



RESEARCH FOUNDATION

RESEARCH FOR THE NFPA MISSION

Fire Safety Challenges of Tall Wood Buildings – Phase 2: Task 5 – Experimental Study of Delamination of Cross Laminated Timber (CLT) in Fire

FINAL REPORT BY:

Daniel Brandon

RISE Research Institutes of Sweden
Borås, Sweden

Christian Dagenais

FPInnovations
Quebec, Canada

March 2018

© 2018 Fire Protection Research Foundation

1 Batterymarch Park, Quincy, MA 02169-7417, USA
Email: research@nfpa.org | Web: nfpa.org/foundation

FOREWORD

Recent architectural trends include the design and construction of increasingly tall buildings with structural components comprised of engineered wood referred to by names including; cross laminated timber (CLT), laminated veneer lumber (LVL), or glued laminated timber (Glulam). These buildings are cited for their advantages in sustainability resulting from the use of wood as a renewable construction material.

Research and testing are needed to evaluate the contribution of massive timber elements to room/compartments fires with the types of structural systems that are expected to be found in tall buildings (e.g. CLT, etc.). Previous research has shown that timber elements contribute to the fuel load in buildings and can increase the initial fire growth rate. This has the potential to overwhelm fire protection systems, which may result in more severe conditions for occupants, fire fighters, property and neighboring property.

There is a need to quantify the contribution of timber elements to compartment fires to assess the relative performance compared to noncombustible structural materials. The contribution of exposed timber to room fires should be quantified for the full fire duration using metrics such as charring rate, visibility, temperature and toxicity. This will allow a designer to quantify the contribution, validate design equations and develop a fire protection strategy to mitigate the level of risk to occupants, fire fighters, property and neighboring property. In addition, the effect of encapsulating the timber as means of preventing or delaying involvement in the fire (e.g. gypsum, thermal barrier) needs to be characterized.

This report is part of a larger project with the goal to quantify the contribution of Cross Laminated Timber (CLT) building elements (wall and/or floor-ceiling assemblies) in compartment fires. This Task 5 report summarizes a model scale experimental study conducted to analyze the delamination behavior of a variety of adhesives in CLT.

The Fire Protection Research Foundation expresses gratitude to the report authors Daniel Brandon, who is with RISE Research Institutes of Sweden located in Borås, Sweden and Christian Dagenais, who is with FPInnovations located in Quebec, Canada. The Research Foundation appreciates the guidance provided by the Project Technical Panelists, the funding provided by the project sponsors, and all others that contributed to this research effort. Special thanks are expressed to the USDA, Forest Service for being a sponsor of this study.

The content, opinions and conclusions contained in this report are solely those of the authors and do not necessarily represent the views of the Fire Protection Research Foundation, NFPA, Technical Panel or Sponsors. The Foundation makes no guaranty or warranty as to the accuracy or completeness of any information published herein.

About the Fire Protection Research Foundation

The [Fire Protection Research Foundation](#) plans, manages, and communicates research on a broad range of fire safety issues in collaboration with scientists and laboratories around the world. The Foundation is an affiliate of NFPA.



About the National Fire Protection Association (NFPA)

Founded in 1896, NFPA is a global, nonprofit organization devoted to eliminating death, injury, property and economic loss due to fire, electrical and related hazards. The association delivers information and knowledge through more than 300 consensus codes and standards, research, training, education, outreach and advocacy; and by partnering with others who share an interest in furthering the NFPA mission.



[All NFPA codes and standards can be viewed online for free.](#)

NFPA's [membership](#) totals more than 65,000 individuals around the world.

Keywords: tall wood buildings, fire safety, tall timber, cross laminated timber, CLT, compartment fire, fire test, delamination, model scale tests, experimental study

Report number: FPRF-2018-05

PROJECT TECHNICAL PANEL

Carl Baldassarra, Wiss, Janney, Elstner Associates
David Barber, Arup
Jim Brinkley, International Association of Fire Fighters
Charlie Carter, American Institute Steel Construction
Kim Clawson, Jensen Hughes
Ronny Coleman, Fireforce One
Sean DeCrane, Battalion Chief (Retired), Cleveland Fire Department, OH
Michael Engelhardt, University of Texas at Austin
Patricia Layton, Clemson
Steven Lohr, Fire Chief, Hagerstown Fire Department, MD
Rick McCullough, Fire Chief (Retired), City of Regina, Saskatchewan,
Canada
Kevin McGrattan, NIST
Ben Johnson, Skidmore, Owings, and Merrill LLP
Paul Shipp, USG Corporation
Ray Walker, Fire Marshal, Vernon, CT, International Fire Marshals
Association
Tracy Vecchiarelli, NFPA Staff Liaison

PROJECT SPONSORS

American Wood Council (AWC)
US Department of Agriculture, Forest Service
Property Insurance Research Group (PIRG):
American International Group, Inc. (AIG)
CNA Insurance
FM Global
Liberty Mutual Insurance
Tokio Marine America
Travelers Insurance
XL Group
Zurich Insurance Group



SAFETY AND TRANSPORT
FIRE RESEARCH



Fire Safety Challenges of Tall Wood Buildings – Phase
2: Task 5 – Experimental Study of Delamination of
Cross Laminated (CLT) Timber in Fire

Daniel Brandon and Christian Dagenais

Fire Safety Challenges of Tall Wood Buildings –
Phase 2: Task 5 – Experimental Study of
Delamination of Cross Laminated (CLT) Timber
in Fire

Daniel Brandon and Christian Dagenais

Abstract

Fire Safety Challenges of Tall Wood Buildings - Phase 2: Experimental Study of Delamination of Cross-Laminated Timber (CLT) in Fire

Recent architectural trends include the design and construction of tall buildings with visible structural members comprised of mass timber. Cross-laminated timber (CLT) is such a material and is increasingly used for tall buildings because of a combination of advantages regarding its structural performance, low environmental impact and more. As timber is a combustible material, CLT can become involved in the fire at locations where it is not protected against the fire. In that case, the CLT contributes to the fuel load of the fire and has an influence on the fire dynamics.

Recent compartment fire tests have shown that bond line failures within cross-laminated timber caused by fire can result in sustained fires that do not extinguish naturally. Due to weakening of the bond line, glued lamellas of the exposed layer of the CLT can delaminate, which can result in a sudden exposure of cold timber to the high temperatures of a fire. This delamination results, therefore, in an increased combustion of exposed timber, and was previously shown to be the cause of continuous fully developed fires and fires that re-intensify after a period of decay.

The study presented in this report aimed to (1) determine whether delamination in compartment fires can be avoided by using robust adhesives and (2) to assess the capability of a small scale test method to identify robust adhesives that do not lead to delamination of CLT in fires.

The study involved a replication of fire conditions recorded in a recent compartment fire test performed earlier for this research project on Fire Safety Challenges of Tall Wood Buildings. These fire conditions were replicated in an intermediate scale furnace test with an exposed CLT specimen. The fire temperatures, oxygen concentration, incident radiant heat flux, CLT temperatures, charring rate and times of delamination resulting from the intermediate scale tests were similar to those of the compartment test, if the same CLT product was used in both specimens. It was shown that some CLT specimens made with other adhesives do not delaminate in the same conditions.

The capability of a small scale Bunsen burner test to identify non-delaminating and delaminating adhesives was assessed. A comparative study showed that there is a good correspondence between results of the intermediate scale furnace test and the small scale Bunsen burner test.

Key words: CLT, Compartment fire, Exposed Wood, Tall Wood Buildings

RISE Research Institutes of Sweden AB

Stockholm 2017

Content

Abstract	1
Content	2
Preface	4
1 Introduction	5
2 Furnace test	6
2.1 Compartment tests by SU et al. (2017).....	6
2.2 Replication of compartment test conditions with a furnace.....	7
2.3 Setup and measurements	10
2.4 Materials and production of specimens	15
2.5 Properties of specimens	16
2.6 Test results and discussion	17
2.6.1 Tests PRF-A and PRF-B.....	17
2.6.2 Tests MF-A and MF-B.....	21
2.6.3 Tests EPI-A and EPI-B.....	24
2.6.4 Tests PU1-A and PU1-B	29
2.6.5 Tests PU2-A and PU2-B	36
2.7 Adhesive performance	40
2.7.1 Char depth	40
2.7.2 Mass loss and heat release.....	41
2.7.3 Summary of signs of delamination	42
2.7.4 Critical bond line temperature	43
2.8 Evaluation of the method	44
2.8.1 Incident heat flux by radiation	45
2.8.2 CLT temperatures	46
2.8.3 Char depth	48
2.8.4 Time of delamination.....	49
3 PS 1 testing	50
3.1 Method.....	50
3.2 Setup and measurements	51
3.3 Materials and production of specimens	51
3.4 Measured properties of specimens	52
3.5 Test results	53
3.6 Validation of method	57
3.7 Discussion of flame test results	57
4 Correspondence between PS-1 and furnace testing	58
Acknowledgements	60

References	61
Appendix I.....	63
Appendix II	67
Appendix III.....	70

Preface

The investigation described in this report has been conducted at:

RISE – Research Institutes of Sweden, and

FP-Innovations, Canada.

The development of the test plan for intermediate scale furnace tests and their execution were done by RISE in Stockholm. Students from the Lund University, Eric Johansson and Anton Svenningsson have helped preparing and conducting intermediate scale furnace tests at RISE in Stockholm.

Specimens for the intermediate scale furnace tests at RISE in Stockholm were made at Innotech Alberta in Edmonton in co-operation with FP-Innovations.

PS1 tests discussed in chapter 3 of this report were planned and conducted by FP-innovations.

1 Introduction

In previous fire tests of compartments comprising exposed CLT, the occurrence of heat delamination considerably increased the duration, heat release rate and damage of the fires (Brandon and Östman, 2016). Heat delamination of CLT occurs due to weakening of the bond line at elevated temperatures and is, therefore, very dependent on the adhesive type of the CLT. In order to obtain a full understanding of fire dynamics in CLT structures, it is necessary to consider heat delamination behavior of a variety of adhesives in CLT. In this study, the focus will be on the behavior of a number of adhesives in fire. It should, however, be noted that the adhesive type by itself does not guarantee a certain behavior in fire.

Performing a series of full scale compartment tests for every type of CLT is expensive. Therefore, there is a need for a small scale method to distinguish adhesives that exhibit heat delamination characteristic from those that do not. This report presents two sets of experiments:

- 1) Intermediate scale furnace tests that simulate the fire exposure and oxygen content of a previous full-scale compartment test (Compartment Test 1-4, Su *et al.* 2017) with CLT specimens made with five different types of structural adhesives;
- 2) Heat performance tests (as detailed in Clause 6.1.3.4 of Voluntary Product Standard PS 1 Structural Plywood (NIST 2010)) of plywood specimens with the same five adhesives as used in the intermediate scale furnace tests.

The intermediate scale furnace test assesses whether and when delamination would have occurred if the CLT manufactured with a given adhesive would have been used in full scale Compartment Test 1-4. Test 1-4 was selected for this study, as it involved a surface area of exposed CLT which is at the upper limit of what is allowed in current regulations. In Test 1-4 the ceiling was exposed, which is known to be more prone to delamination than exposed walls (Klippel et al., 2016). Additionally, Annex B of the current 2018 version of PRG-320 requires full-scale testing to ensure that the CLT does not exhibit fire re-growth when subjected to an exposure similar to FPRF Test 1-4. This report includes a discussion of the suitability of the furnace test as an alternative for the current method described in Annex B.

In addition to the furnace tests, it is assessed whether a small scale heat performance test would be a suitable and economical method to differentiate delaminating adhesives from non-delaminating adhesives used for face bonding CLT elements. The correspondence between both test methods is used for the evaluation of the small scale heat performance test for the identification of robust adhesives.

Given that the project is intended for the North American market, it was agreed that the intermediate scale tests would be performed to assess different adhesives compliant to the 2012 edition of ANSI/APA PRG 320. The five adhesives evaluated in this study are: two one-component polyurethanes (PU1 and PU2) one melamine formaldehyde (MF), one emulsion polymer isocyanate (EPI) and one phenol resorcinol formaldehyde (PRF). The CLT elements used in the FPRF Compartment Test 1-4 were manufactured using the PU1 adhesive.

2 Furnace test

Intermediate scale furnace tests were performed of CLT with different adhesive types. The implemented temperatures and oxygen content were based on full scale compartment fire tests by Su et al. (2017). The intermediate scale tests aimed to replicate the most extreme fire temperatures measured by plate thermometers in the compartment fire test, in order to assess whether delamination would occur if other CLT products were used. The tests were performed in a furnace with internal dimensions of 1.0 x 1.0 x 1.0m. Furnace tests at this scale are cost-efficient and allow a close-up study of the delamination behavior. An assessment of delamination in the intermediate scale fire test was performed using (1) measurements of the bond line temperatures, (2) measurements of the char depths and charring rates (3) a video made of approximately 50% of the exposed surface, (4) estimations of the total mass loss during the tests and (5) assessment of sudden changes of air temperature and oxygen content of the exhaust air.

The intermediate scale tests were performed to assess different adhesives of the following types: Poly-urethane (PU) Melamine Formaldehyde (MF); Emulsion Polymer Isocyanate (EPI); Phenol Resorcinol Formaldehyde (PRF). Two of the tests were performed of the CLT product with Polyurethane (PU1) adhesive used in the FPRF compartment fire tests. Additionally, two tests of CLT specimens with an enhanced polyurethane adhesive aiming to eliminate heat delamination (PU2) were conducted. In order to assess the repeatability to some extent, the tests were repeated twice.

2.1 Compartment tests by SU et al. (2017)

Six full scale compartment fire tests have been performed as part of the FPRF research project on fire safety challenges of tall timber buildings (Su et al., 2017). In this report, data from these tests are used. Therefore, the setup of these compartment tests is briefly discussed here.

All compartment tests had inner dimensions of 9.1 x 4.6 x 2.7m and comprised of a structure completely made of CLT. Four compartments had a rough opening of 1.8 x 2.0m and two compartments had a rough opening of 3.6 x 2.0m. Typical apartment furniture was placed in the compartments, resulting in a density of the moveable fire load of 550MJ/m². The study aimed to quantify the contribution of exposed CLT to a fire and, therefore, involved compartments with different surfaces exposed. Table 1 shows an overview of exposed surfaces and surfaces protected with a specified number of 15.9mm type-X gypsum board layers (GB) of each test.

In this report the compartment tests are referred to as ***Compartment Test 1-1***, ***Compartment Test 1-2*** etc. Results of Compartment Test 1-4 are used throughout this report. Compartment Test 1-4 had an exposed CLT ceiling and all walls protected with three layers of type X gypsum boards.

Table 1 Test matrix of CLT compartments for fire tests (Su et al. 2017)

Test name	Name in this report	Rough opening in wall W2	Compartment surface				
			W1 9.1m x 2.7m	W2 4.6m x 2.7m	W3 9.1m x 2.7m	W4 4.6m x 2.7m	Ceiling 9.1m x 4.6m
1-1	Compartment Test 1-1	1.8m wide x 2.0m high	3GB	3GB	3GB	3GB	3GB
1-4	Compartment Test 1-4		3GB	3GB	3GB	3GB	Exposed
1-5	Compartment Test 1-5		Exposed	3GB	3GB	3GB	3GB
1-6	Compartment Test 1-6		Exposed	3GB	3GB	3GB	Exposed
1-2	Compartment Test 1-2	3.6m wide x 2.0m high	2GB	2GB	2GB	2GB	2GB
1-3	Compartment Test 1-3		Exposed	2GB	2GB	2GB	3GB

2.2 Replication of compartment test conditions with a furnace

The aim of the furnace tests was subjecting CLT specimens to a replication of the fire exposure that was observed in Compartment Test 1-4. A successful method should lead to comparable material damage, *i.e.* wood temperatures, charring rates and times of delamination in the simulated and simulating tests, if the same CLT product is used.

Oxygen concentration of the air in a compartment or a furnace has a significant influence on the char oxidation and pyrolysis of wood (Weng, Hasemi, Fan 2005). It is, furthermore, noted that previous small scale fire tests (Brandon et al. 2015) at atmospheric oxygen concentration (20.9%) with relatively low incident heat fluxes (with respect to post-flashover compartment fires) resulted in significantly higher charring rates than seen in any previous post flashover compartment fire test (Brandon and Östman, 2016). Therefore, it is considered important to perform the test in an enclosed environment in which the oxygen content can be regulated to simulate the oxygen concentration measured in Test 1-4. In air with high oxygen concentrations, significant oxidation can take place, which leads to a shrinkage of the char layer. This leads to a decrease of thermal protection the char provides to the uncharred timber, which leads to an increased charring rate. However, a recent study (Schmid *et al.*, 2016) has shown that char contraction is not significant for oxygen concentrations under 5%.

The thermal exposure to the specimen is dependent on radiative and convective heat flux, which can be written as:

$$\dot{q}''_{rad} = \varepsilon(\dot{q}''_{inc} - \sigma T_s^4) \quad (1)$$

and

$$\dot{q}''_{con} = h_c (T_G - T_S) \quad (2)$$

Where: \dot{q}''_{rad} is the radiative heat flux to or from a surface;

ε is the thermal emissivity;

\dot{q}''_{inc} is the incident heat flux by radiation;

σ is the Stefan Boltzmann constant;

T_S is the surface temperature;

\dot{q}''_{con} is the convective heat flux to or from a surface;

h_c is a convection heat transfer coefficient;

T_G is the gas temperature.

A black body radiation temperature introduced by Wickström (2016) will be used:

$$T_R = \sqrt[4]{\frac{\dot{q}''_{inc}}{\sigma}} \quad (3)$$

Where T_R is the black body radiation temperature.

The total heat flux to or from a surface is equal to the sum of the radiative heat flux and convective heat flux:

$$\dot{q}'' = \varepsilon (\dot{q}''_{inc} - \sigma T_S^4) + h_c (T_G - T_S) \quad (4)$$

or

$$\dot{q}'' = \sigma \varepsilon (T_R^4 - T_S^4) + h_c (T_G - T_S) \quad (5)$$

Where \dot{q}'' is the black body radiation temperature.

In furnace tests, the radiation temperature and the gas temperature cannot be controlled independently. Therefore, a single fire temperature T_F , is needed that replaces the radiation temperature T_R and the gas temperature T_G and results in the same total heat flux to a surface. The fire temperature always has a value between the radiation temperature and the gas temperature.

$$\dot{q}'' = \sigma \varepsilon (T_F^4 - T_S^4) + h_c (T_F - T_S) \quad (6)$$

Where T_F is the fire temperature.

The fire temperature can be found using the surface temperature of an object that does not absorb heat ($\dot{q}'' = 0$): the adiabatic surface temperature T_{AST} .

$$\dot{q}'' = 0 = \sigma \varepsilon (T_F^4 - T_{AST}^4) + h_c (T_F - T_{AST}) \quad (7)$$

Solving the equation above leads to:

$$T_F = T_{AST} \quad (8)$$

Therefore, the fire temperature can be approximated from the surface temperature of an object that only absorbs an insignificant amount of heat, such as a plate thermometer that is positioned inside a fire testing furnace. In Section 2.3 the use of a plate thermometer to determine the incident radiant heat flux is discussed.

The exposure within the furnace is controlled by aiming for similar plate thermometer temperatures as measured in compartment fire test 1-4. Additionally, the oxygen concentration measured under the ceiling in the full scale compartment fire test is replicated in the furnace. In test 1-4 delamination of the second layer of lamellas caused the temperature to rise and the oxygen content to drop between 120 minutes and the end of the test at 160 minutes after ignition. In order to assess whether delamination would occur, with other CLT specimens, the effects of delamination of the second layer of lamellas in the original test were ignored and the target temperature and oxygen curve were extrapolated to resemble that of a decaying fire without delamination (Figure 1). In the fully developed stage the oxygen content of the compartment test was approximately 0% for the majority of the time. In the furnace this oxygen content is difficult to achieve. As it was recently shown that there is no significant char contraction due to oxidation at oxygen concentrations under 5% (Schmid et al., 2016), it was chosen to allow the oxygen content to be in between 0 and 5% during the fully developed phase of the intermediate scale furnace test.

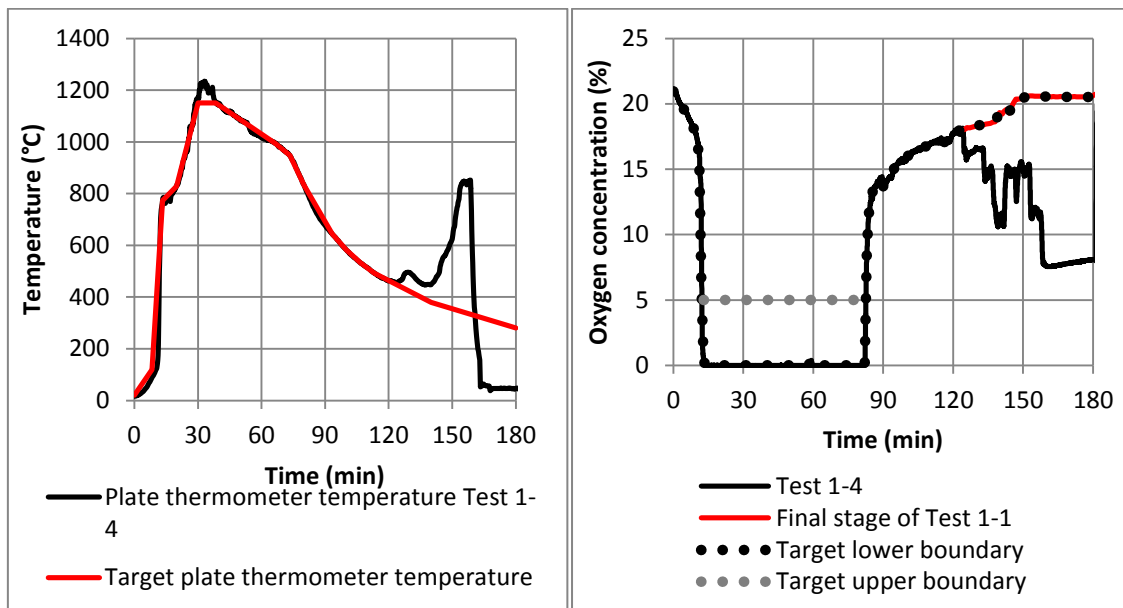


Figure 1: Target temperature and oxygen content and the original measurements of compartment tests

A recent study resulted in a method to predict the char and delamination behavior of CLT in standard fire resistance tests without considering the presence of mechanical loads (Klippel and Schmid, 2017). The method was validated with results of numerous standard fire resistance tests, both, with and without mechanical loads, which indicates that there is no significant correlation between mechanical loading and delamination or charring behavior. The study presented herein focusses on the delamination and charring behavior of CLT. Therefore, mechanical loads are not considered in this study.

2.3 Setup and measurements

CLT specimens of 1400 by 600 mm were placed on top of the furnace, as shown in Figure 2 to 4. An area of 1000 by 600mm was exposed to the fire of the furnace. Two plate thermometers were installed 100 and 150mm below the exposed timber surface (see Figure 3 and 4), similar to Compartment Test 1-4. A K-type thermocouple was positioned close to the upper plate thermometer in order to determine the gas temperature for incident radiant heat flux calculations.

The oxygen content of leaving air was measured in the exhaust and was adjusted by controlling the air and nitrogen inlet of the furnace, so that the oxygen content was similar to that measured under the ceiling of the replicated compartment test.

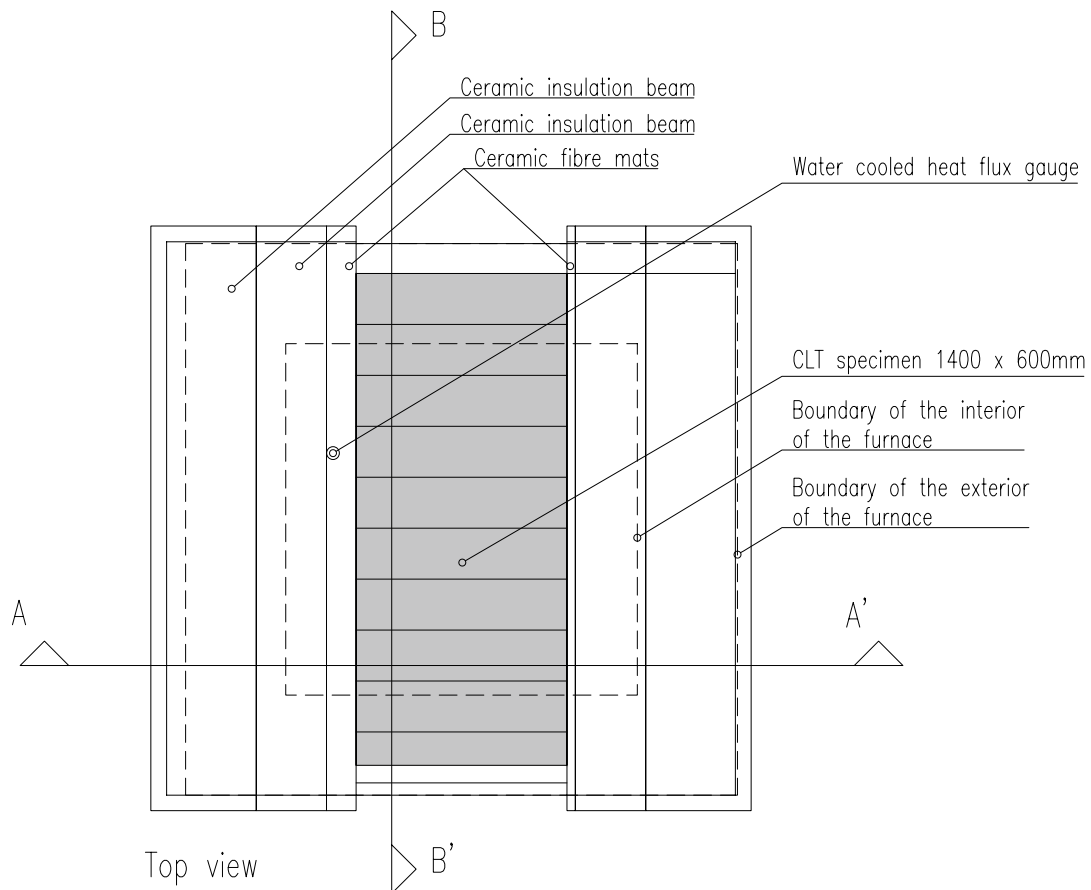


Figure 2: Top view of the test setup

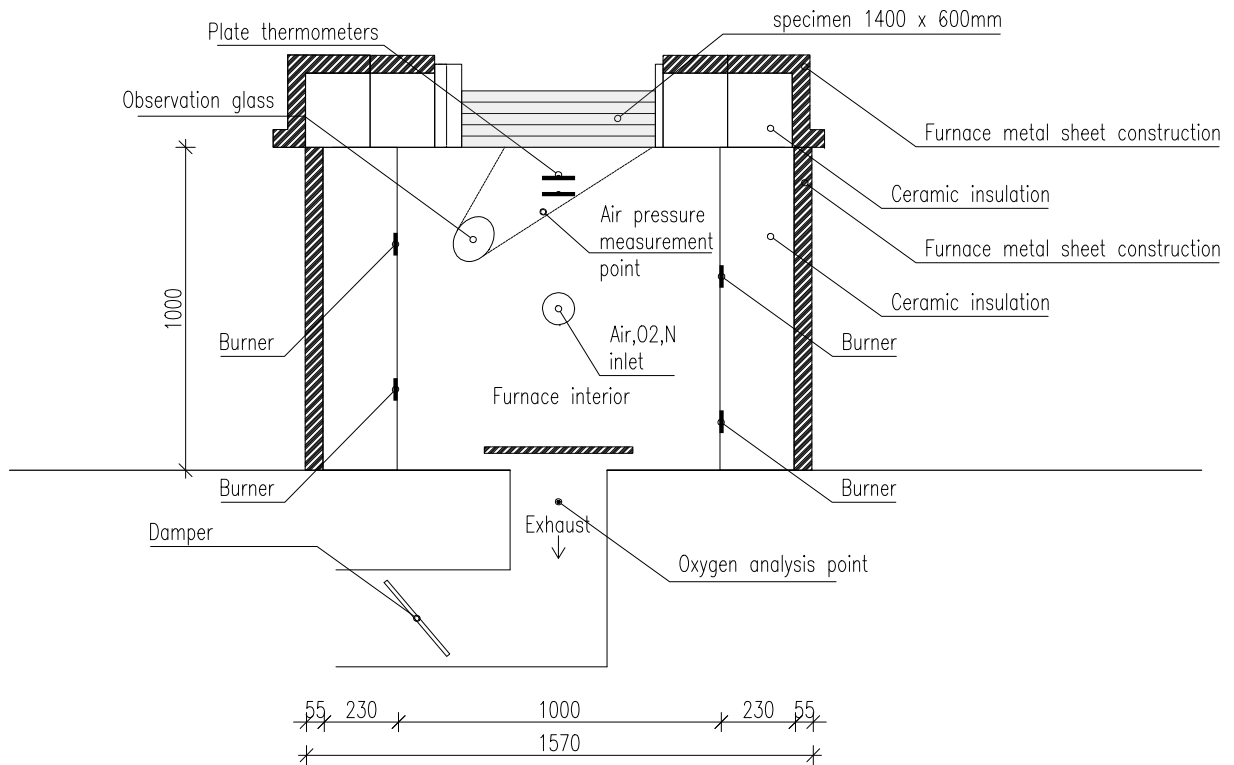


Figure 3: Section A-A' of the test setup

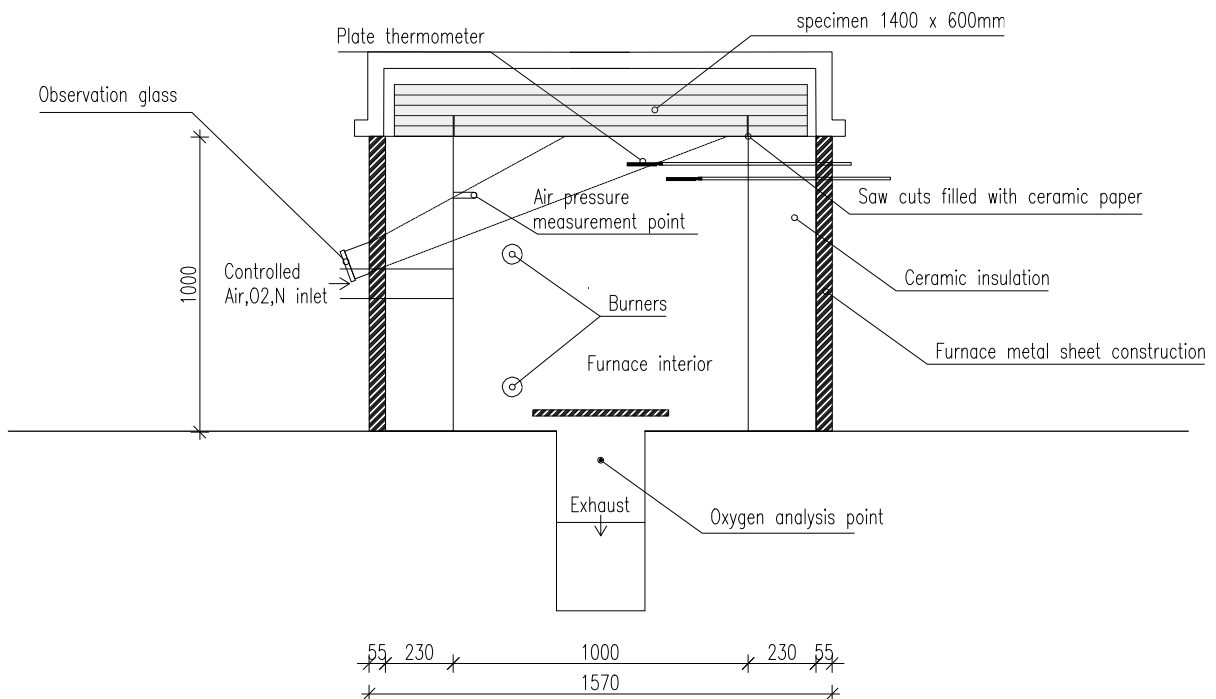


Figure 4: Section B-B' of the test setup

The incident heat flux by radiation was calculated using plate thermometer and thermocouple measurements (Wickström, 2016):

$$\dot{q}_{inc} = \sigma T_{PT}^4 - \frac{h_c}{\varepsilon_{PT}} (T_{G;TC} - T_{PT}) \quad (9)$$

Where σ is the Stefan Boltzmann constant

T_{PT} is the temperature measured by the plate thermometer

$T_{G;TC}$ is the gas temperature approximated by a thermocouple near the plate thermometer

ε_{PT} is the emissivity of the plate thermometer

It should be noted that a thermocouple measurement is influenced by direct radiation and does not measure the true gas temperature. However, section 2.8.1 includes a discussion of the consequences of this error on the incident radiant heat flux calculated.

A water cooled incident heat flux meter was used to estimate the value of the parameter h_c / ε_{PT} . However, it will be shown in the discussions of the tests that this parameter has no significant influence on the calculations of the incident heat flux from the plate thermometer. Due to limited robustness of the water cooled incident heat flux gauge, the measurements were not repeated.

The mass loss and the heat release of the each specimen give an additional indication of delamination, as delamination results in an increased heat release rate and mass loss rate. For an estimation of the total contribution (heat release) of the specimen during the test, the weight loss of dry timber (excluding moisture) was estimated. Prior to the test, each specimen was weighed and its density was determined. Additionally, the moisture content was determined (according to section 2.5) so that the dry density of the specimen could be estimated. In order to determine the dry weight of the specimen after the test, the exposed section of the specimen that was exposed was dried in an oven at 120°C for 8 days to evaporate the moisture inside the specimen. The total heat released was estimated with the heat of combustion, obtained from literature:

$$Q_{CLT} = \Delta m_{dry} \cdot \chi \cdot H_{wood} \quad (10)$$

Where: Δm_{dry} is the mass loss of the timber excluding mass of moisture;

χ is the combustion efficiency (between 0 and 1.0);

H_{wood} is the heat of combustion of dry wood (18.75 MJ/kg; Krajnc, 2015).

Thermocouples positioned inside the CLT were used for determining the temperature profile and charring rates and the occurrence of delamination. To determine the temperatures and charring rates correctly, thermal conduction along the thermocouples should be limited, by placing the thermocouples parallel to the isotherms (horizontally) (Brewer, 1967). To determine the occurrence of delamination, it is important that thermocouples are positioned exactly in the bond line. Therefore, these thermocouples were embedded in the bond line prior to gluing of the CLT specimens. Additionally, for comparisons with Compartment Test 1-4 also two sets of three thermocouples have been positioned in the direction perpendicular to the isotherms. Each of these sets had had a tip installed at 20, 35 and 70mm distance from the exposed side, the same way as done in Compartment Test 1-4.

Figure 5 shows the positions of the thermocouples from the top, front and side view. Additionally, Figure 6 shows a close-up of the front view. Metal sheathed 1.5mm diameter type K thermocouples were inserted in 1.5mm diameter holes, which were drilled with a pillar drill. The thermocouples that were positioned parallel to the isotherms (perpendicular to the heat flow) were positioned in four series of six thermocouples, measuring the temperatures in the lowest three lamellas. The thermocouples of each series were positioned at different depths, with 15 and 20 mm increments, so that the thermocouple tips were at the same distance from the exposed surface as the thermocouples in Compartment Test 1-4. The charring rates were determined from the time at which each subsequent thermocouple of one series measures 300°C.

The uncharred depth was measured using a resistograph, which recorded the resistance and distance of a drill that was drilled at constant velocity through the timber. The drilling started from the unexposed side of the specimen. A sharp drop of resistance was measured once the drill reached the char layer, which allowed to determine the thickness of the uncharred sections. The char depth was calculated by subtracting the uncharred depth from the original thickness of the specimen. The measurement was performed consistently at the same four locations of each specimen. These locations were at 20 cm distance from both edges of the exposed surface and at 20 cm distance from the supported ends.

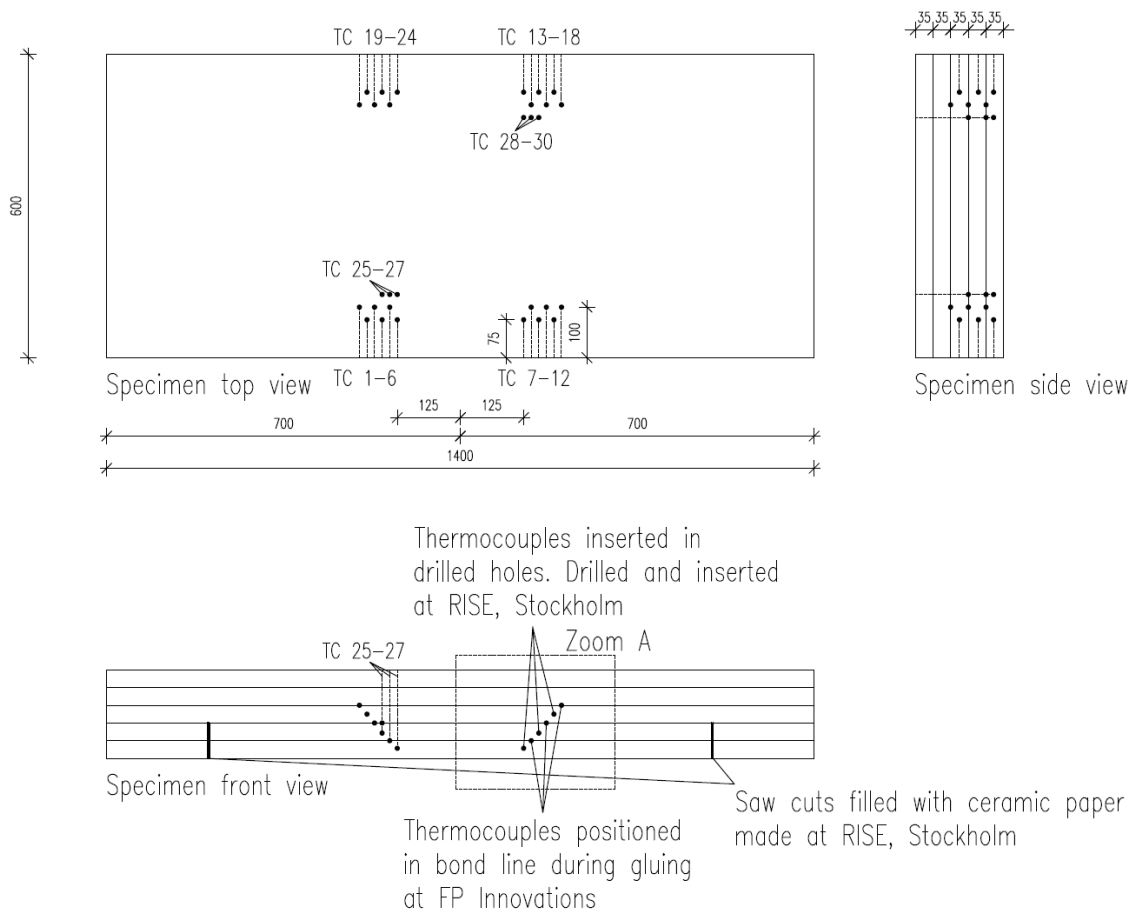


Figure 5: Top view, front view and side view of the specimens with indicated locations of thermocouples

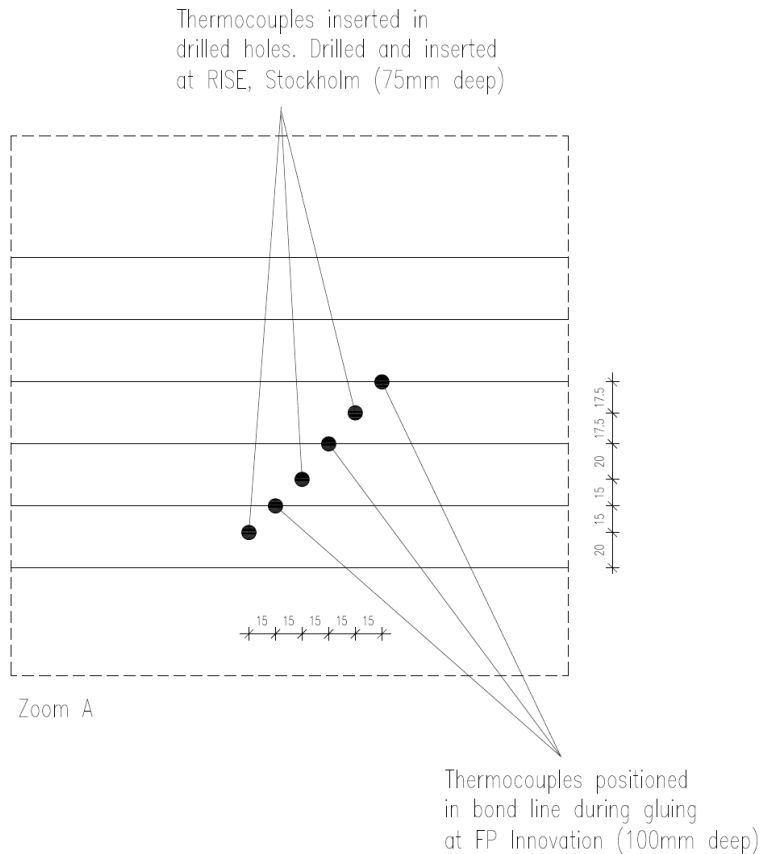


Figure 6: Locations and distances of thermocouples.

The time of delamination is determined visually from a recorded video of approximately 50% of the specimen's surface and by identifying rapid temperature increases measured in the bond line and in the falling lamellas. For this study the criteria used to identify delamination from temperature increases are based on temperature measurements within the CLT of Compartment Test 1-4 (Figure 7). Maximum rates of temperature increase in the CLT at depths of 20 and 35mm were approximately 40°C/min, in roughly the first 40 minutes after flashover. After the rate of temperature increase started to reduce, suddenly a significantly faster temperature increase was observed by thermocouples in the first lamella. The recorded plate thermometer and thermocouple temperatures within the compartment did not show a clear cause of this rapid temperature increase in the CLT. Therefore, the rapid temperature increase indicates that a piece of char fell-off or a lamella delaminated which suddenly exposed the thermocouples in the first lamella to the fire. A temperature increase exceeding 100°C within 1 minute in the bond line or within the exposed lamella could successfully be used as a criterion to indicate that the thermocouple became suddenly exposed to the fire, as shown in Figure 7. In the cooling phase this increase is less rapid as the difference between gas temperatures and bond line temperatures is potentially smaller. In the cooling phase, a temperature increase of 100°C within 5 minutes was used as a criterion to indicate char fall-off or delamination. The time at which this occurred corresponded well with the reported time of the second flashover at 150 minutes (Su et al., 2017).

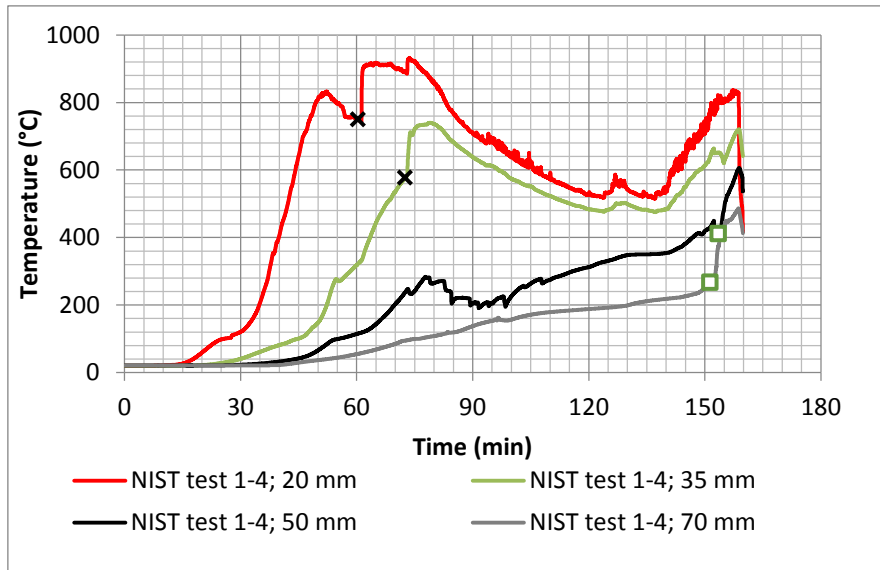


Figure 7: Temperatures in the exposed CLT of the ceiling of Compartment Test 1-4.

2.4 Materials and production of specimens

Eight 5-ply CLT panels were constructed at Innotech Alberta in Edmonton (AB) through a joint collaboration between FPIInnovations and Innotech Alberta. The CLT panels were 1,400 mm long by 620 mm wide by 175 mm thick. The major strength axis of the CLT was along the 1,400 mm. The CLT panels were then sent to Stockholm, Sweden for fire testing at RISE.

Nominal 2x4 graded Spruce-Pine-Fir (SPF) lumber were purchased from a certified Canadian CLT plant. The layup configuration followed the E1 stress grade detailed in ANSI/APA PRG 320, with the exception that all laminations were machine stress-rated (MSR) 1950fb-1.7E SPF lumber rather than having visually-graded SPF No.3 lumber in the transverse layers. The lumber boards had no finger-joints in order to limit the potential influence of a finger-joint failure occurring first during the fire test. The lumber boards were conditioned to approximately 12% moisture content and surfaced from both sides down to 35 mm in thickness less than 24 h prior to gluing.

The appropriate number of lumber boards were then tightly placed side-by-side to cover the required area and secured together using plywood strips. This procedure was repeated for all five layers to facilitate manipulations and insertion into the hydraulic press. It is noted that the press is designed for oriented strand board (OSB), which typically requires heating of the platens to accelerate the curing process. No heat was used for pressing the CLT panels in this study.

The adhesives were uniformly applied using rollers on one side of the lumber boards only, for every layer. The mass of each layer was measured to ensure that sufficient adhesive was applied. Two CLT panels were made using each adhesive. The adhesive spread rate, open and close assembly times, applied pressure as well as pressing and **curing times were done in accordance with the adhesive suppliers' recommendations** and technical data sheets. Representatives of the PU2 and PRF witnessed the CLT manufacturing. Table 2 provides the gluing parameters used for the CLT panels.

Additional pictures of the specimen preparation and gluing can be found in Appendix III.

Table 2 CLT gluing parameters

Layer (top to bottom)	Mass of adhesive (g) per layer							
	Type of Adhesive							
	One- Component Polyurethane ⁽¹⁾		Emulsion Polymer Isocyanate		Melamine- Formaldehyde		Phenol- Resorcinol- Formaldehyde	
	PU2-1	PU2-2	EPI1-1	EPI2-2	MF-1	MF-2	PRF-1	PRF-2
Spread Rate	30 lb / 1000 ft ²		50 lb / 1000 ft ²		50 lb / 1000 ft ²		80 lb / 1000 ft ²	
Assembly Time	70 min		20 min		40 min		80 min	
Press Time	210 min		120 min		190 min		16 h ⁽²⁾	
Pressure	150 psi		150 psi		150 psi		150 psi	
4 th - 5 ^h	174	174	216	216	295	295	358	358
3 rd - 4 th	171	171	226	226	268	268	393	393
2 nd - 3 rd	181	181	222	221	283	283	384	384
1 st - 2 nd	198	198	241	241	275	275	371	371
Targeted Mass	132		216		265		354	
Notes:								
⁽¹⁾ PU2 required a water-based primer to be sprayed at 20 g/m ² for 60 min prior to glue application.								
⁽²⁾ Due to equipment constraint, it was agreed with the adhesive supplier to turn off the hydraulics after 4 hours and leave the CLT panels under the platens self-weight (± 15 psi) overnight without affecting the bond performance.								

In addition to these eight CLT panels, a pair of commercial CLT panels was also obtained in attempt to replicate those used in the FPRF compartment fire tests. These commercial CLT panels were labelled as “PU1-1” and “PU1-2” as they were manufactured using a one-component PU adhesive conforming to the 2012 edition of ANSI/APA PRG 320. The gluing process is deemed conforming to the adhesive supplier and the CLT manufacturer’s quality control process.

2.5 Properties of specimens

An average moisture content was estimated by oven-drying an undamaged and cold part of the specimens after the test at approximately 800 cm². The weight of the block was determined before and after they were positioned in an oven at 120°C for 8 days. The moisture content and wet density of the specimens is show in Table 3. The first letters of the specimen/test names indicate the type of adhesive present in the CLT. Two tests were performed corresponding to each adhesive.

The gap size between lamellas of the same layer varied between 0 and 1.5 mm. Occasionally, the gaps were bigger near the corners of lamellas. Figure 8 shows a typical cross-section of a specimen.

Table 3 Density and moisture content of CLT specimens

Specimen/test name	Wet density(kg/m ³)	Moisture content (%)
MF-A	536	14.7
MF-B	527	11.8
PRF-A	530	14.9
PRF-B	531	15.1
EPI-A	527	13.8
EPI-B	530	11.1
PU1-A	507	11.4
PU1-B	504	12.0
PU2-A	527	11.3
PU2-B	535	11.1

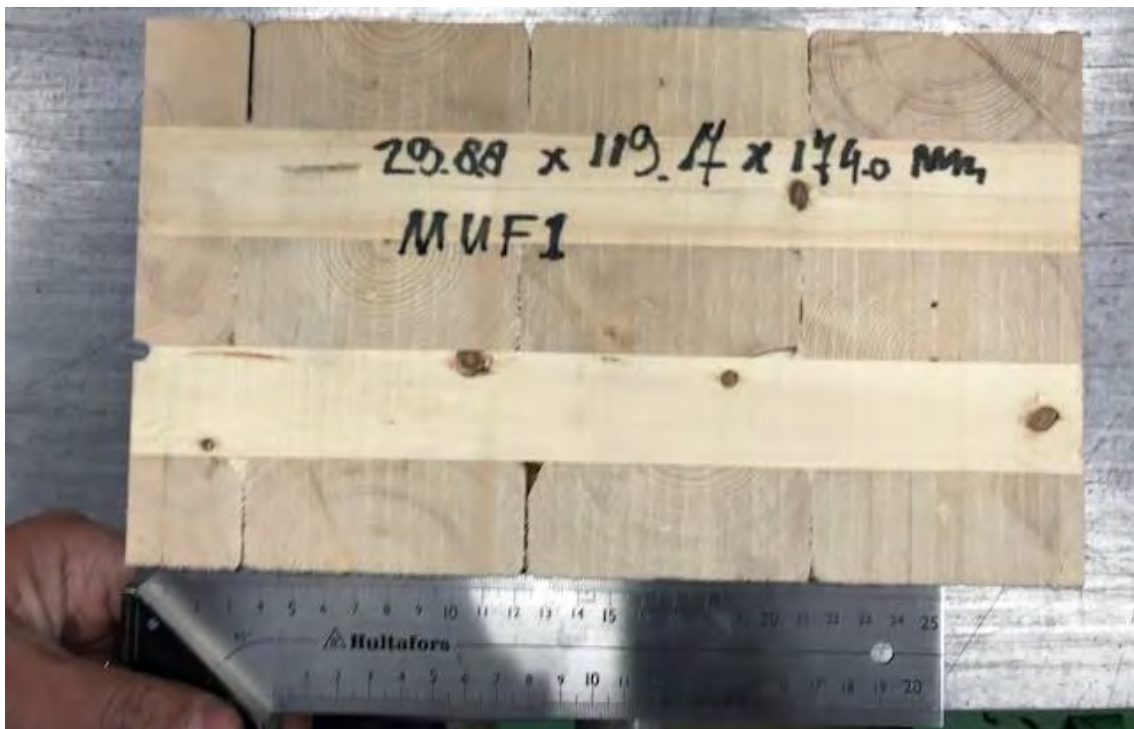


Figure 8: typical cross section of the CLT specimens

2.6 Test results and discussion

The sub-sections below present results of the intermediate scale furnace tests. Each sub-section shows results corresponding to CLT with a different adhesive. Additional results can be found in Appendix I and II.

2.6.1 Tests PRF-A and PRF-B

This sub-section summarizes the main results of tests PRF-A and PRF-B. Figure 9 shows the average plate thermometer temperature together with the target temperature. Figure 10 shows the measured oxygen concentration together with the target oxygen concentration for the duration of the test. No complications arose for the control of the temperature and oxygen content.

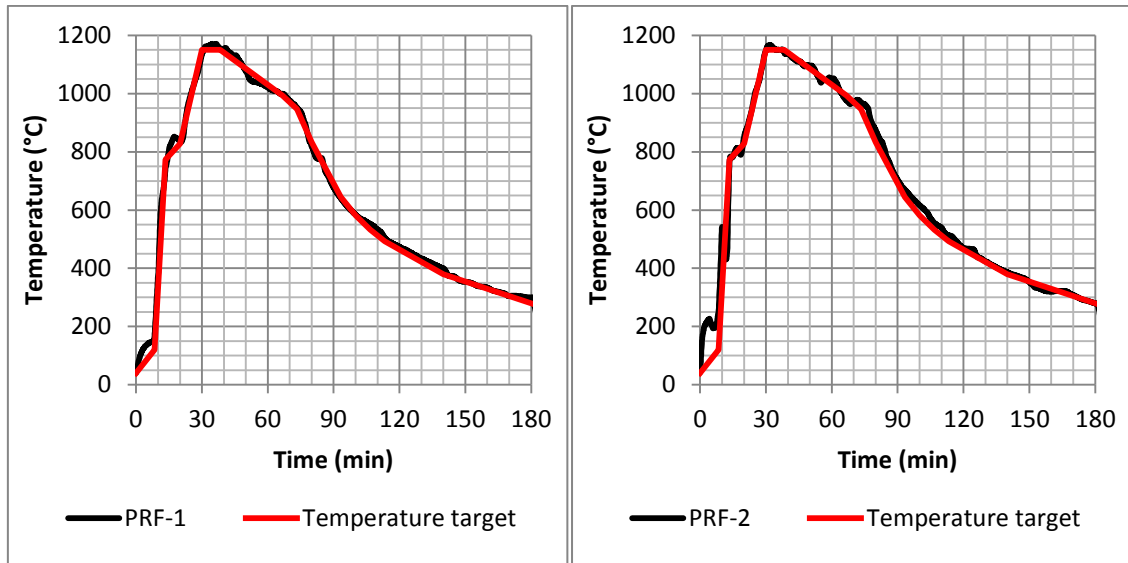


Figure 9: Average temperature measured by the plate thermometers of PRF-A (left) and PRF-B (right)

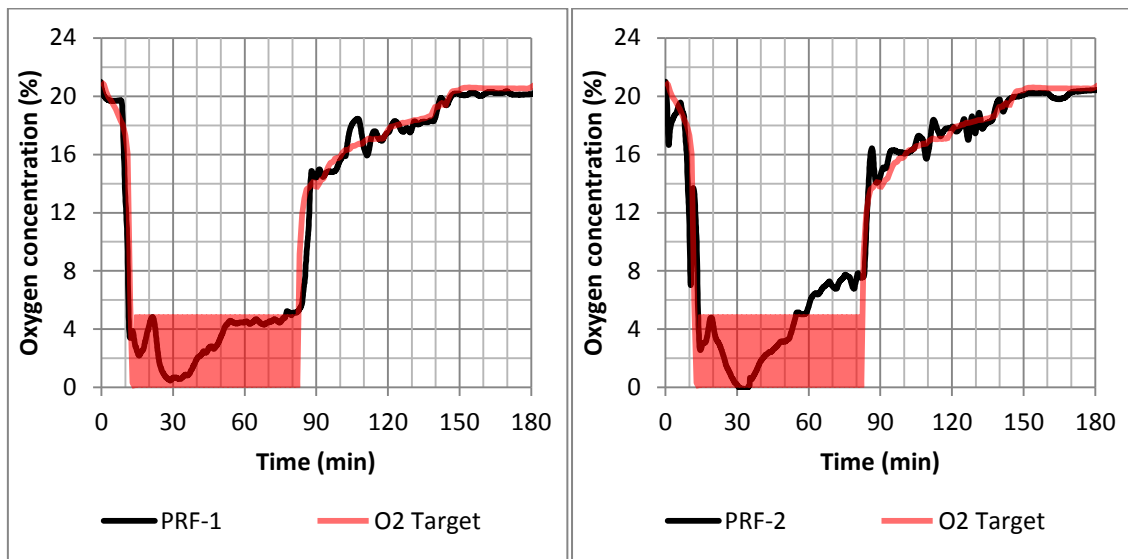


Figure 10: Oxygen concentration of PRF-A (left) and PRF-B (right)

Figure 11 and Figure 12 show the CLT temperatures at 20, 35, 50 and 70mm from the exposed surface. The thermocouples of these series were positioned parallel to the isotherms, to prevent significant thermal conduction along the thermocouples. Thermocouples 13 and 15 of PRF were not taken into account for the indication of delamination and for the determination of the charring rate as they showed clear signs of malfunction. The same criteria of temperature increase as used in Section 2.3 for Compartment Test 1-4 were used to indicate delamination for PRF-A and PRF-B. According to these criteria, there is no indication of delamination given by the thermocouples of PRF-A. There is however one thermocouple in PRF-B, TC 8, showing a temperature increase exceeding $100^{\circ}\text{C}/\text{min}$, at the time indicated in Figure 12. The video camera filming approximately half of the specimen's surface, however, did not record delamination at the same time. The video camera showed two instances at which a small amount of char fell down into the furnace. However, as the surface was small (approximately 1 to 3 percent of the visible surface) and the shape of the lamella could

not be recognized in the video, this was not identified as delamination. Relevant frames of the video can be found in Appendix I.

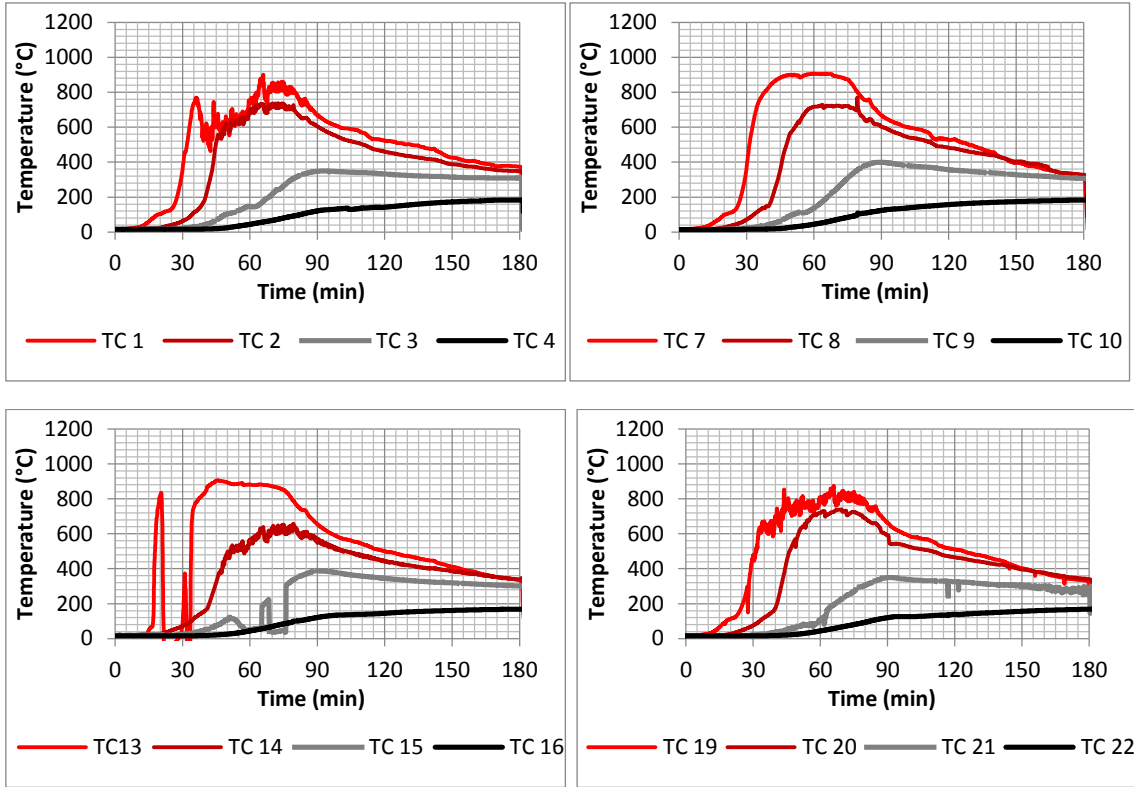


Figure 11: CLT temperatures at 20, 35, 50 and 70mm depth at four locations PRF-A

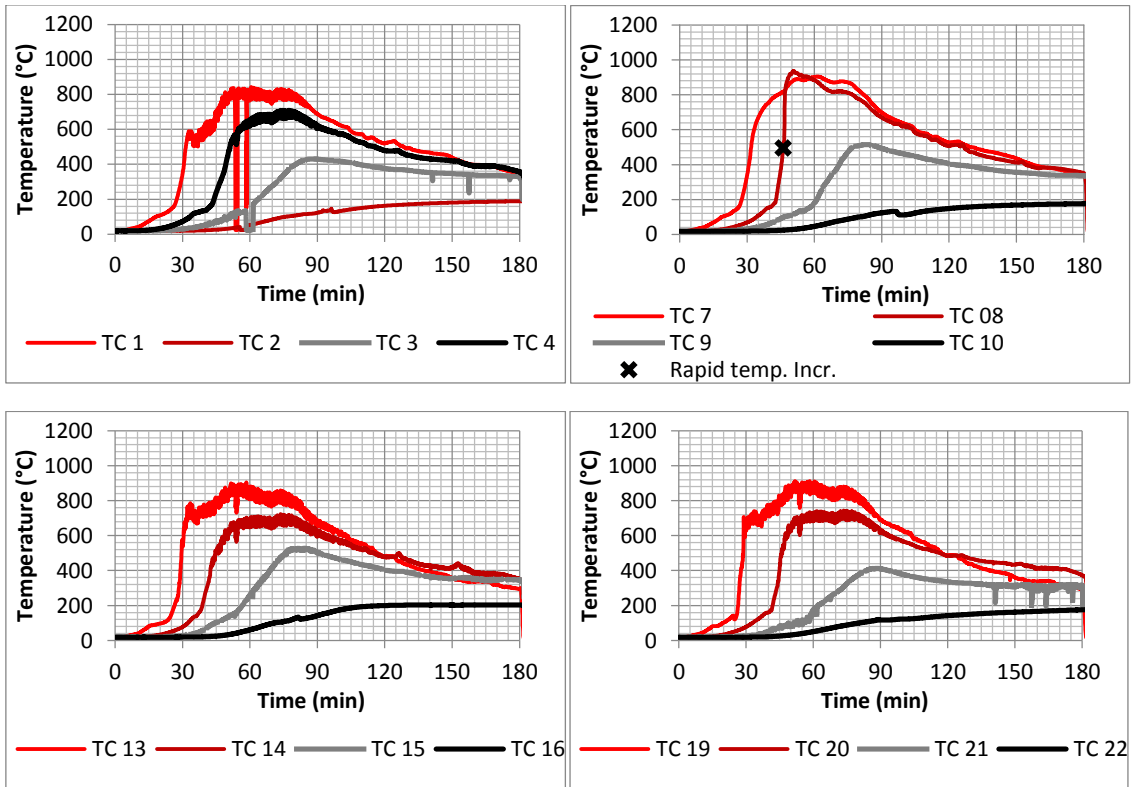


Figure 12: CLT temperatures at 20, 35, 50 and 70mm depth at four locations PRF-B

Charring rates were determined from four thermocouple sets assuming that wood turns into char at 300°C (Buchanan, 2001). For the determination of charring rates, only the thermocouples positioned parallel to the isotherms were considered, in order to avoid erroneous results. 300°C was measured in all thermocouples at 50mm depth, but not at 70mm depth. Figure 13 shows the depth of the char layer during the test based on temperature measurements. Additionally, the average and the maximum char depths measured after the test are indicated. The measured charring depth suggests that the charring rate sharply reduces after approximately 70 minutes, which is approximately when the decay phase starts. The results of the four char depth measurements with a resistograph are shown in Table 4.

Table 5 shows the measured properties related to the mass loss of dry timber and the estimated total heat release of the CLT.

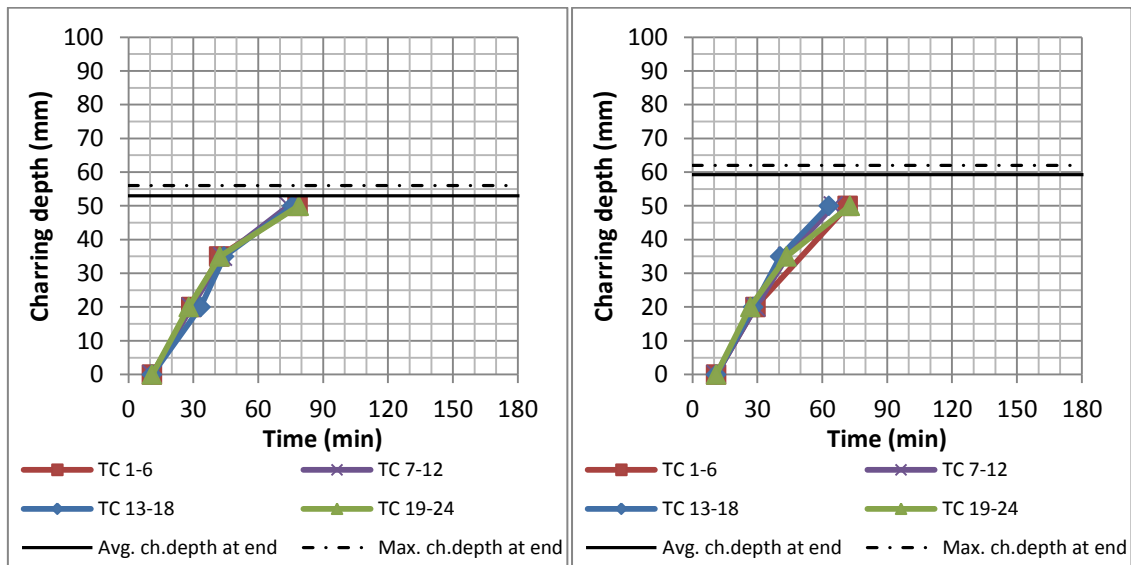


Figure 13: Charring depth during and at the end of PRF-A (left) and PRF-B (right)

Table 4 Charring depths at the end of the test

Charring depth (mm)	PRF-A	PRF-B
Measurement 1	56	61
Measurement 2	49	61
Measurement 3	51	53
Measurement 4	56	62
Average	53	59

Table 5 Mass loss and total heat release per square meter

Test name	Estimated char depth (mm)	Initial dry weight per surface area (kg/m ²)	Mass loss of dry timber per surface area (kg/m ²)	Percentage of mass of dry timber lost	Estimated heat release(MJ/m ²) for 100% combustion efficiency
PRF-A	53	80.7	22.2	28%	416
PRF-B	59	80.8	21.7	27%	408

2.6.2 Tests MF-A and MF-B

Results of the two tests with a Melamine Urea Formaldehyde (MF), MF-A and MF-B are shown in this sub-section.

Figure 14 shows the average plate thermometer temperature together with the target temperature. Figure 15 shows the measured oxygen concentration together with the target oxygen concentration for the duration of the test. No complications arose for the control of the temperature and oxygen content.

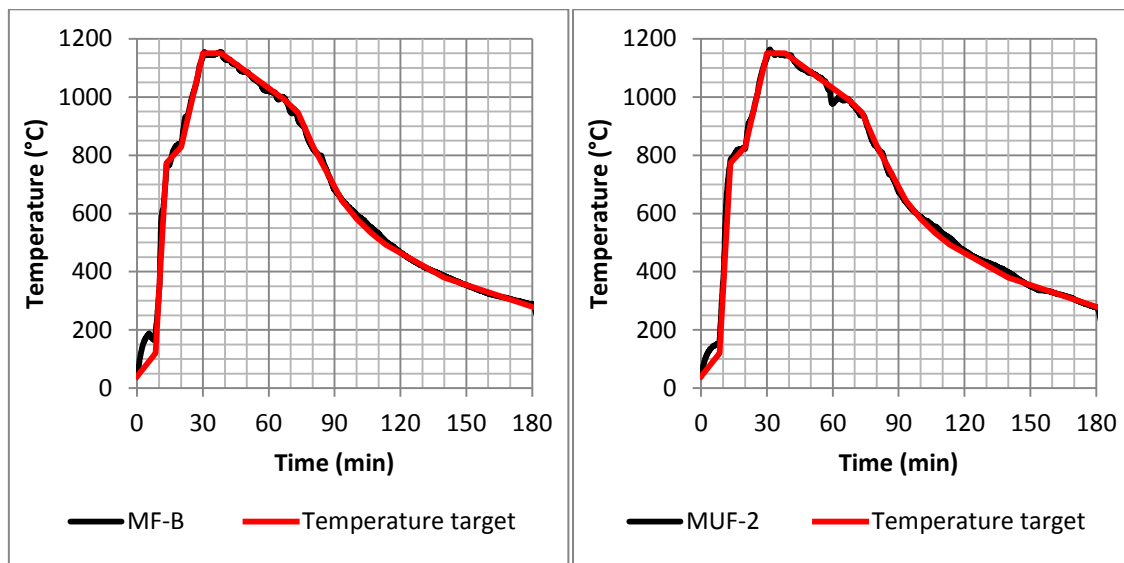


Figure 14: Average temperature measured by the plate thermometers of MF-A (left) and MF-B (right)

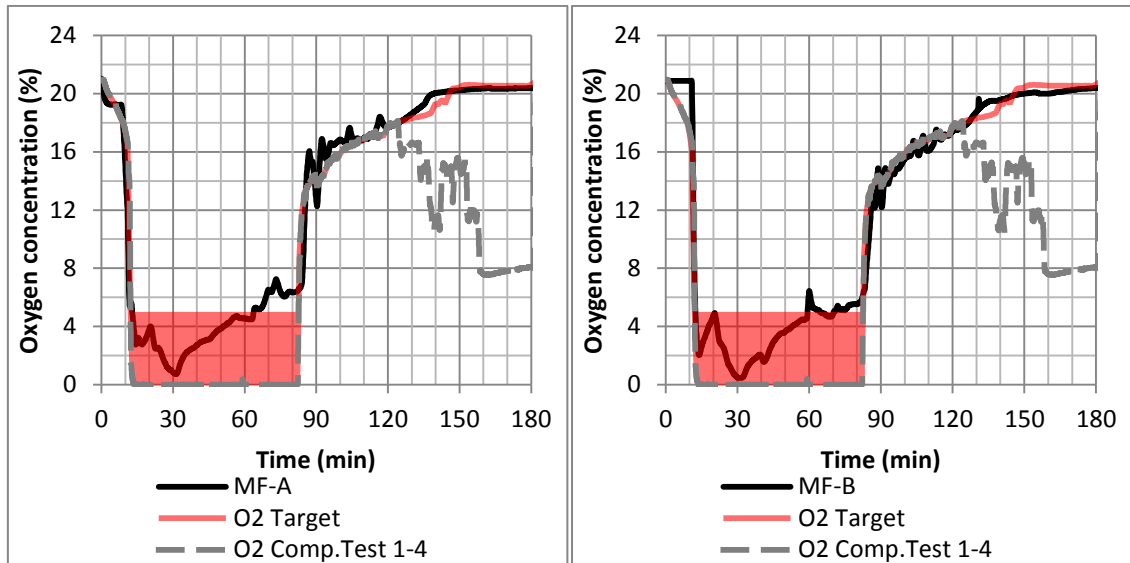


Figure 15: Oxygen concentration of MF-A (left) and MF-B (right)

Figure 16 and Figure 17 show the CLT temperatures at 20, 35, 50 and 70mm from the exposed surface. As explained previously, the thermocouples of these series were positioned parallel to the isotherms. According to the criteria specified in Section 2.3, there is no indication of delamination given by the thermocouples of MF-A. There is, however, one thermocouple in MF-B, TC 8, showing a temperature increase exceeding $100^{\circ}\text{C}/\text{min}$, at the time indicated in Figure 16. The video camera filming approximately half of the specimen's surface, however, did not record delamination at that time. The video of MF-A did not show any falling char. The video of MF-B showed a only small area of char falling at approximately 40 minutes. It should be noted that the camera was replaced during MF-B, which took approximately 15 minutes (at 50 to 62 minutes), potentially missing video evidence of falling char. However, there was no evidence found of additional char falling after the new camera was installed. Relevant frames of the video can be found in Appendix I.

Charring rates were determined in a similar way as was done for tests that were already discussed in sub-section 2.6.1. 300°C was measured in all thermocouples at 50mm depth, but it was not measured at 70mm depth. Figure 18 shows the depth of the char layer during the test based on temperature measurements. Additionally, the average and the maximum char depths measured after the test are indicated. The measured char depth suggests that the charring rate sharply reduces after approximately 70 minutes, which is approximately when the decay phase starts. The results of the four char depth measurements with a resistograph are shown in Table 6.

Table 7 shows the measured properties related to the mass loss of dry timber and the estimated total heat release of the CLT assuming a heat of combustion of $18.75 \text{ MJ}/\text{kg}$ for dry timber.

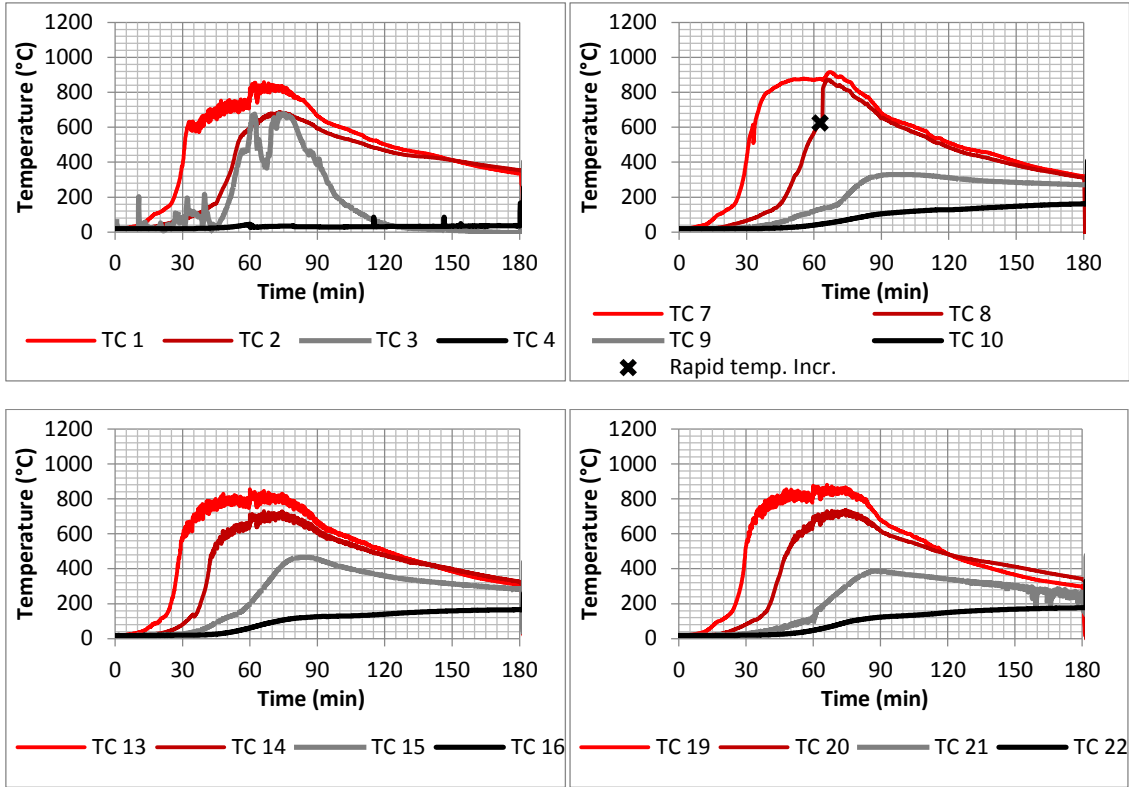


Figure 16: CLT temperatures at 20, 35, 50 and 70mm depth at four locations MF-A

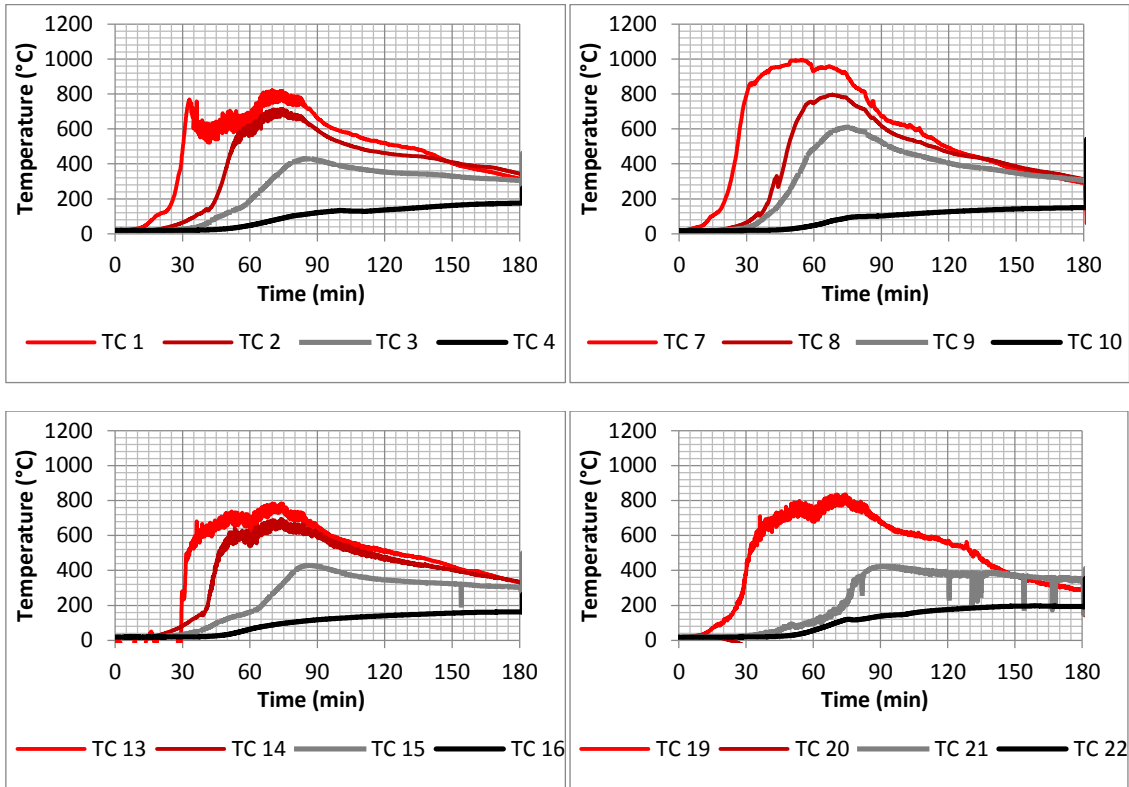


Figure 17: CLT temperatures at 20, 35, 50 and 70mm depth at four locations MF-B

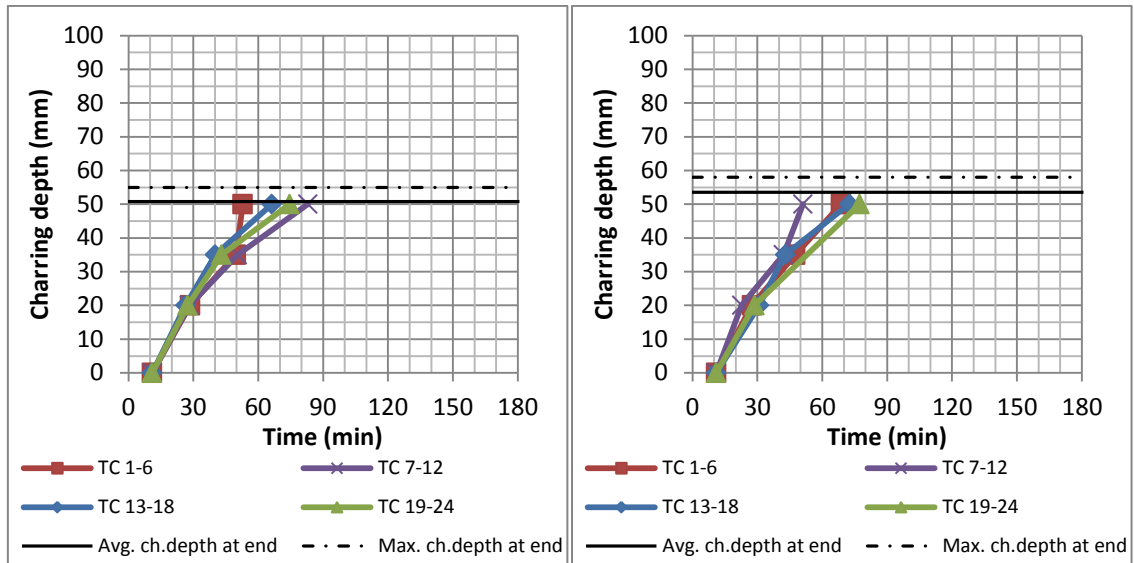


Figure 18: Charring depth during and at the end of MF-A (left) and MF-B (right)

Table 6 Charring depths at the end of the test

Charring depth (mm)	MF-A	MF-B
Measurement 1	46	53
Measurement 2	53	58
Measurement 3	55	52
Measurement 4	49	51
Average	51	54

Table 7 Mass loss and total heat release per square meter

Test name	Estimated char depth (mm)	Initial dry weight per surface area (kg/m ²)	Mass loss of dry timber per surface area (kg/m ²)	Percentage of mass of dry timber lost	Estimated heat release (MJ/m ²) for 100% combustion efficiency
MF-A	51	81.8	21.8	27%	408
MF-B	54	82.5	22.0	27%	412

2.6.3 Tests EPI-A and EPI-B

Results of the two tests with Emulsion Polymer Isocyanate (EPI) adhesive are summarized in this sub-section.

Figure 14 shows the average plate thermometer temperature together with the target temperature. Figure 20 shows the measured oxygen concentration together with the target oxygen concentration for the duration of the test. No complications arose for the control of the temperature and oxygen content.

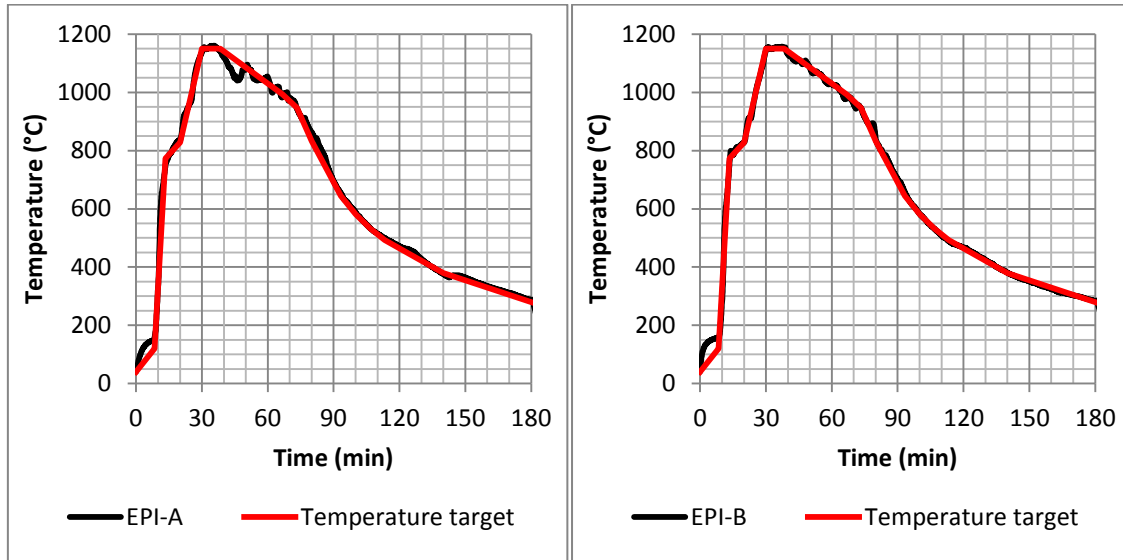


Figure 19: Average temperature measured by the plate thermometers of EPI-A (left) and EPI-B (right)

Figure 21 and Figure 22 show the CLT temperatures at 20, 35, 50 and 70mm from the exposed surface, measured using thermocouples that were positioned parallel to the isotherms. According to the criteria specified in 2.3, there is no indication of delamination given by the thermocouples of EPI-A and EPI-B. However, char fall-off was seen in the video of EPI-B at a relatively late stage. First, falling of small parts of a charred lamella was observed between 68 and 90 minutes into the test. After approximately 90 minutes, a significant part of a charred lamella fell into the furnace, as can be seen in the frames of the video in Figure 23. This char fall-off, however, did not seem to influence the temperatures in the furnace significantly and no adjustments had to be made to follow the target oxygen concentration and temperature. The char fall-off took place 40 to 60 minutes after the char line had surpassed the bond line, thereby distinguishing it from a delamination, in which a bond line fails before the char front surpasses it. At this stage the 300°C isotherm had surpassed all thermocouples at 50mm depth, indicating that there was a char layer with a thickness of at least 15mm in the second lamella. The bond line temperature was approximately 600°C, which was less than 100°C lower than the fire temperature at that point. Therefore, surface temperatures of the newly exposed second lamella did not increase as rapidly as seen in other tests of this study. The video of EPI-A showed only minor falling of char at approximately 1:13 h. Frames of that video can be found in Appendix I.

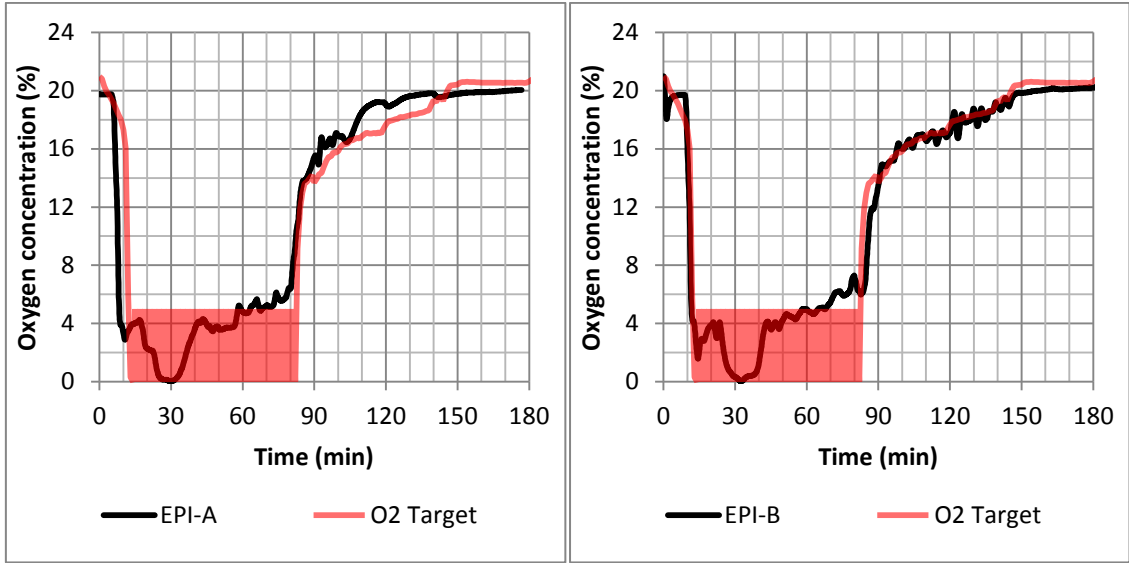


Figure 20: Oxygen concentration of EPI-A (left) and EPI-B (right)

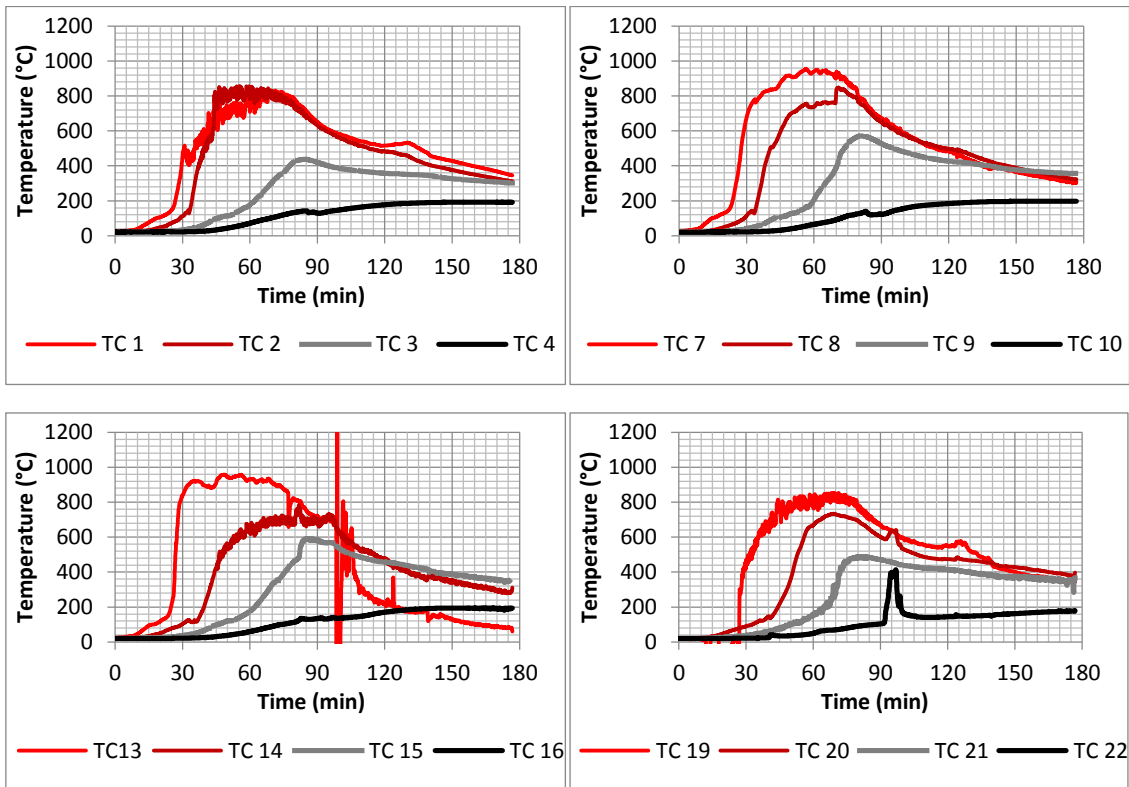


Figure 21: CLT temperatures at 20, 35, 50 and 70mm depth at four locations EPI-A

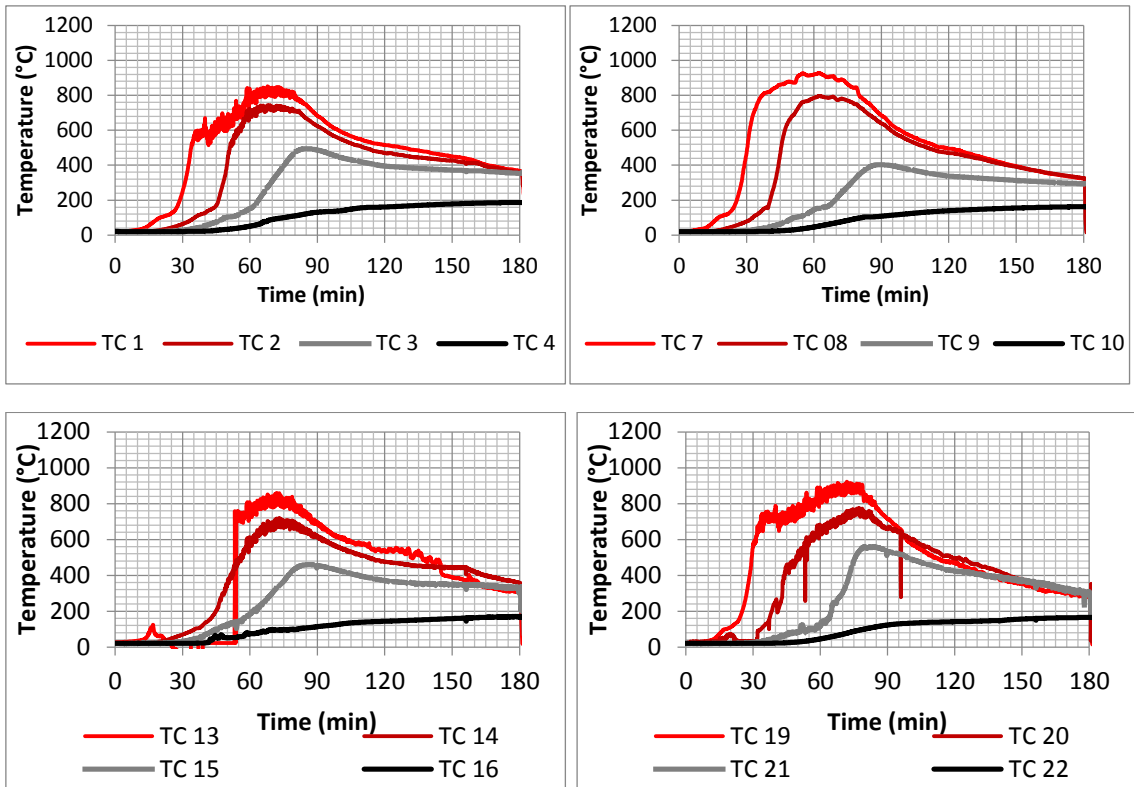
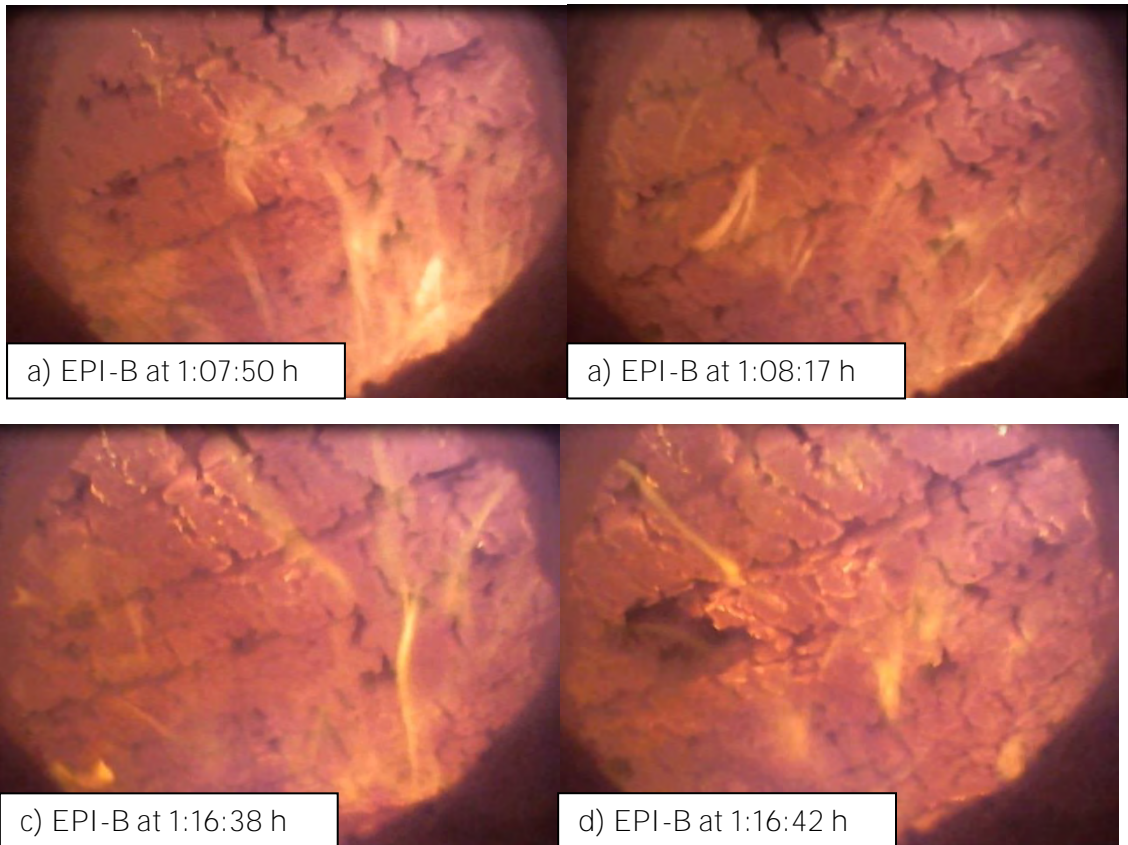


Figure 22: CLT temperatures at 20, 35, 50 and 70mm depth at four locations EPI-B



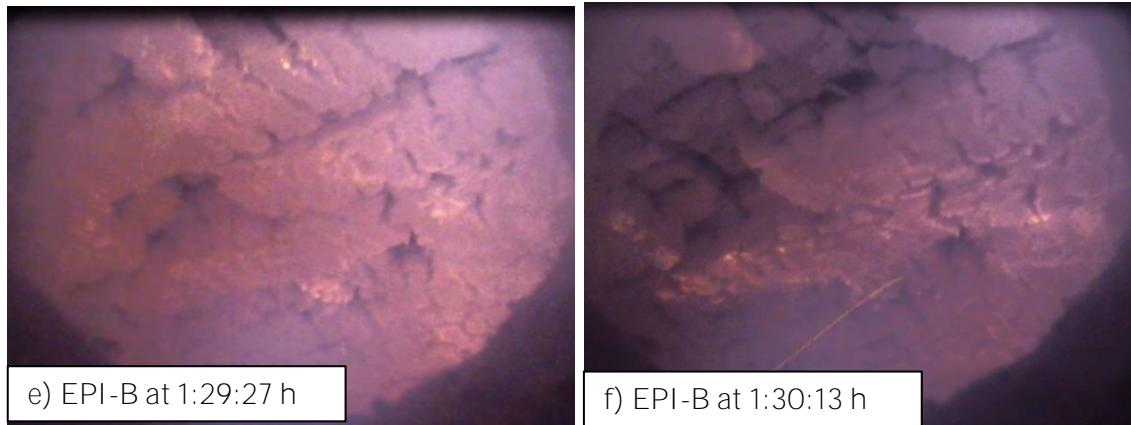


Figure 23: Frames of the video showing times and locations of falling parts.

Charring rates were determined in a similar way as was done for tests that were already discussed earlier in this report. 300°C was measured in all thermocouples at 50mm depth, but it was not measured at 70mm depth. Figure 24 shows the depth of the char layer during the test based on temperature measurements. Additionally the average and the maximum char depths measured after the test are indicated. The measured charring depth suggests that the charring rate sharply reduces after approximately 70 minutes, which is approximately when the decay phase starts. The results of the four char depth measurements with a resistograph are shown in Table 6.

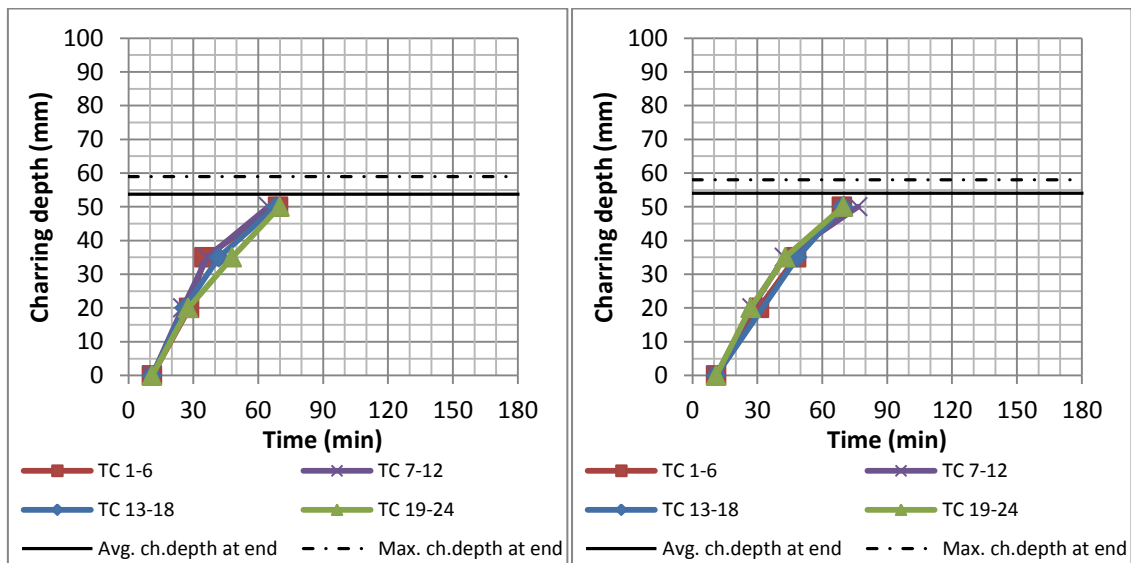


Figure 24: Charring depth during and at the end of EPI-A (left) and EPI-B (right)

Table 9 shows the mass loss of dry timber and the estimated total heat release of the CLT. The heat release was estimated assuming a heat of combustion of 18.75 MJ/kg for dry timber and a combustion efficiency of 1.0.

Table 8 Charring depths at the end of the test

Charring depth (mm)	EPI-A	EPI-B
Measurement 1	59	51
Measurement 2	49	58
Measurement 3	50	52
Measurement 4	57	55
Average	54	54

Table 9 Mass loss and total heat release per square meter

Test name	Estimated char depth (mm)	Initial dry weight per surface area (kg/m ²)	Mass loss of dry timber per surface area (kg/m ²)	Percentage of mass of dry timber lost	Estimated heat release(MJ/m ²) for 100% combustion efficiency
EPI-A	54	81.1	24.6	30%	462
EPI-B	54	83.4	26.2	31%	492

2.6.4 Tests PU1-A and PU1-B

Tests PU1-A and PU1-B consist of the same CLT that was used in full scale Compartment Test 1-4 (Su et al., 2017). In contrast with the other specimens, this CLT is commercially produced. The aim of these two tests is to validate the testing method, by comparing results of Compartment Test 1-4 with results of the presented intermediate scale furnace tests. For this, the measured incident radiant heat flux, temperatures inside the specimens, charring depths, heat release and times of delamination are compared in Section 2.8. The results of PU1-A and PU1-B will be summarised in this sub-section.

The plate thermometer temperatures of test PU1-A and PU1-B are shown in Figure 25. The oxygen measurements of both tests are shown in Figure 26. In both tests delamination of the exposed layer occurred during the fully developed phase of the fire. As a consequence of this, the oxygen concentration dropped to zero percent after approximately 50 minutes. Similar to the other tests discussed in this section, the burners were shut off during the decay phase. However, due to delamination of the second layer of lamellas, the temperatures increased naturally in PU1-A at approximately 2:30h. After delamination of the exposed layer, the oxygen content could not be controlled to the same level of accuracy, as was done in the tests of other specimens.

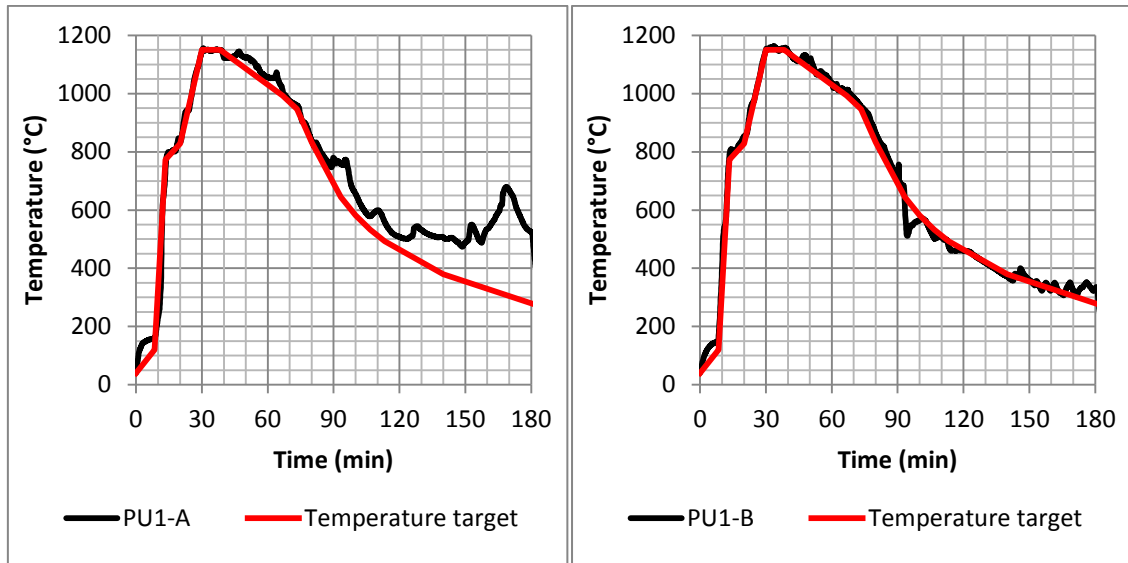


Figure 25: Average temperature measured by the plate thermometers of PU1-A (left) and PU A2 (right)

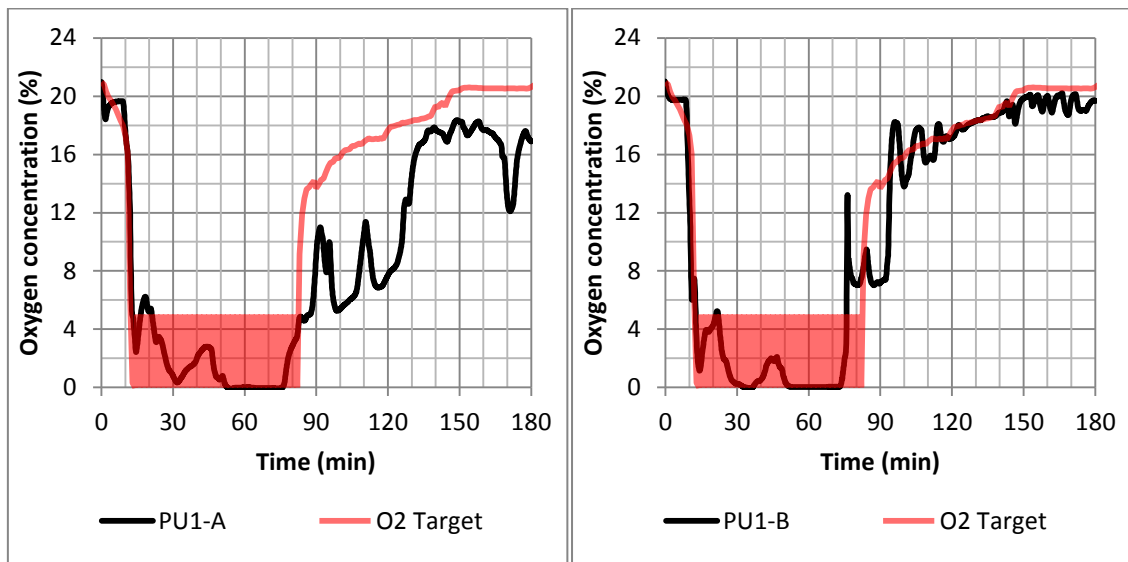


Figure 26: Oxygen concentration of PU1-A (left) and PU A2 (right)

Temperatures measured with thermocouples positioned parallel to the grain at depths of 20mm, 35mm, 50mm and 70mm are shown in Figure 27 and Figure 28 for specimens PU1-A and PU1-B, respectively. According to the criteria specified in Section 2.3, a sudden temperature rise measured by multiple thermocouples indicated delamination. The time and temperature corresponding to these steep temperature rises are shown in the figures. For test PU1-A thermocouples TC4 and TC8 are not considered for the determination of delamination times, as the measurements indicated a defect of the thermocouples. Additional thermocouples positioned perpendicular to the isotherms also showed sudden increases of temperatures inside the lamellas and bond lines (as will be seen further in this report in Section 2.8.2). The measurements indicated that delamination of the first layer occurred after 45 to 65 minutes and delamination of the second layer started at approximately 140 minutes. In test PU1-B only two thermocouples indicated delamination of the second layer, indicating there was only partial delamination of this layer in this test.

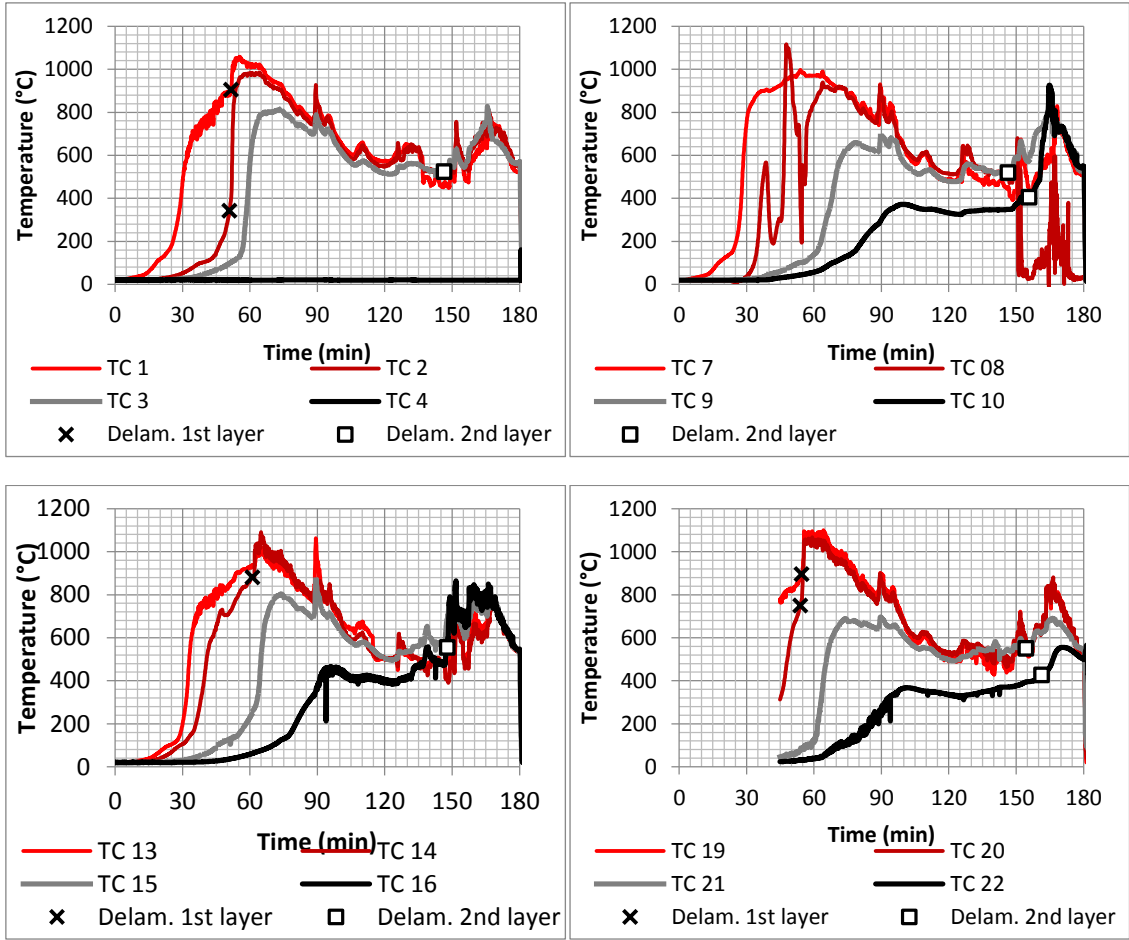
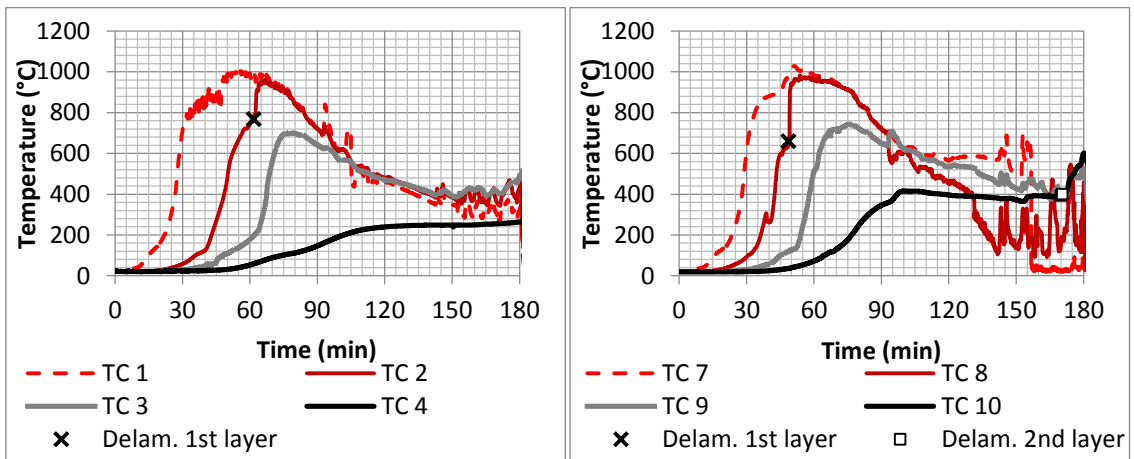


Figure 27: Temperatures measured in the first two plies of specimen PU1-A and in the bond lines of these plies and an indication of delamination according to specified criteria



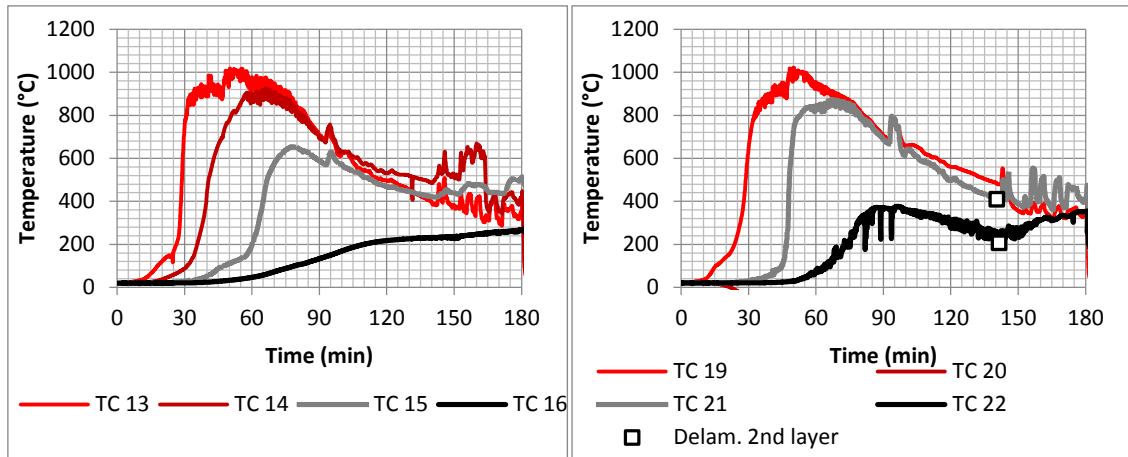


Figure 28: Temperatures measured in the first two plies of specimen PU1-B and in the bond lines of these plies and an indication of delamination according to specified criteria

Video recordings showed clear delamination during tests PU1-A and PU1-B. At 50:55min of PU1-A the first part of a lamella visibly fell into the furnace (see Figure 29 b). At this period smoke developed rapidly in the furnace, due to lack of oxygen. This smoke development was not seen in tests with CLT of other adhesives. At 51:37 a large part of the exposed layer fell into the furnace (see Figure 29 c) and within a few seconds the furnace was filled with thick smoke, which made it not possible to see the specimen until the decay phase (see Figure 29 d).

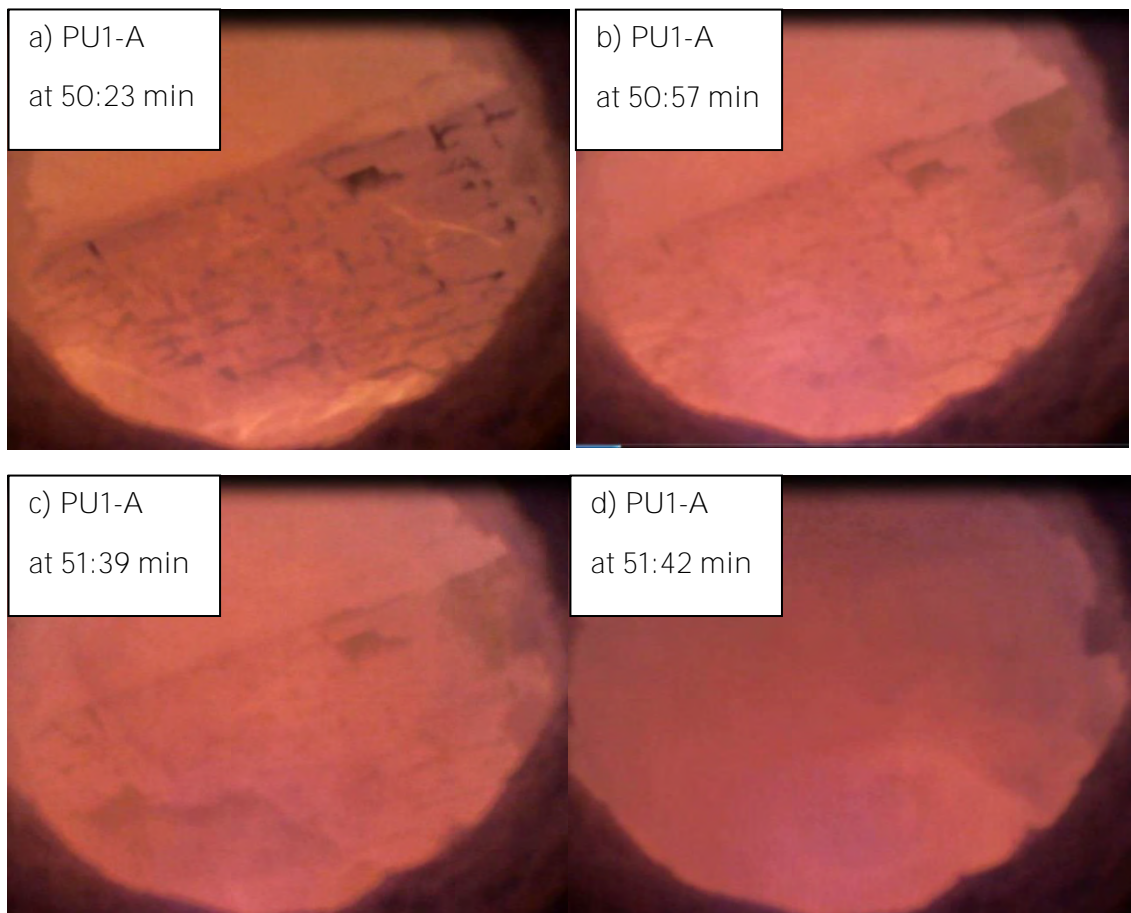


Figure 29: Photos of the exposed surface in test PU1-A during delamination of the exposed ply

The only light in the furnace was emitted by the burning specimen. During the decay phase of the fire, the video screen became dark and an increase of light indicated an increased amount of combustion (Figure 30a). Flaming on the surface was observed at 2:30h during PU1-A (Figure 30b). Due to the flames, falling of the lamella could not be seen in the video. However, it could be seen that a part of the second layer was still in place at 2:38h (Figure 30c). At 2:44h the intensity of the flames increased, indicating that a significant part of the third layer of lamellas became exposed.



Figure 30: Photos of the exposed surface in test PU1-A during delamination of the second ply

The video of PU1-B showed part of the exposed layer of lamellas falling at 42:30 min and 2 seconds later at 42:32 min (Figure 31b-c). At 47:30min another significant part of the first layer fell (Figure 31d), which was quickly followed by the development of thick smoke in the furnace (Figure 31e).

In the decay phase of PU1-B, visible glowing started after approximately 2:30 hours (Figure 32a). Visible flames were observed at 2:36h (Figure 32b), however, the source of the flames was outside of the visible area. At 2:48h partial delamination was observed, causing a short flash of light (Figure 32c). However, no sustained flaming was observed. At 2:53h another flash of light was observed coming from location that was not visible by the camera (Figure 32d) and no additional evidence of delamination was seen until the end of the test.

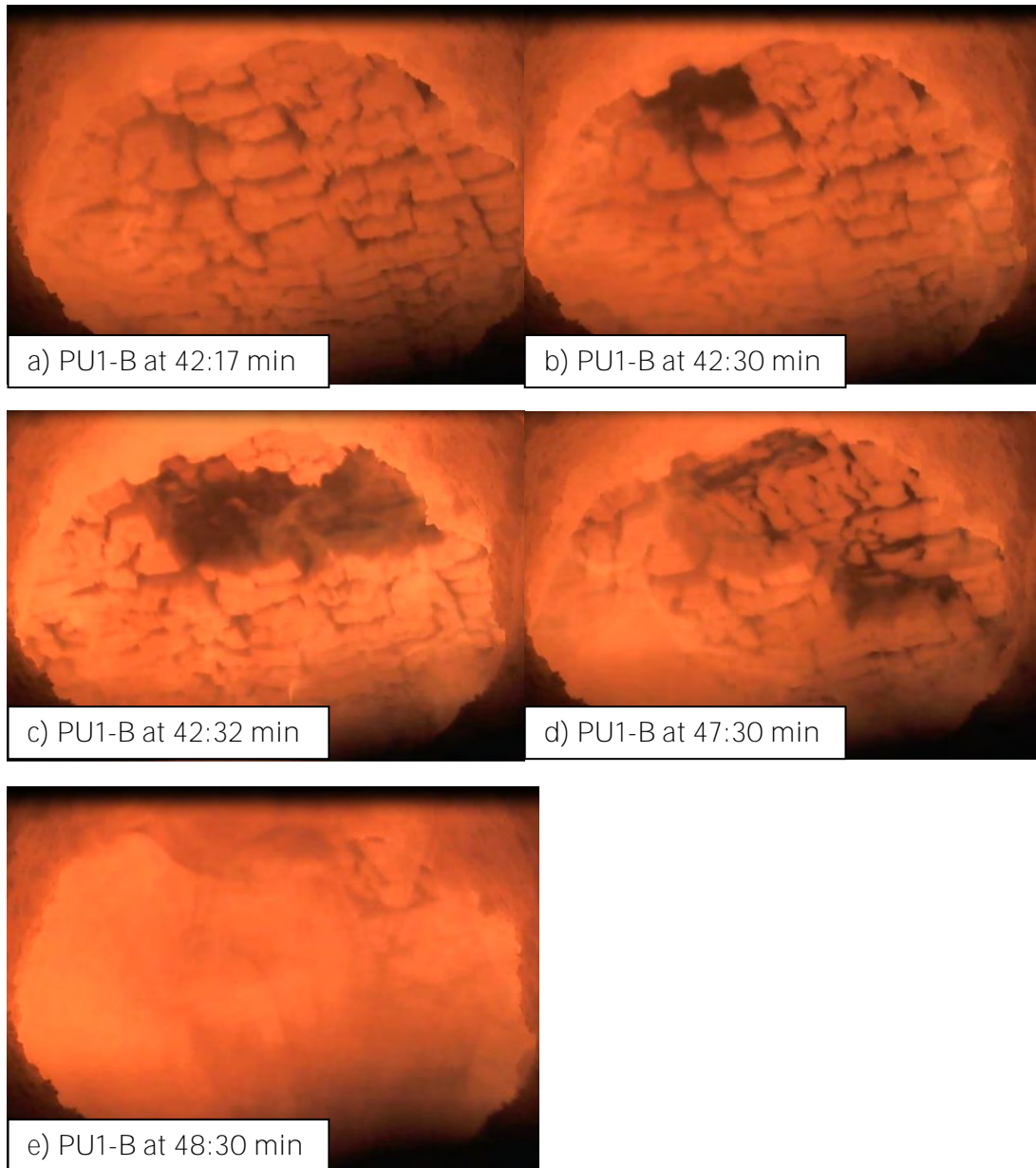
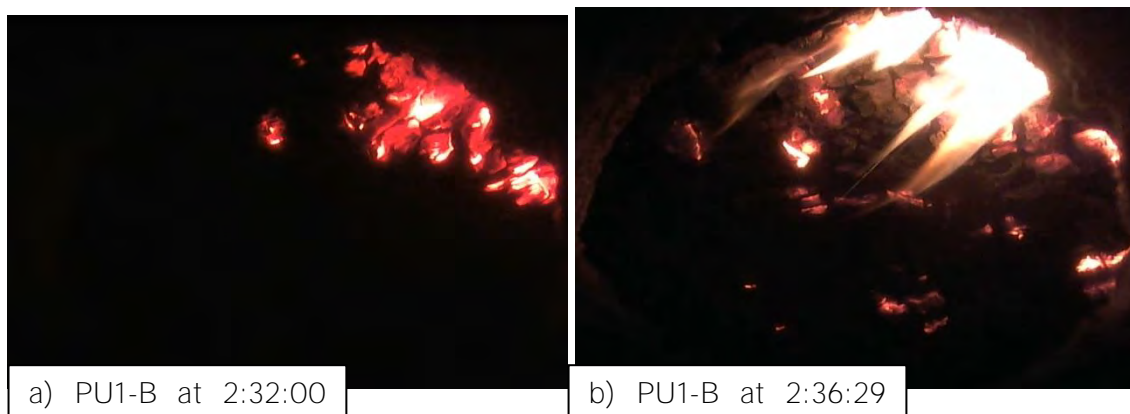


Figure 31: Photos of the exposed surface in test PU1-B during delamination of the exposed ply



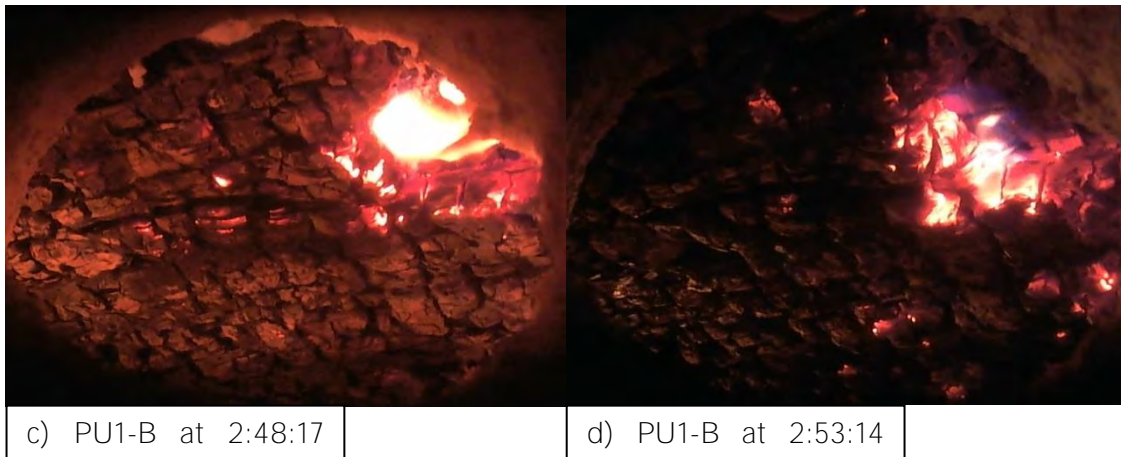


Figure 32: Photos of the exposed surface in test PU1-B during delamination of the second ply

The thickness of the char layer was estimated using the char temperature of wood of approximately 300°C. The char depth during the test was determined using the four sets of thermocouples positioned parallel to the isotherms. Figure 33 shows the determined charring depths corresponding PU1-A and PU1-B. In PU1-A the 300°C isotherm reached three out of four thermocouples at a depth of 87mm at the end of the test. This corresponds well with the charring depths measured at the end of the test (see Table 10), indicating that the thermocouples that were positioned parallel to the isotherm accurately measured the temperatures. In PU1-B the 300°C isotherm only reached two out of four thermocouples in the second bond line.

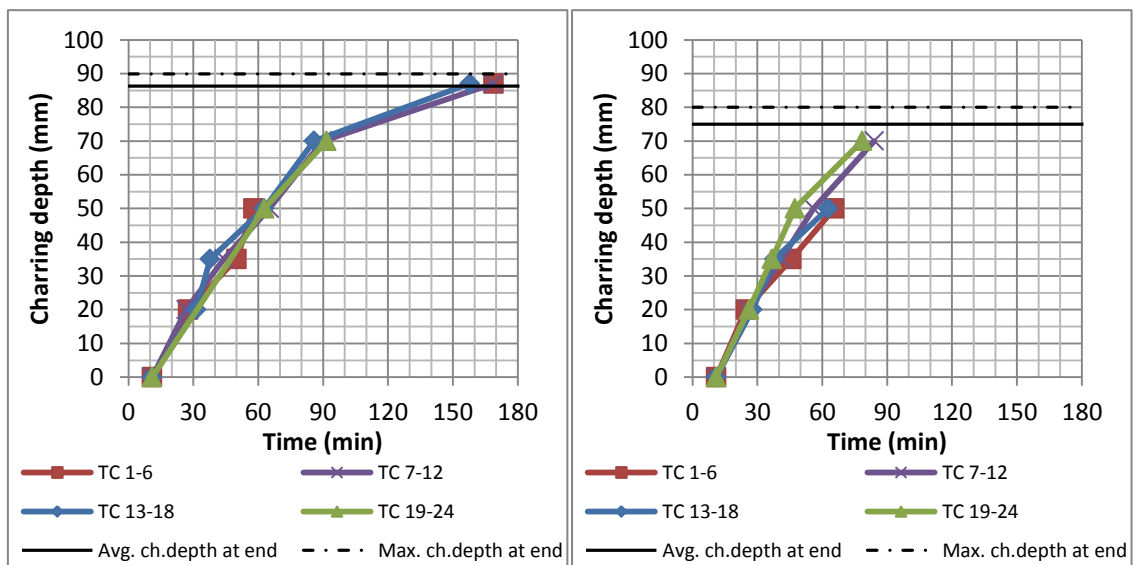


Figure 33: Charring depth during PU1-A (left) and PU1-B (right)

Table 10 Charring depths

Charring depth	PU1-A (mm)	PU1-B (mm)
Measurement 1	87	74
Measurement 2	88	72
Measurement 3	81	74
Measurement 4	90	80
Average	86	75

Table 11 shows the mass loss of dry timber and the estimated total heat release of the CLT. The heat release was estimated assuming a heat of combustion of 18.75 MJ/kg for dry timber (Krajnc, 2015).

Table 11 Mass loss and total heat release per square meter

Test name	Estimated char depth (mm)	Initial dry weight per surface area (kg/m ²)	Mass loss of dry timber per surface area (kg/m ²)	Percentage of mass of dry timber lost	Estimated heat release(MJ/m ²) for 100% combustion efficiency
PU1-A	86	79.6	34.6	44%	650
PU1-B	75	78.7	32.0*	41%*	599*

0.8 kg lamella's that fell 2 minutes after the test was stopped is included in the mass loss

2.6.5 Tests PU2-A and PU2-B

The two tests with the additional one-component Poly Urethane (PU2) adhesive are referred to as PU2-A and PU2-B in this report. This section shows the results of these two tests.

Figure 34 shows the average plate thermometer temperature together with the target temperature. Figure 35 shows the measured oxygen concentration together with the target oxygen concentration for the duration of the test. No complications arose for the control of the temperature and oxygen content.

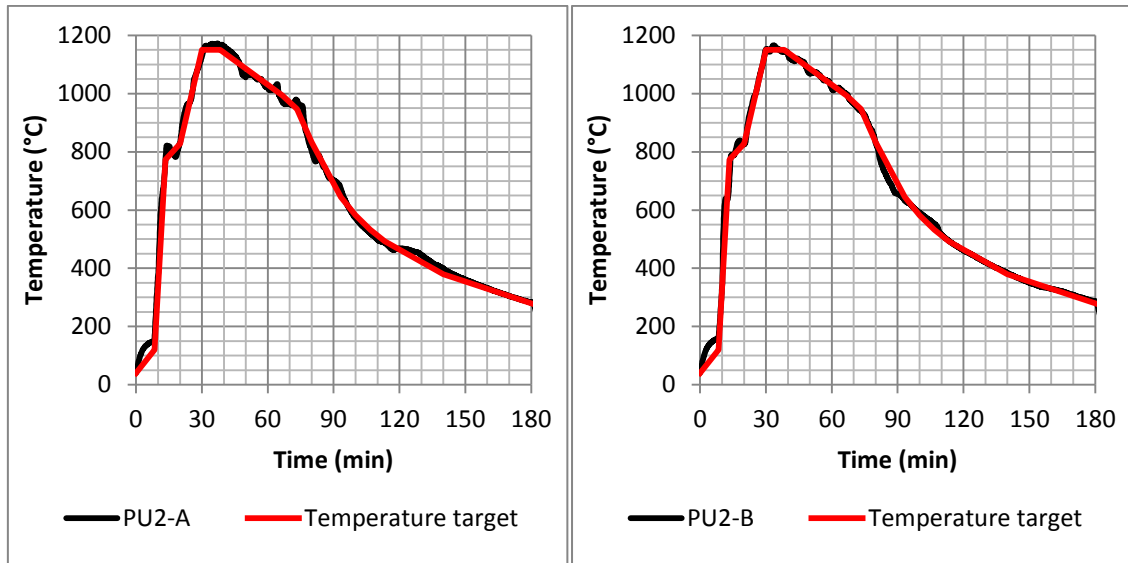


Figure 34: Average temperature measured by the plate thermometers of PU2-A (left) and PU2-B (right)

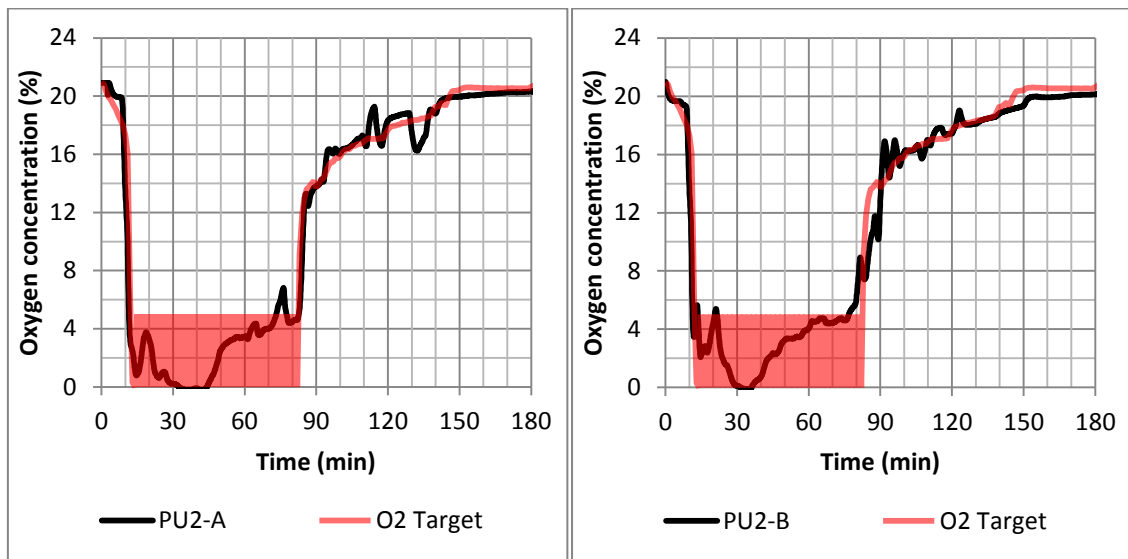


Figure 35: Oxygen concentration of PU2-A (left) and PU2-B (right)

Figure 36 and Figure 37 show the CLT temperatures at 20, 35, 50 and 70mm from the exposed surface, measured using thermocouples that were positioned parallel to the isotherms. Thermocouples TC15 of PU2-A and TC 3 and 7 of PU2-B were disregarded as they show clear signs of malfunction. The temperature jumps measured by TC 14, 15, 16 and 22 were likely caused by an electrical disturbance in one of the data loggers. The temperature jumps were seen at exactly the same time in measurements made with the same data logger. Therefore, measurements from these thermocouples are not considered for the determination of delamination. According to the criteria specified in 2.3, there is no indication of delamination given by the thermocouples of PU2-A and PU2-B. **The video camera filming approximately half of the specimen's surface did also not record delamination during the test.** The videos of PU2-A and PU2-B showed no signs of delamination. Frames of the videos can be found in Appendix I.

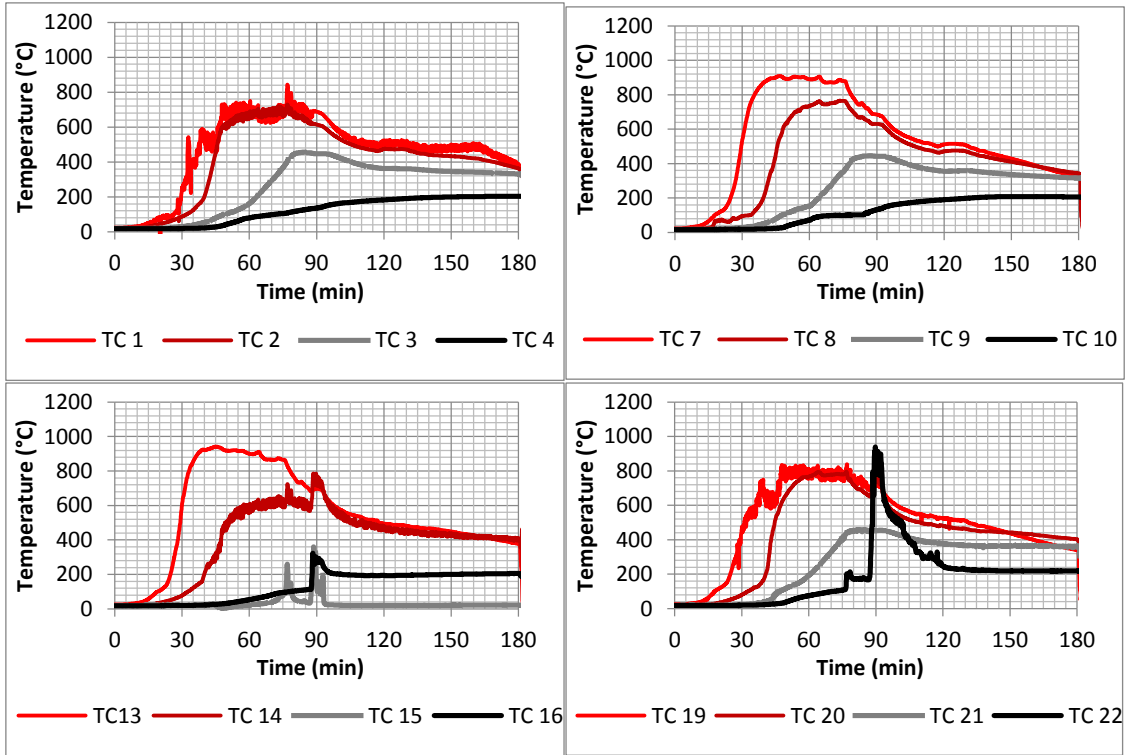


Figure 36: CLT temperatures at 20, 35, 50 and 70mm depth at four locations PU2-A

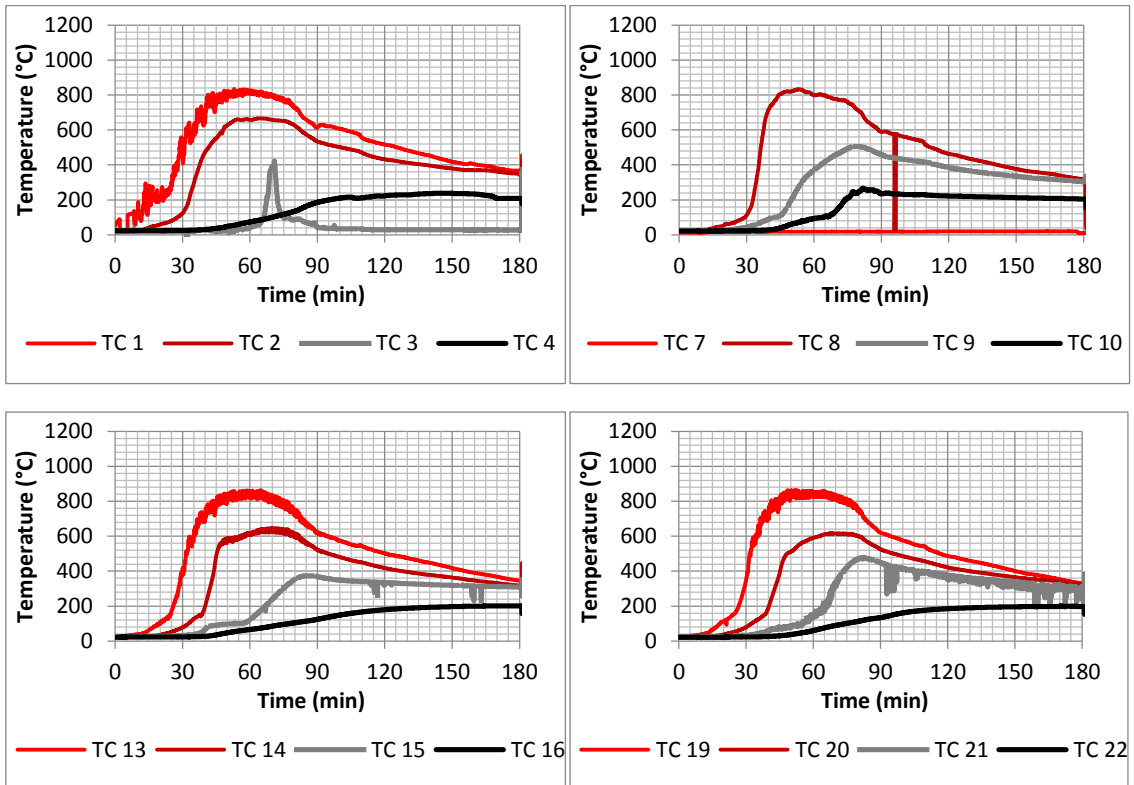


Figure 37: CLT temperatures at 20, 35, 50 and 70mm depth at four locations PU2-B

Charring rates were determined in a similar way as was done for tests that were already discussed earlier in this report. 300°C was measured in all thermocouples at 50mm depth, but it was not measured at 70mm depth. Figure 38 shows the depth of the char layer during the test based on temperature measurements. Additionally, the average and the maximum char depths measured after the test are indicated. The measured charring depth suggests that the charring rate sharply reduces after approximately 70 minutes, which is approximately when the decay phase starts. The results of the four char depth measurements with a resistograph are shown in Table 6.

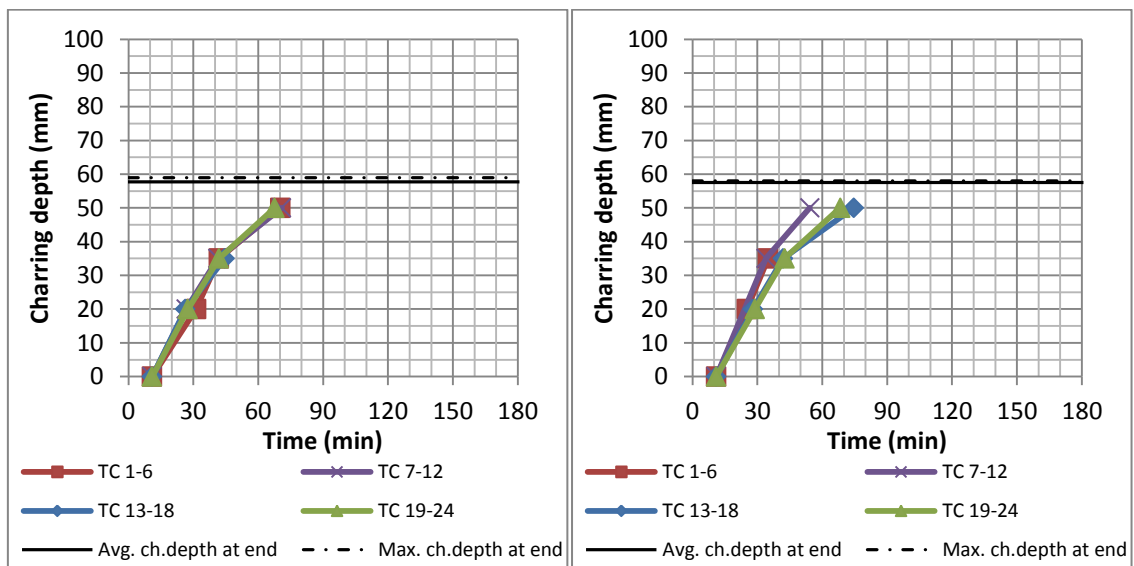


Figure 38: Charring depth during and at the end of PU2-A (left) and PU2-B (right)

Table 12 Charring depths at the end of the test

Charring depth (mm)	PU2-A	PU2-B
Measurement 1	58	58
Measurement 2	57	58
Measurement 3	57	57
Measurement 4	59	57
Average	58	58

Table 13 shows the measured properties related to the mass loss of dry timber and the estimated total heat release of the CLT.

Table 13 Mass loss and total heat release per square meter

Test name	Estimated char depth (mm)	Initial weight surface (kg/m ²)	dry per area	Mass loss of dry timber per surface area (kg/m ²)	Percentage of mass of dry timber lost	Estimated heat release(MJ/m ²) for 100% combustion efficiency
PU2-A	58	80.9		22.6	28%	423
PU2-B	58	82.7		23.3	28%	437

2.7 Adhesive performance

This section shows comparisons of charring behaviour and the mass loss corresponding to the different adhesives tested. Furthermore, critical bond line temperatures of an adhesive prone to delamination are determined.

2.7.1 Char depth

The depth of the char layer can be seen as a measure of fire damage of the CLT panel. Figure 39 shows the average charring depth for each type of adhesive. The data point corresponding to 180 minutes is obtained from char depth measurements after the test. The other data is obtained from measurements of thermocouples that were positioned parallel to the isotherms.

It can be seen that the average charring depth of the PU1 specimens was significantly higher than that of all other specimens. A small difference is already seen at 60 minutes, which was during the delamination phase of the first layer of lamellas. Even though the decay phase started around the same time, the char depth of the PU1 specimens increased significantly after 60 minutes.

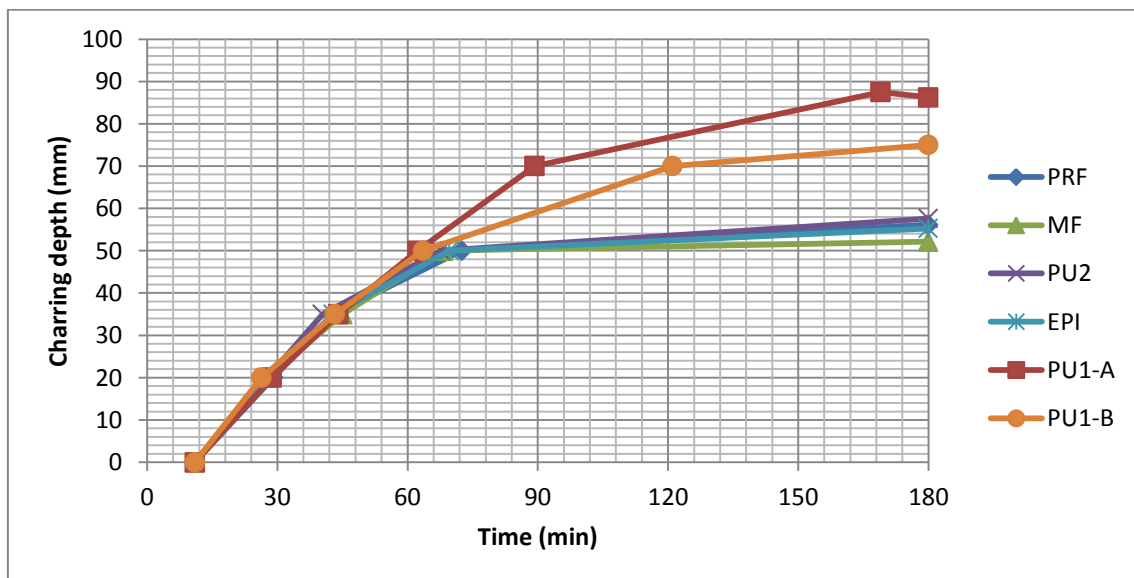


Figure 39: Charring depth throughout tests

Box-plots of the char depth measured using a resistograph are shown in Figure 40. It can be seen that the range of char depths measured in the PRF specimens, correspond to the range of char depths measured in the MF, EPI and PU2 specimens. All char depths measured in PU1 specimens after the test exceeded those of other specimens.

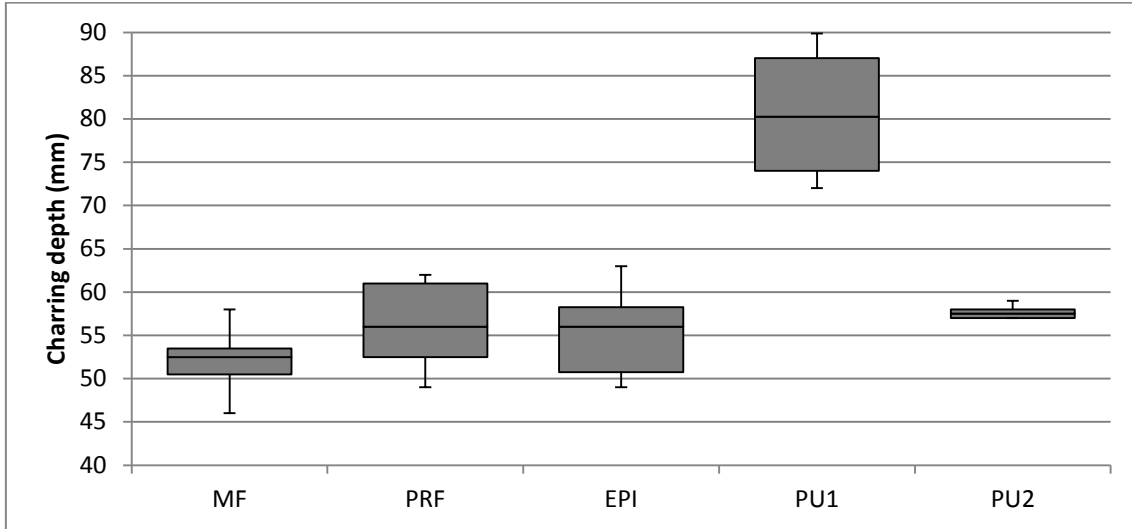


Figure 40: Charring depth at end of test.

2.7.2 Mass loss and heat release

The total mass loss of dry timber per area of exposed surface corresponding to different tests is shown in Figure 41. It can be seen that the specimens that showed clear delamination on the camera recordings (EPI-B; PU1-A and; PU1-B) lost more mass of dry timber during the fire test. The mass loss of PU1-A and PU1-B is, however, significantly higher than that of EPI-B. The heat release can be estimated from the mass loss of the dry timber, by assuming that all falling char and combustibles produced by the burning wood completely combust.

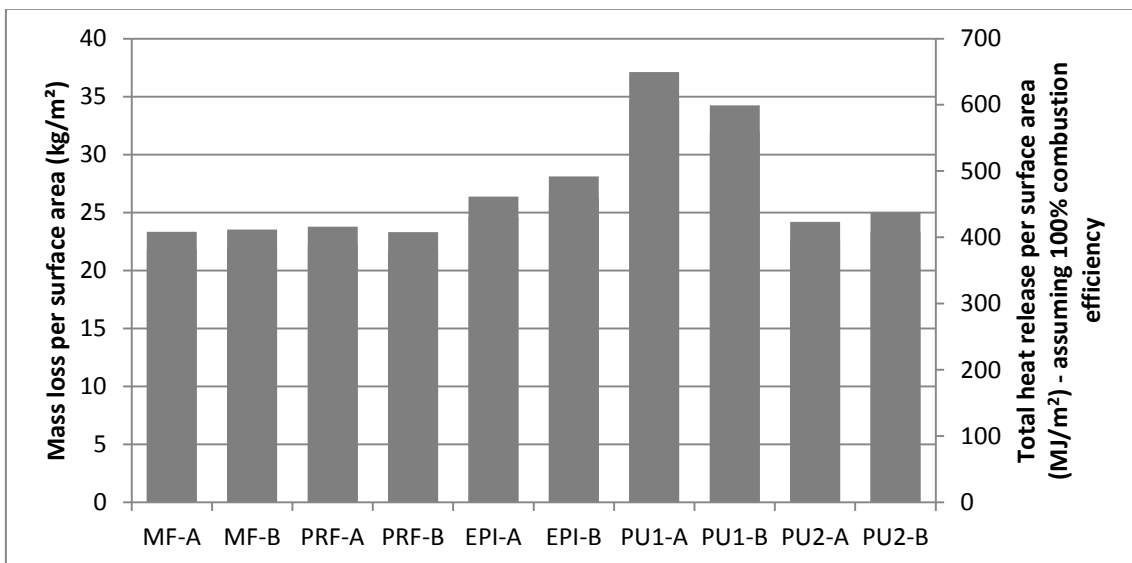


Figure 41: Mass loss of dry timber at end of test.

2.7.3 Summary of signs of delamination

A summary of indications of delamination discussed earlier is given in Table 14. Strong evidence of delamination is shown in bold characters.

Table 14 Indications of delamination

Test name	Temperature & O ₂ & Inc. radiant heat flux	Temperatures in the 1st ply or bond line*	Temperatures in the 2nd ply or bond line*	Char depth	Mass loss & heat release rate	Video camera
PRF-A	No indication	No indication	No indication	No indication	No indication	Small piece of char falls. Approx. surface: 100 cm ²
PRF-B	No indication	1 out of 12 thermocouples showed an accelerated temperature rise	No indication	No indication	No indication	Small piece of char falls. Approx. surface: 25 cm ²
MF-A	No indication	No indication	No indication	No indication	No indication	No indication
MF-B	No indication	1 out of 12 thermocouples showed an accelerated temperature rise	No indication	No indication	No indication	Small piece of char falls. Approx. surface: 100 cm ²
EPI-A	No indication	No indication	No indication	No indication	No indication	No indication
EPI-B	No indication	No indication	No indication	No indication	No indication	Char fall-off observed after 90 minutes. Approx. surface: 450 cm²
PU1-A	Oxygen content automatically dropped to zero during the fully developed phase. Temperatures started to increase at approx. 2:30h because of delamination	7 out of 12 thermocouples showed an accelerated temperature rise	8 out of 10 thermocouples showed an accelerated temperature rise	Significantly increased charring depth**	Significantly increased mass loss and heat release**	Full delamination of the first ply. More than half of the visible surface of the second ply delaminated
PU1-A	Oxygen content automatically dropped to zero during the fully developed phase.	8 out of 12 thermocouples showed an accelerated temperature rise	3 out of 10 thermocouples showed an accelerated temperature rise	Significantly increased charring depth**	Significantly increased mass loss and heat release**	Full delamination of the first ply. Approximately 10% of the visible surface of the second ply delaminated
PU2-A	No indication	No indication	No indication	No indication	No indication	Small piece of char falls. Approx. surface: 25 cm ²
PU2-B	No indication	No indication	No indication	No indication	No indication	No indication

* Sudden increases of local temperature can be related to pieces of char locally falling or the entrance of the fire in cracks already present in the wood.

**Relative to results of PRF-A and PRF-B

2.7.4 Critical bond line temperature

For the development of engineering methods, it is important to know the critical bond line temperature that leads to delamination. From the compartment tests by Su *et al.* (2017) it could not be concluded whether the bond line fails before the char line surpasses the bond line, as only a part of the temperature measurements suggested that bond line temperatures were lower than 300°C. The same was seen in tests PU1-A and PU1-B. To get knowledge of the critical bond line temperature it was chosen to study the distribution of temperatures at which delamination occurs. In order to get as many data as possible, critical temperatures identified in all compartment tests presented by Su *et al.* and in furnace test PU1-A and PU1-B are all used for this analysis.

The critical bond temperature was only determined from temperature measurements in the bond line. The time of delamination and the corresponding bond line temperature was determined as discussed in Section 2.6.4. The distribution of bond line temperatures at the identified moment of delamination is shown in Figure 42. It can be seen that critical temperatures ranged between 200 and 900°C. However, critical temperatures between 200 and 400°C are significantly more frequent. Figure 43 suggests that the critical temperature is also dependent on the duration of the heating process. This figure distinguishes measurements made with thermocouples positioned parallel to the isotherms from measurements made with thermocouples perpendicular to the isotherms. However, both types of measurements indicate that delamination can take place before the bond line is charred and that an assumed critical temperature of 200°C is conservative. The sharp lower limit of the critical temperature could be related to the required performance at 220°C of ANSI/PRG320, which this CLT complies to.

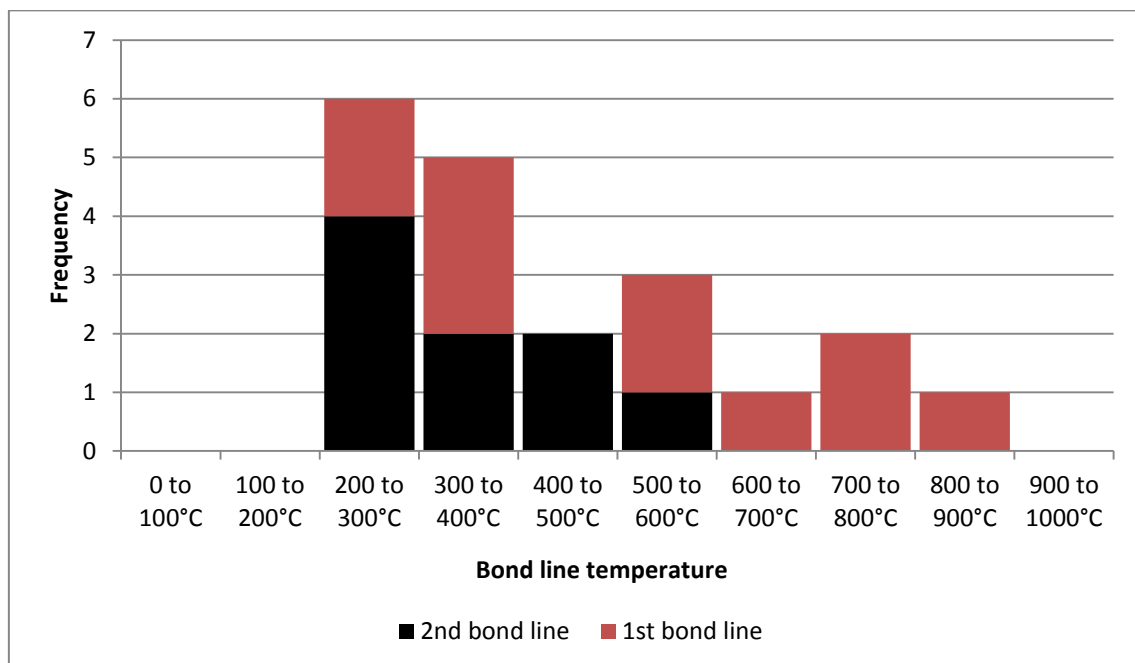


Figure 42: Distribution of bond line temperatures during delamination of the first and second layer in PU specimens and compartment tests.

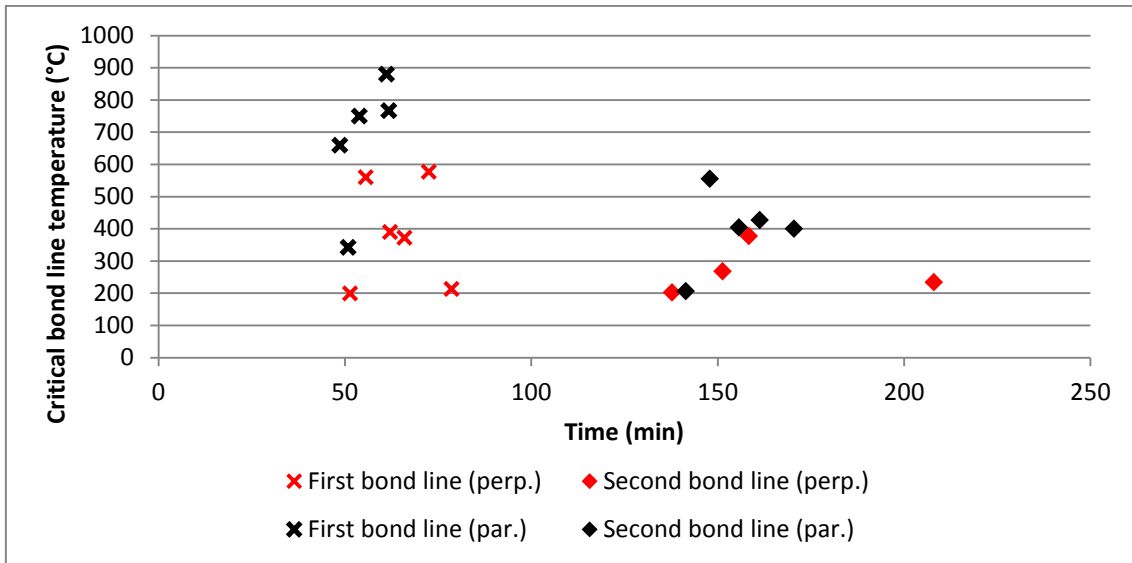


Figure 43: Critical bond line temperature and time of delamination of the first and second layer in PU1 specimens and compartment tests.

Another indication of the temperatures in the bond line can be seen in Figure 44. Delamination of a significant part of second ply occurred after approximately two minutes after the end of test PU1-B. The timber at the bond line is only partially charred, indicating that the temperatures varied from below the charring temperature ($\pm 300^{\circ}\text{C}$) to above the charring temperature.



Figure 44: Specimen of test PU1-B after the test.

2.8 Evaluation of the method

Results of PU1-A and PU1-B are compared with results of Compartment Test 1-4 (Su *et al.*, 2017) for validation of the testing method. As mentioned before, a successful test method should result in comparable material temperatures, char depths, times of delamination and heat release, if the same type of CLT is tested.

2.8.1 Incident heat flux by radiation

The incident heat flux by radiation, calculated from plate thermometer and gas temperature measurements of test PU2-A and PU2-B according to eq.9, is shown together with the incident heat flux determined from Compartment Test 1-4 in Figure 45. The value of the heat flux was calculated assuming convection coefficients of 0 and 25 W/(m²/K), to show that the heat flux by convection to or from the plate thermometer is negligible in this test. As the two curves show a strong resemblance, it is concluded that the calculation is insensitive to deviations of the emissivity and the convection coefficient. This is related to the strong resemblance between the gas temperature (approximated using a thermocouple) and the plate thermometer temperature measured in the furnace.

Concerning a potential error made by approximating the gas temperature using a thermocouple, sensitivity analysis showed that an error of 100°C of the gas temperature measurement, only results in an error of 1.2% of the calculated maximum incident radiant heat flux corresponding to a convection coefficient of 25 W/(m²/K). The low sensitivity for the error of the gas temperature, is related to the insignificance of the convective heat flux in comparison with the radiative heat flux in the high temperatures of the furnace test.

In test PU2-A an additional water cooled heat flux meter was installed as discussed in Section 2.3. The water cooled heat flux meter measures the total heat flux to a surface with a temperature that is low, but usually unknown. For this test a built-in thermocouple was positioned to measure the temperature of the sensor, in order to estimate the convective heat flux. Figure 45 includes heat fluxes measured using the water cooled heat flux gauge corresponding to convection coefficients of 0 and 15W/m²K. Because of the maximum capacity of the heat flux gauge of 200kW/m², the heat flux gauge was removed from the furnace for a period of approximately 35 minutes. The heat fluxes determined with a plate thermometer and a water cooled heat flux gauge were similar for a convection coefficient to the surface of the heat flux gauge of 15W/m²K for the first period until approximately 70 minutes. Later in the decay phase the convection coefficient dropped to approximately zero.

In two instances the incident radiant heat flux of Compartment Test 1-4 exceeded that of PU2-A and PU2-B. The temperatures of Compartment Test 1-4 exceeded the maximum allowed temperature of the furnace for a few minutes. Therefore, the maximum heat flux of the furnace is lower than the maximum heat flux of the compartment test. The second increase of radiant heat flux seen in the compartment test was caused by delamination of the CLT with PU1 adhesive. The incident heat flux by radiation of other tests is given in Appendix II.

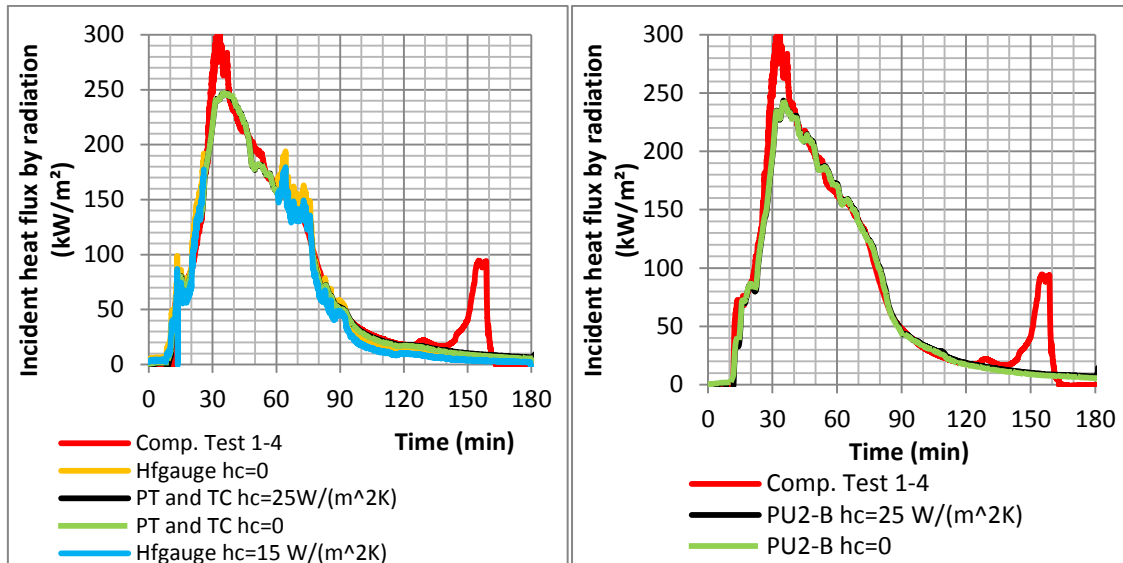


Figure 45: Incident heat flux by radiation of test PU2-A (left) and PU2-A (right)

2.8.2 CLT temperatures

Due to the size of the CLT slabs in Compartment Test 1-4, it was not possible to measure temperatures with thermocouples positioned parallel to the isotherms. For comparisons it was chosen to install extra sets of thermocouples in the same way as was done in Compartment Test 1-4. Figure 46 shows the temperatures corresponding to these thermocouples. Especially in the decay phase the temperatures correspond well with each other. In the heating phase the heating rate at each specified depth varied in different positions of the furnace specimens. However, there is a clear resemblance between the curves of the different tests. In results of, both, the compartment test and the furnace test, a sudden increase was measured at approximately 60 minutes. This jump indicates delamination, which occurred approximately at the same time in all tests with PU1 adhesive. A second temperature increase was seen in Compartment Test 1-4 indicating delamination of the second ply. Although the temperatures deeper in the specimen seemed very similar, this increase was not seen in PU1-B. Localized delamination was witnessed with video recordings and measurements of other sets of thermocouples. However, this delamination was not significant enough to increase the fire temperature significantly. A significant part of the exposed surface delaminated approximately 2 minutes after the test was stopped (Figure 44). Temperatures measured within the CLT of test PU1-A were similar to the temperatures measured in the CLT of Compartment Test 1-4 until the end of the test, indicating that the test successfully replicated relevant fire conditions of the compartment test.

For a comparison, Figure 47 shows temperatures measured in non-delaminating CLT. The sudden increase of temperatures in specimens PU2-A and PU2-B did not occur, indicating that there was no delamination. From approximately 60 minutes, the temperatures of both tests start to deviate. This deviation indicates a difference of performance between PU1 and PU2 specimens. Similar results of other tests are shown in Appendix II. None of the additional results in Appendix II indicated delamination.

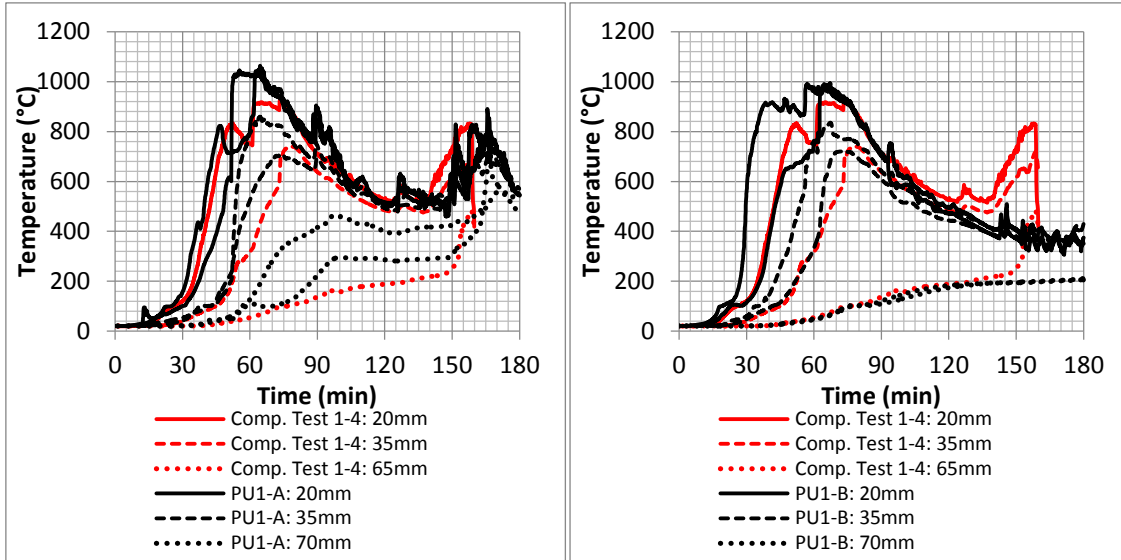


Figure 46: temperatures of PU1-A, PU1-B and Compartment Test 1-4 at different depths. In PU1-B thermocouples were installed at 50mm instead of 70mm depth

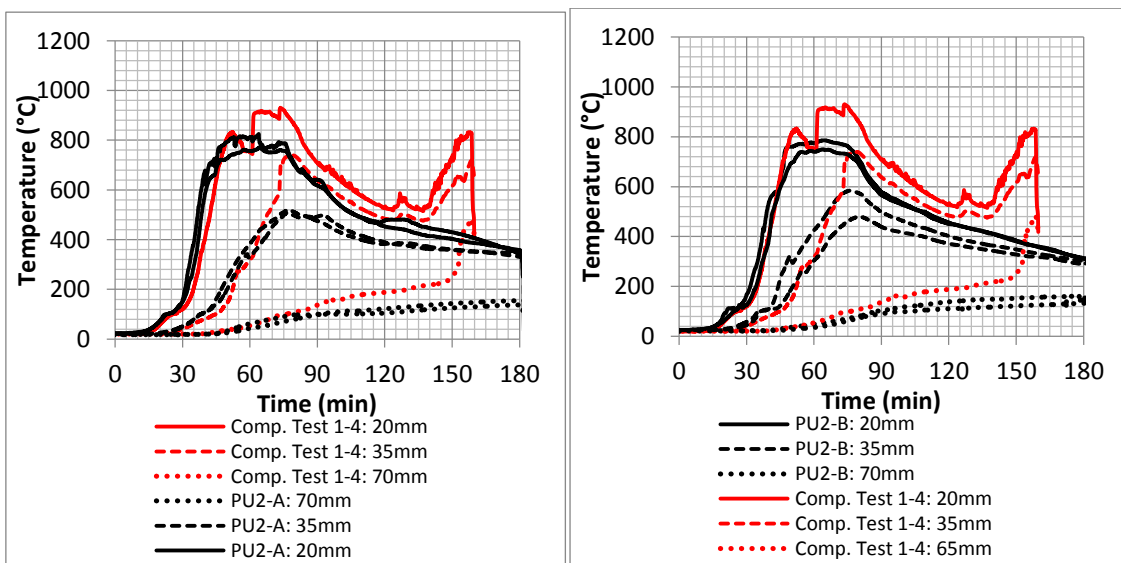


Figure 47: temperatures of PU2-A, PU2-B and Compartment Test 1-4 at different depths

The importance of positioning thermocouples parallel to the isotherms for materials with low conductivity has been shown a long time ago, for example in a study conducted at NASA (Brewer, 1967). It is understood that it is not possible to place thermocouples parallel to the isotherms in specimens with large dimensions. Therefore, it is necessarily to show the effect of errors made, when measuring with thermocouples positioned in the direction of the heat flow (perpendicular to the isotherms). Figure 48 shows measurements of thermocouples positioned in both directions from the same depths. The temperature measurements at each depth are significantly dependent on the direction of the thermocouple. Especially at a depth of 35mm significant temperature differences close to 400°C can be seen. Therefore, care should be taken if results from thermocouples positioned parallel to the isotherms have to be interpreted.

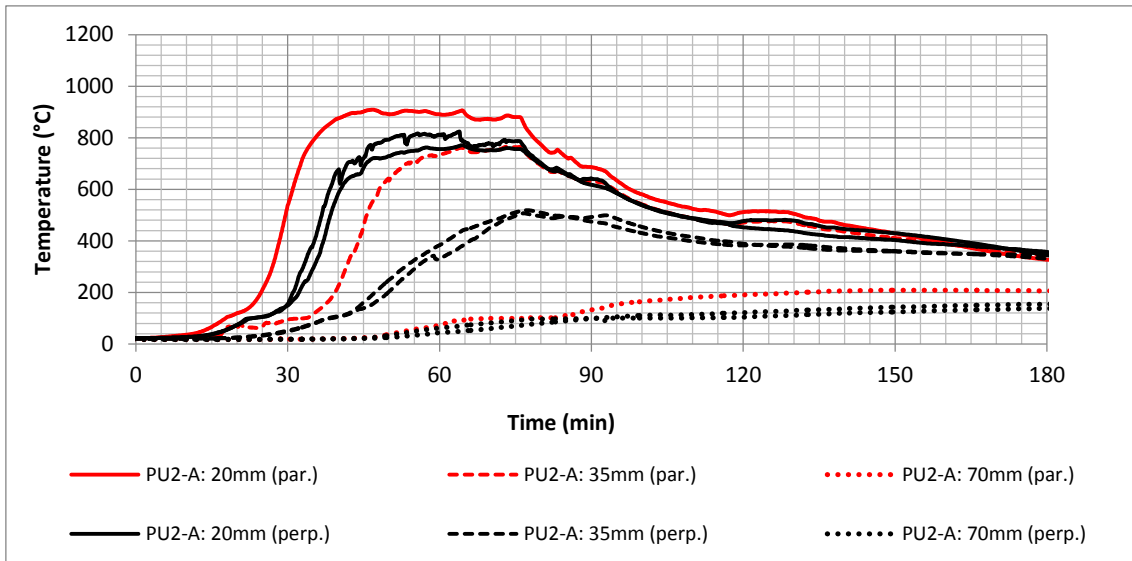


Figure 48: temperatures of PU2-A measured with thermocouples perpendicular and parallel to the isotherms

2.8.3 Char depth

The char depth was measured after Compartment Test 1-4, which allows comparisons with charring depths resulting from the furnace tests. It should, however, be noted that Compartment Test 1-4 was 20 minutes shorter, as it was extinguished after 160 minutes. For a direct comparison with Compartment Test 1-4, the average char depths at 160 minutes were estimated using linear interpolation (Figure 49). Based on a study of the uncertainty of thermocouple locations and temperature measurements, the expanded total uncertainty for the interpolated char depth is estimated to be ± 0.9 mm (95 % confidence). The estimated charring depth of the specimens of PU-A at 160 minutes corresponds well with the charring depth of Compartment Test 1-4, because the largest difference of average char depth of the two test methods is only 5mm. It should be noted that there was significant spatial (24mm) variation in char depth across the ceiling, as measured after Test 1-4. For both intermediate scale tests of the same CLT product (PU1), the spatial variation of char depth measured was 9 mm. The spatial variation of charring depth measured in tests with other adhesives varied between 2 and 9 mm. However, the resemblance between the average charring rates measured in the PU1 specimens of both tests, indicates that the furnace test successfully replicated relevant fire conditions of the compartment test.

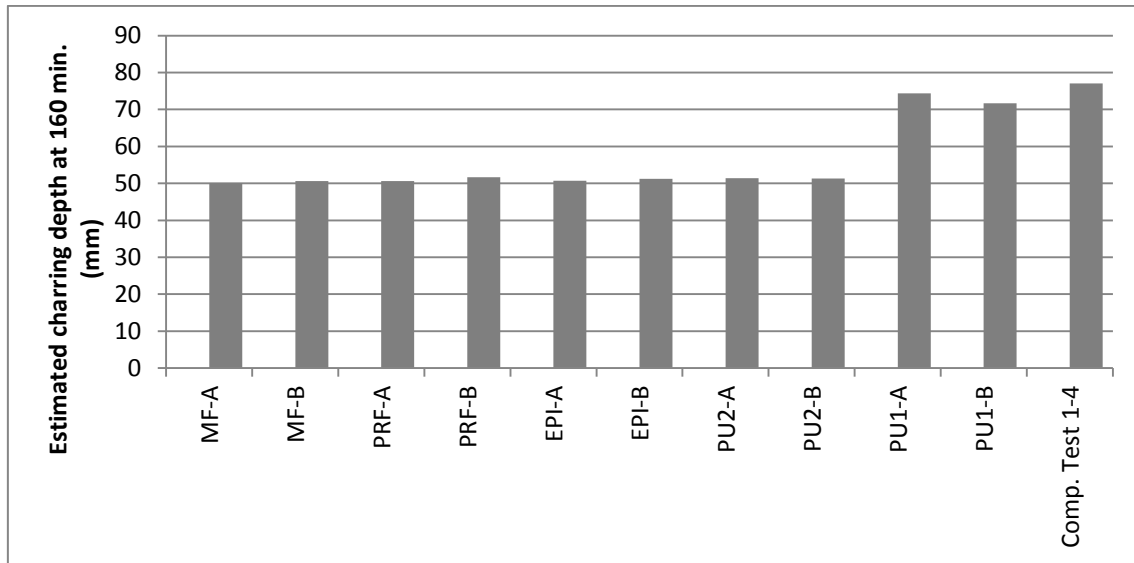


Figure 49: Estimated charring depth at 160 min using linear interpolation.

2.8.4 Time of delamination

In order to validate the test method further, the time of delamination of Compartment Test 1-4 and PU1-A and PU1-B are compared. The time of delamination was determined from thermocouple measurements using the criteria given in Section 2.3.

Figure 50 shows box-plots of the time of delamination, determined from thermocouples in the first two plies and the first two bond lines. Delamination of the first ply occurred at around 60 minutes in the furnace and compartment test. Delamination of the second ply started at approximately 150 minutes. In test PU1-B, the majority of the thermocouples did not indicate delamination. Video recordings, showed that only partial delamination of the second ply occurred within 3 hours testing time. However, after the test was ended, at approximately 182 minutes, a significant part of the second layer of lamellas delaminated. Therefore, the box plot for delamination of the second layer of PU1-B is not complete. As most of the second layer fell at 182 minutes it is expected that the upper limit of that box plot would have been at 182 minutes if the test would have been longer. Times of delamination determined from Compartment Test 1-4 were in the range of delamination times determined from PU1-A and PU1-B. This indicates that the test successfully replicated relevant fire conditions of the compartment test.

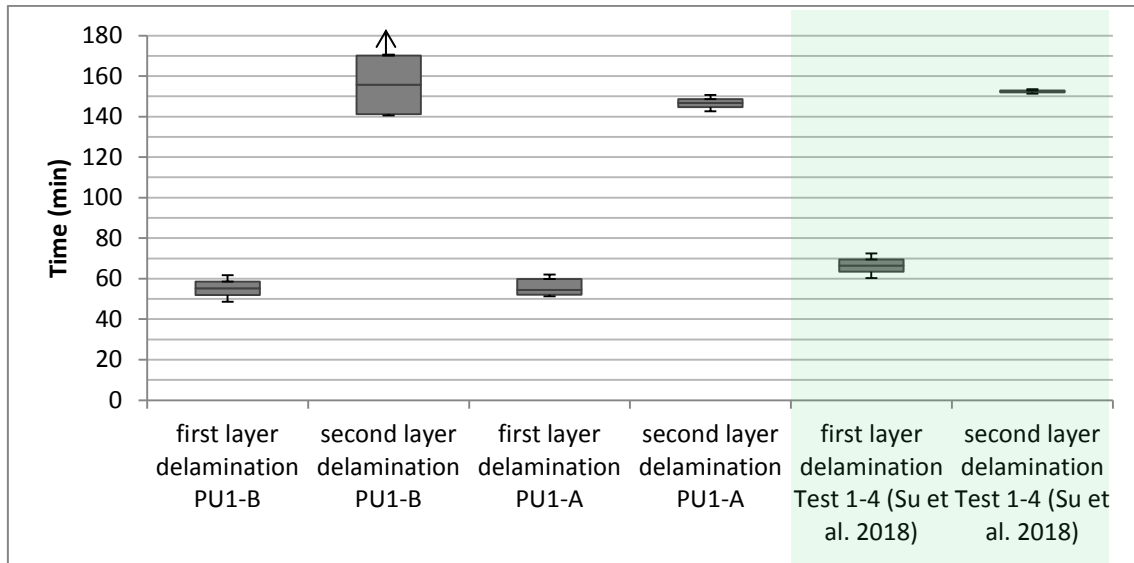


Figure 50: Time of delamination determined from thermocouple measurements

3 PS 1 testing

The heat performance test, as described in Clause 6.1.3.4 of the Voluntary Product Standard PS 1 Structural Plywood (NIST, 2010), is conducted to determine whether a structural adhesive exhibits heat delamination that could potentially impact the charring behavior of a product when compared to traditional (unglued) lumber. It is noted that the result from this test method is currently not a mandatory pass/fail requirement in the 2012 edition of ANSI/APA PRG 320. PS1 testing was performed in this research to determine if the PS 1 test, intended for plywood, also provides useful data on the performance of adhesives used in CLT. At the time the research was performed, the tests were relevant with respect to the change of ANSI/APA PRG 320. The tests are presented in this report as they can be relevant for the development of new products prior to performing required standard tests. The tests discussed in this chapter were conducted at FP-Innovations.

According to the standard terminology of adhesives in ASTM D907 (2015), **delamination is defined as “the separation of layers in a laminate because of failure of the adhesive, either in the adhesive itself or at the interface of the adhesive and the adherent”**. If an adhesive exhibits heat delamination characteristics, ANSI/APA PRG 320 requires that appropriate design adjustments are to be provided. However, since it is a product manufacturing standard, it does not provide any guidance or recommendations on the matter for designing for fire resistance.

3.1 Method

The PS 1 heat performance test requires a plywood test specimen to be placed on a small scale apparatus as shown in Figure 51, and to be exposed to a 800 to 900°C flame from a Bunsen-type burner for a period of 10 minutes, or until a brown charred area appears on the unexposed side (back side), whichever occurs first. Visual observations of the charred surface are then made based on the extent of veneer delamination, if any.

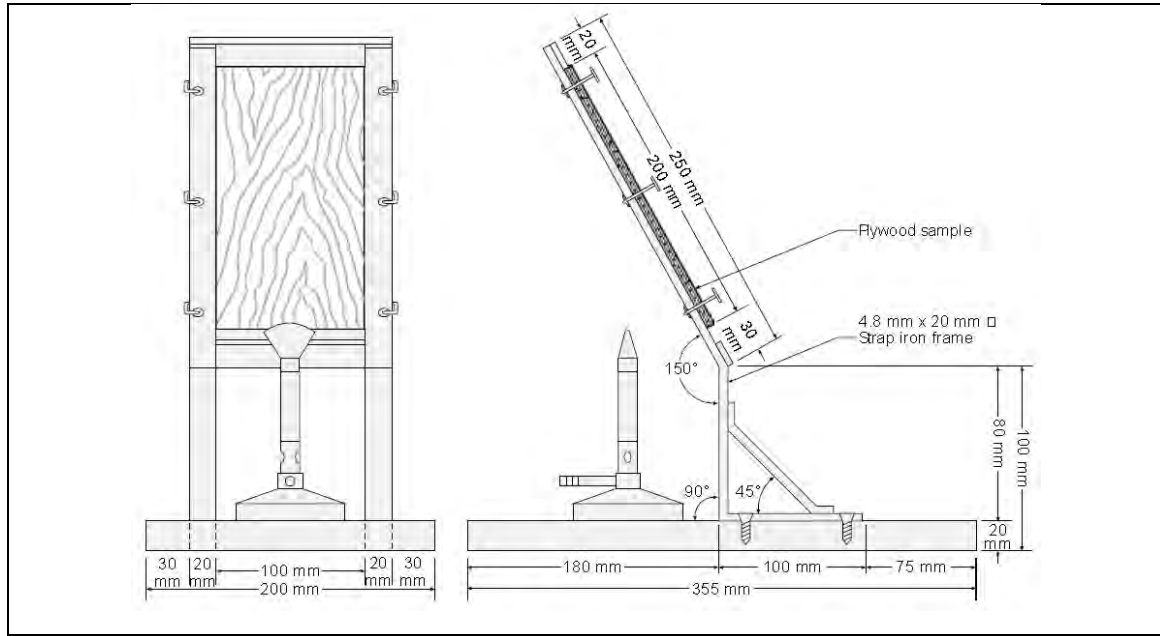


Figure 51: Schematic of apparatus, as presented in NIST (2010)

3.2 Setup and measurements

The experimental setup consists in an inclined metallic frame designed in such a way that the top of the burner is positioned at 25.4 mm from the specimen surface and that its flame is 38.1 mm high. The flame shall impinge on the specimen face at 50.2 mm from the bottom end. During the test, the specimen is secured to the metallic frame using 6 bolts and nuts.

After the test, the sample is removed from the apparatus and the bond lines are examined for delamination by separating the charred plies with a sharp, chisel-like instrument. The PS1 heat performance test criteria are considered met if there is no delamination in any specimen of the set of a given adhesive.

3.3 Materials and production of specimens

PS 1 does not provide clear guidance with respect to preparation of the plywood specimen for heat performance evaluation. As such, it was agreed, based on recommendations by APA-EWS, that wood veneers or slices be used for specimen preparation. A-Grade Douglas-Fir veneers with a thickness of 3.2 mm were purchased from a Western Canadian supplier, with original dimensions of 1.2 x 2.4 m. The veneers were free from knots or other defects, and conditioned to approximately 12% moisture content before gluing.

Five (5) billets of 5-ply plywood, 203 x 305 mm, were prepared in accordance with the adhesive **manufacturer's recommendations (spread rate, open-/assembly-/close-times, pressure, etc.)**, as detailed in subsection 2.4 of this report. Each billet was further cut down to 160 x 203 mm test specimens from the center portion of the billet. The major strength axis of the plywood test specimen was oriented along the 203 mm direction (wood grain of the 1st, 3rd and 5th plies run parallel to the 203 mm direction).

Figure 52 shows a typical test specimen, which was similar for the five adhesives, prior to flame testing. Additional pictures of the specimen preparation and gluing can be found in Appendix II.



Figure 52: Plywood specimen (PU1-1) prior to flame testing

3.4 Measured properties of specimens

After gluing, the plywood specimens were conditioned to approximately 12% moisture content before flame testing. Table 15 provides the density for each plywood test specimen.

Table 15 Density of Douglas-Fir plywood specimens

Specimen	Density of plywood specimens (kg/m ³)				
	Type of Adhesive				
	PU1	PU2	EPI	MF	PRF
1	572	548	540	601	607
2	547	569	562	638	576
3	554	585	606	593	605
4	532	609	581	616	622
5	568	562	557	620	569
Average (std. dev.)	555 (16)	575 (23)	569 (25)	614 (18)	603 (19)

3.5 Test results

All specimens made with PU1 exhibited heat delamination of the 1st veneer. Peeling was visually observed starting 4.0 to 6.5 min into the test. Given that there was clear visual evidence of heat delamination (Figure 53a), no chisel-like instrument was needed to assess whether the specimens passed or failed.

Three of the five EPI specimens exhibited heat delamination of the 1st veneer. They, however, delaminated to a much less degree than that of the PU1 specimens. Some EPI specimens required a closer review using the chisel-like instrument. Peeling of the 1st veneer was nevertheless visually observable for specimens EPI-1, EPI-2 and EPI-3 (Figure 53). Heat delamination was noted to occur after approximately 7 to 7.5 min of flame exposure.

The PU2, MF and PRF specimens did not show signs of heat delamination. A charred surface was observed on all specimens (Figure 54). There was no peeling or detachment of the 1st veneer observed during and after the tests.

Table 16 provides the test results as it relates to whether delamination was observed or not. Table 17 shows the mass loss (in % of the initial mass). Figure 55 to Figure 59 show the specimens after the flame testing.

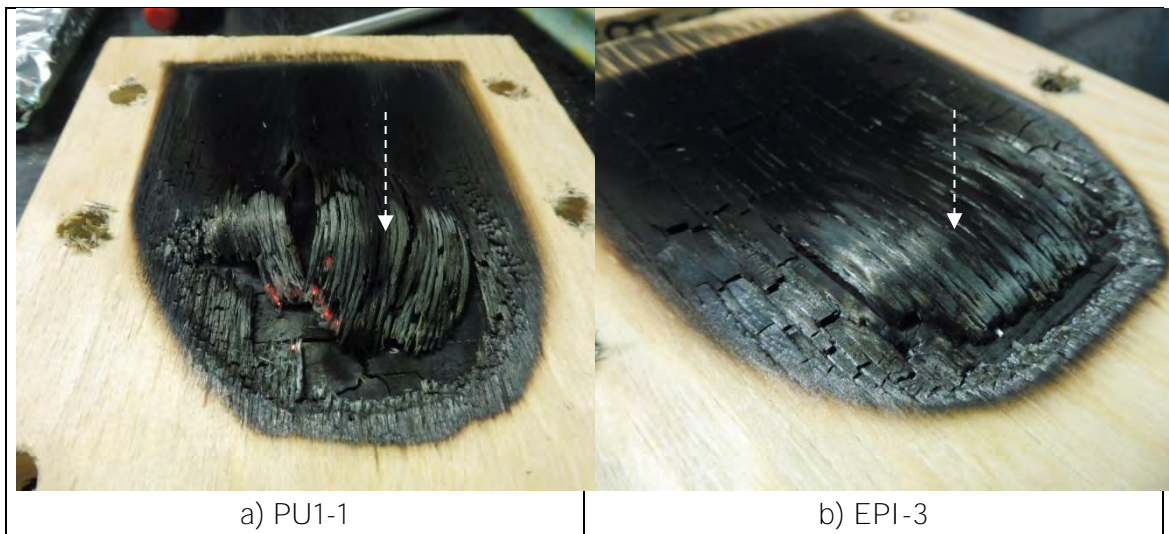


Figure 53: Specimens exhibiting heat delamination (1st ply peeling off)

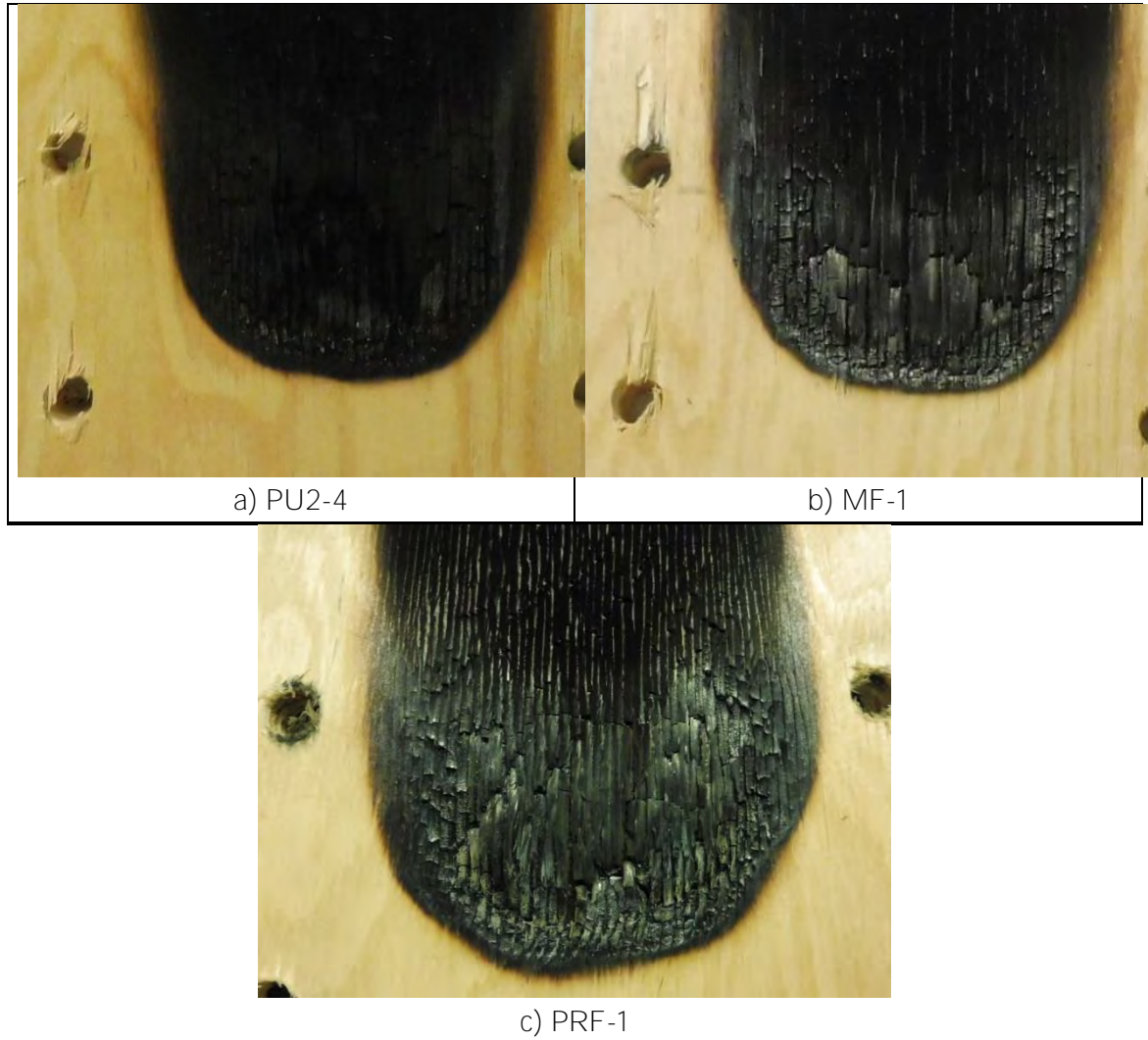


Figure 54: Specimens not exhibiting heat delamination

Table 16 PS 1 heat performance test results

Specimen	Heat Delamination (Y/N)				
	Type of Adhesive				
	PU1	PU2	EPI	MF	PRF
1	Y	N	Y	N	N
2	Y	N	Y	N	N
3	Y	N	Y	N	N
4	Y	N	N	N	N
5	Y	N	N	N	N
Outcome	Fail	Pass	Fail	Pass	Pass

Y = heat delamination occurred, N = no delamination.

Table 17 Mass loss of specimens during heat exposure

Specimen	Mass Loss				
	Type of Adhesive				
	PU1	PU2	EPI	MF	PRF
1	6.1%	5.0%	6.4%	5.7%	5.4%
2	5.1%	5.9%	5.6%	4.7%	4.7%
3	5.4%	6.6%	6.1%	5.4%	4.5%
4	6.3%	5.2%	4.7%	4.6%	5.3%
5	6.4%	5.2%	5.1%	5.0%	4.5%



Figure 55: PU1-1 specimen after PS 1 flame testing

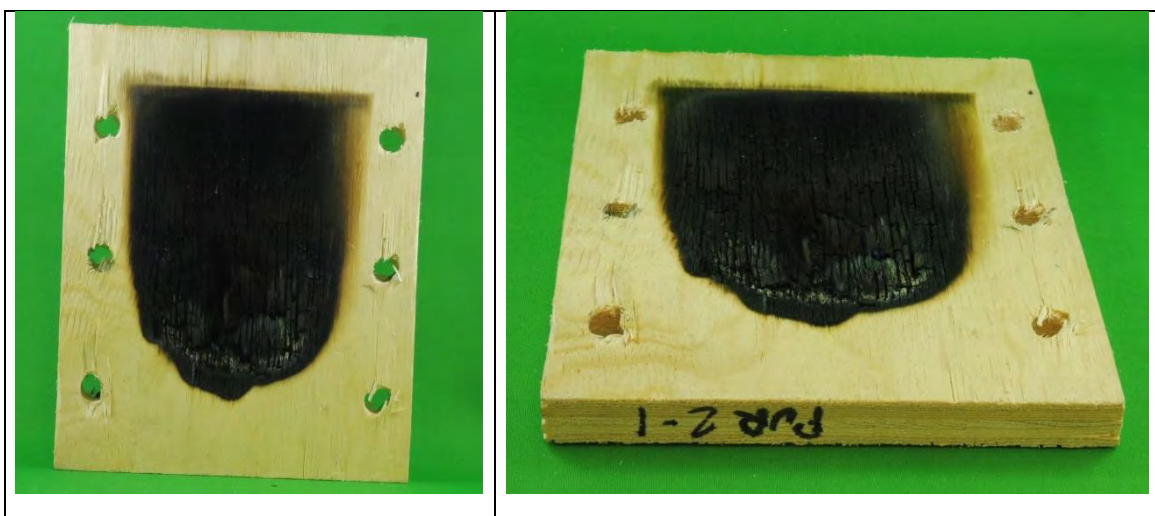


Figure 56: PU2-1 specimen after PS 1 flame testing

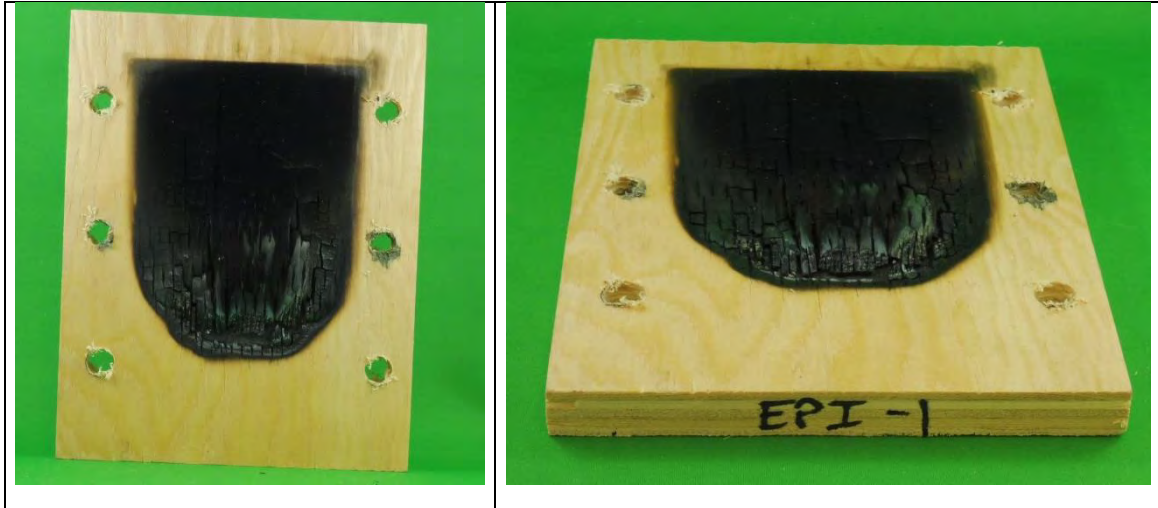


Figure 57: EPI-1 specimen after PS 1 flame testing



Figure 58: MF-1 specimen after PS 1 flame testing

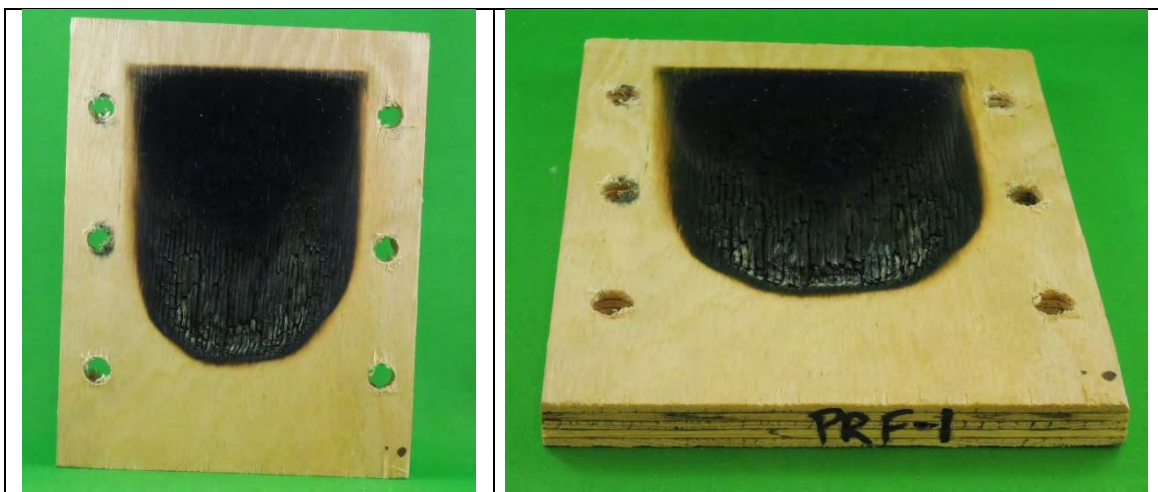


Figure 59: PRF-1 specimen after PS 1 flame testing

3.6 Validation of method

The intent of the PS 1 flame test is to evaluate whether an adhesive would exhibit heat delamination characteristic when exposed to a standard flame exposure across the plywood veneers. It is acknowledged that the PS 1 flame exposure is not intended to replicate either a standard or design fire exposure, and is also not necessarily a guarantee that a satisfactory flame test of a given adhesive would not result in heat delamination of an engineered wood product made with this given adhesive in either a standard or a real fire condition. It can also be argued that heat transfer through a plywood made of thin veneers is not the same as that of a CLT made of dimensional lumber boards (typically 35 mm in thickness). However, the test method has been proven satisfactory for plywood over the years, suggesting that it might be suitable for other wood products.

Based on the results, the PS 1 flame test method does seem to provide insight related to adhesives prone to heat delamination. Some of the tested adhesives clearly showed signs of heat delamination where it was visually observed that the 1st veneer was peeling off and detaching itself from the 2nd veneer during the flame exposure. There was no need for using the chisel-like instrument. Further discussion on its validity and correspondence with furnace tests is given in Section 4 of this report.

3.7 Discussion of flame test results

Based on results of the full scale fire tests 1-3 to 1-6 and the intermediate scale furnace tests of CLT made with PU1 adhesive, it was expected that the PS 1 test would demonstrate delamination for this type of adhesive. PRF is a heavily cross-linked polymer, indicating that PRF adhesives do not soften significantly during heating. Additionally, numerous fire tests have been performed with this adhesive type, as this adhesive type was traditionally used in most engineered timber products. Fire test results of specimens with the specific MF adhesive with high strength at elevated temperatures were available to the authors. Therefore, it was expected that CLT with these two adhesives would not exhibit delamination.

Due to limited experience with PU2 and EPI adhesive in fire tests the expectations of these results were uncertain. The PU2 provided satisfactory results as it did not exhibit delamination. This new PU2 has been specially designed by its manufacturer for providing greater fire performance than that of traditional polyurethane, in an attempt to eliminate the fall-off characteristic observed in most small scale to large scale CLT fire tests.

The failure of the EPI adhesive to pass the PS1 test, was no expect given it is an approved adhesive for glue-laminated timber in the U.S. It is noted however that PS 1 flame test is not an adhesive performance requirement for manufacturing glue-laminated timber in North America, and may not be the most appropriate test to measure the fire performance of adhesives used for face-bonding glulam and/ or CLT products.

4 Correspondence between PS-1 and furnace testing

The various structural adhesives evaluated in this study have been tested in accordance with numerous different standards and test methods, as shown in Table 18. As such, it is not surprising that different performances are obtained when these adhesives are tested beyond their scope of accreditation.

Table 18 North American adhesive certifications

Adhesive	Test Method / Product Standard				
	CSA O177	CSA O112.9	CSA O112.10	ANSI 405	ASTM D7247
PU1	-	-	Y	Y	Y
PU2 ⁽¹⁾	Y ^(1,2)	Y ⁽¹⁾	-	Y ⁽¹⁾	Y ⁽¹⁾
EPI	-	-	Y	Y	Y
MF	-	Y	-	Y	Y
PRF	Y	Y	-	Y	Y

⁽¹⁾ At the time of writing the report, the adhesive manufacturer indicated that certification under these standards was on-going.
⁽²⁾ Adhesive already tested and met delamination requirements set forth in Annex A.2 of CSA O177 (confidential external report).
 Y – Specifies adhesives that have been tested to the requirements of the given standard.

At the time the research was conducted, the US glulam manufacturers complied with ANSI 405-2013, which required adhesives to pass the requirements of ASTM D2559, ASTM D1151, ASTM D7247 Elevated Temperature test, CSA O112.9 B2 Creep Resistance test, ASTM D1183 and a durability test from either ASTM D3434 or CSA O112.9 (Section 5.5 – block shear test after boil-dry-freeze cycles). The D7247 test procedure evaluated relative bond line strength loss at a minimum target bond line temperature of 220°C, not at the char front temperature of approximately 300°C. However, the current 2018 versions of ANSI 405 for glulam and PRG-320 for cross-laminated timber, now require compliance with CSA O177 wherein the adhesive must conform to CSA O112.9 or CSA O112.7 “*Resorcinol and Phenol-Resorcinol Resin Adhesives for Wood (Room and Intermediate Temperature Curing)*”. Additionally, Annex B of the 2018 version of PRG-320 requires additional full-scale testing to ensure that the CLT does not exhibit fire re-growth when subjected to severe exposures such as those in the FPRF test series.

In Canada, CSA O177 requires that adhesives used in glue-laminated timber must conform to CSA O112.9 or CSA O112.7 “*Resorcinol and Phenol-Resorcinol Resin Adhesives for Wood (Room and Intermediate Temperature Curing)*”. Moreover, bond line fire performance is to be evaluated from either the mandatory Annex A.2 small-scale flame test and ASTM D7247 at a minimum target bond line temperature of 220°C, or from a full-scale fire-resistance test in accordance to CAN/ULC S101 (which is similar to ASTM E119). It is noted that the mandatory bond line fire performance

evaluation in the Canadian glue-laminated timber standard is significantly different than what is required in the US.

Table 19 Heat delamination in intermediate scale furnace tests and PS1 tests

Specimen	Heat Delamination (Y/N)				
	Type of Adhesive				
	PU1	PU2	EPI	MF	PRF
Intermediate scale furnace specimen A	Y	N	N	N	N
Intermediate scale furnace specimen B	Y	N	N ¹	N	N
PS 1 specimen 1	Y	N	Y	N	N
PS 1 specimen 2	Y	N	Y	N	N
PS 1 specimen 3	Y	N	Y	N	N
PS 1 specimen 4	Y	N	N	N	N
PS 1 specimen 5	Y	N	N	N	N
PS 1 outcome	Fail	Pass	Fail	Pass	Pass

Y = heat delamination occurred, N = no delamination.

¹Char fall-off of the first lamella occurred at a late stage in this test.

As shown in Table 18, all five adhesives used in this study are approved for use in accordance with the US glue-laminated timber standard ANSI 405-2013. However, based on the PS 1 flame test an intermediate scale furnace test results presented in Table 19, one can observe that qualification to ANSI 405-2013 does not guarantee adequate fire performance when used for elements. This is most likely related to the changing grain directions of subsequent glued lamella layers. In contrast with CLT, glue-laminated has all laminations oriented in the same direction. Two adhesives (PU1 and EPI) failed the PS 1 flame testing. The same two adhesives showed delamination and/or char fall-off during the intermediate scale furnace tests.

When analyzing the Canadian adhesive standards' requirements, the test results suggest that adhesives certified in accordance with the full requirements set forth in CSA O177 would result in successful PS 1 flame tests. Moreover, the test results suggest that adhesives certified in accordance with the full requirements set forth in CSA O112.9 would result in successful PS 1 flame tests. The PU1 and EPI adhesives used in this study are the only adhesives certified to CSA O112.10 and they failed the PS1 flame test. As mentioned before, CLT specimens with these adhesives (PU1 and EPI) showed delamination and/or char fall-off during the intermediate scale furnace tests. However, as the exposure conditions of the PS 1 tests and the intermediate scale furnace tests are significantly different, the amount of adhesives tested does not allow drawing strong conclusions regarding the correspondence between the two tests.

It should be noted that after the experimental research conducted for this study, ANSI 405-2013 and ANSI/APA PRG 320-2012 were revised. The new 2018 version of the standards require compliance with CSA O177 which involves a flame exposure that is similar to the PS1 flame tests. Although this research project did not involve tests according to CSA O177, the resemblance between CSA O177 and the PS 1 test suggests that the tests described in CSA O177 could also provide insight into the potential delamination behavior of CLT.

5 Recommendations and conclusions

Intermediate scale furnace tests aiming to replicate the conditions of a compartment fire test (Test 1-4 by Su et al. 2018) have been performed. The referenced compartment fire test is used as the basis for current regulations in the 2018 version of ANSI/APA PRG 320. A replication of the relevant conditions of this compartment fire in an intermediate scale fire testing furnace that leads to the same damage if the same product is tested, therefore, provides a (less expensive) alternative method for future CLT product standards. Comparisons of the charring rates, material temperatures and times of delamination of the same CLT product in both test methods, indicated that the furnace test successfully replicated relevant conditions of the compartment fire test. Therefore, the intermediate scale furnace test is recommended as an alternative to the testing method described in Annex B of the 2018 version of ANSI/APA PRG 320, for future updates.

In addition to the intermediate scale furnace tests, PS1 testing was performed in this research to determine if the PS 1 test, intended for plywood, also provides useful data on the performance of adhesives used in CLT. The tests were originally performed to be considered for inclusion in the 2018 version of ANSI/APA PRG 320. Although the tests were not included in the standard, the tests are presented in this report as they can be relevant for the development of new products prior to performing required full scale tests. Comparisons of results showed that the same two (out of five) adhesives showed delamination or char fall-off in the intermediate scale furnace tests and the PS1 tests. However, as the exposure conditions of the PS 1 tests and the intermediate scale furnace tests are significantly different, the amount of adhesives tested does not allow drawing strong conclusions regarding the correspondence between the two tests. Further research would be needed to validate the PS1 tests as an alternative for currently required testing methods.

Acknowledgements

The authors gratefully acknowledge the Fire Protection Research Foundation, Property Insurance Research Group, U.S. Department of Agriculture, U.S. Forest Service and the American Wood Council for the financial support that made this project possible.

The authors gratefully acknowledge Amanda Kimball, Joseph Su, Matthew Hoehler, Birgit Östman, Casey Grant and the technical panel for their help with the test plan.

Eric Johansson, Anton Svenningsson, Alar Just and Mattia Tiso are acknowledged for their help with preparing and performing the intermediate scale furnace tests.

Grant Reekie from Innotech Alberta is acknowledged for producing the specimens of this research project.

References

AITC 405 (2008) Adhesives for use in Structural Glued Laminated Timber. American Institute of Timber Construction, USA.

ANSI 405 (2013) Adhesives for use in Structural Glued Laminated Timber. American National Standards Institute, USA.

ANSI/APA PRG 320 (2012) Standard for Performance-Rated Cross-Laminated Timber, New York, NY: American National Standards Institute.

ANSI/APA PRG 320 (2018) Standard for Performance-Rated Cross-Laminated Timber, New York, NY: American National Standards Institute.

ASTM D1151-00 (2013) Standard Practice for Effect of Moisture and Temperature on Adhesive Bonds. ASTM International, PA, USA.

ASTM D1183-03 (2011) Standard Practices for Resistance of Adhesives to Cyclic Laboratory Aging Conditions. ASTM International, PA, USA.

ASTM D2559 (2016) Standard Specification for Adhesives for Bonded Structural Wood Products for Use Under Exterior Exposure Conditions. ASTM International, PA, USA.

ASTMD3434-00(2013) Standard Test Method for Multiple-Cycle Accelerated Aging Test (Automatic Boil Test) for Exterior Wet Use Wood Adhesives. ASTM International, PA, USA.

ASTM D7247-17 (2017) Standard Test Method for Evaluating the Shear Strength of Adhesive Bonds in Laminated Wood Products at Elevated Temperatures. ASTM International, PA, USA.

ASTM E119-16a (2016) Standard Test Methods for Fire Tests of Building Construction and Materials. ASTM International, PA, USA.

ASTM D907-15 (2015) Standard Terminology of Adhesives. ASTM International, PA, USA.

Brandon D., Östman B. (2016) Fire Safety Challenges of Tall Wood Buildings – Phase 2: Literature Review. NFPA report: FPRF-2016-22, SP Technical Research Institute of Sweden.

Brandon D., Maluk C., Ansell P.M., Harris R., Walker P., Bisby L., Bregulla J. (2015) Fire Performance of Metal Free Timber Connections. Proceedings of the Institution of Civil Engineers, 168: 173-186.

Brewer W. (1967) Effect of thermocouple wire size and configuration on internal temperature measurements in a charring Ablator, National Aeronautics and space Administration, Washington DC.

Buchanan (2001) Structural Design for Fire Safety. Wiley.

CAN/ULC S101 -14 (2014) Standard methods of fire endurance tests of building construction and materials. ULC Standards, Canada.

CSA O112.9-10 (R2014) - Evaluation of adhesives for structural wood products (exterior exposure). CSA, Canada.

CSA O177-06 (R2015) Qualification Code for Manufacturers of Structural Glued-Laminated Timber. CSA, Canada.

Klippel M, Schmid J, Frangi A (2016) Fire Design of CLT – comparison of design concepts. In Falk A, Dietsch P, Schmid J, ***Proceedings of the Joint Conference of COST Actions FP1402 & FP 1404***. KTH Royal Institute of Technology, Stockholm, Sweden.

Klippel M, Schmid J (2017) Design of Cross-Laminated Timber in Fire. ***Structural Engineering International***, 27(2): pp. 224-230.

Krajnc N. (2015) Wood Fuels Handbook. Food and Agriculture Organization of the United Nations, Pristina, 2015.

NIST (2010) Voluntary Product Standard PS 1-09 – Structural Plywood, Gaithersburg, MD: National Institute of Standard and Technology.

O112.10-08 (R2017) - Evaluation of Adhesives for Structural Wood Products (Limited Moisture Exposure). CSA, Canada.

Schmid J., Santomaso A., Brandon D., Wickström U., Frangi A. (2017) Timber under real fire conditions – the influence of oxygen content and gas velocity on the charring behaviour. *Journal of Structural Fire Engineering*.

Su J. Lafrance P-S. Hoehler M. Bundy M. (2018) ***Cross Laminated Timber Compartment Fire Tests for Research on Fire Safety Challenges of Tall Wood Buildings*** – Phase 2. NRC Canada, Ottawa, Canada.

Weng, Hasemi, Fan (2005) Predicting the pyrolysis of wood considering char oxidation under different ambient oxygen concentrations. ***Combustion and Flame*** 145: 723-729.

Wickström U. (2016) ***Temperature Calculation in Fire Safety Engineering***. Springer International Publishing AG, Switzerland.

Appendix I

Additional pictures of the furnace tests.



a) Lumber planed to 35 mm in thickness



b) Layers prior to gluing



c) Glue application (PRF)



d) Thermocouple placed at a glue line



e) Press apparatus



f) CLT specimens (EPI-2 and PU2-2)

Figure 60: Manufacturing process of the CLT specimens

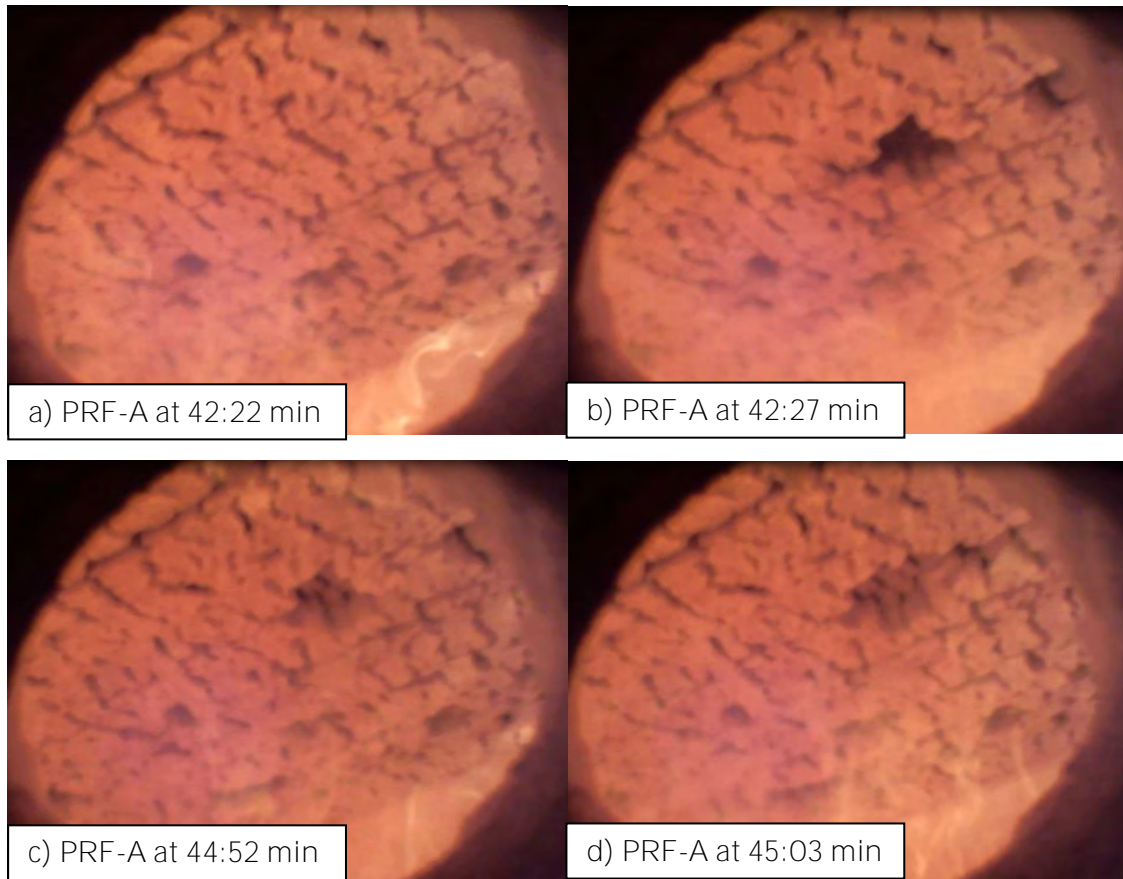


Figure 61: Frames of the video right before and after local falling of char during PRF-A.

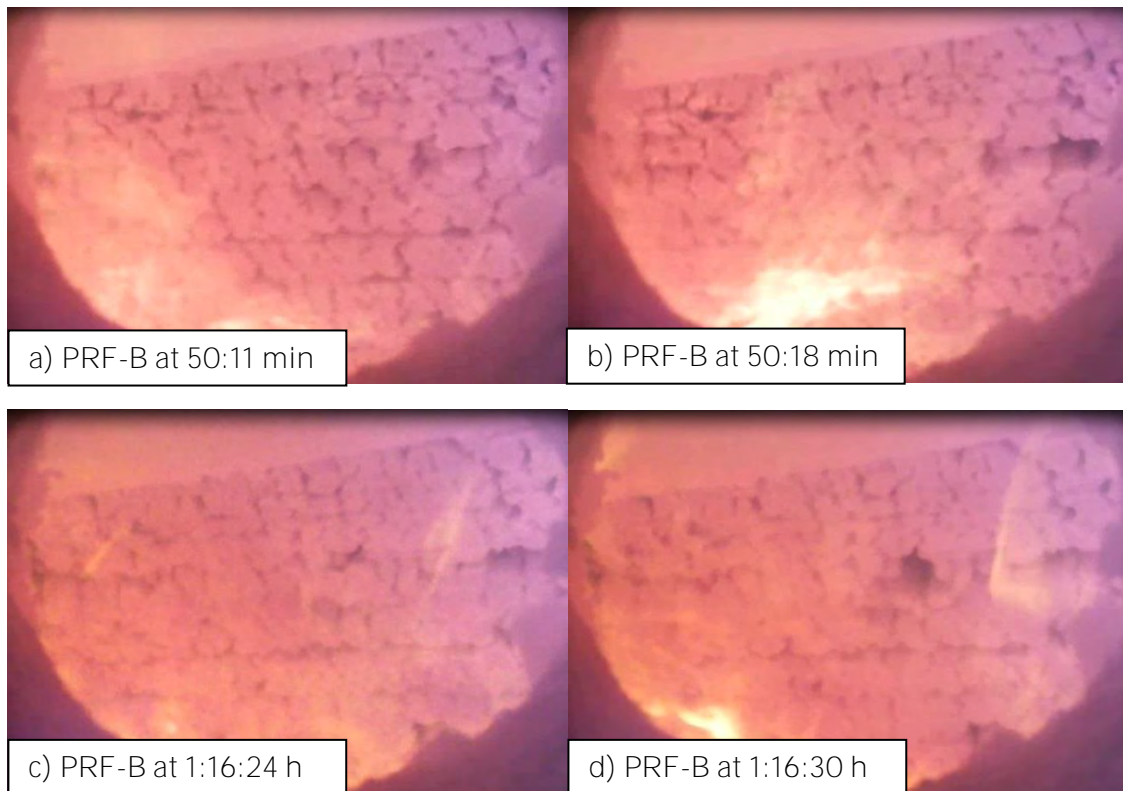


Figure 62: Frames of the video right before and after local falling of char during PRF-B.

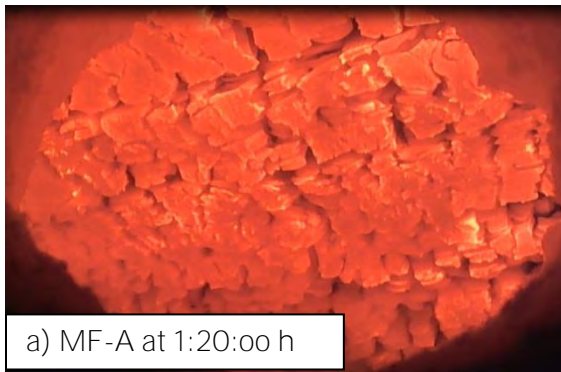


Figure 63: Frame of the video after 80 minutes without falling char MF-A.

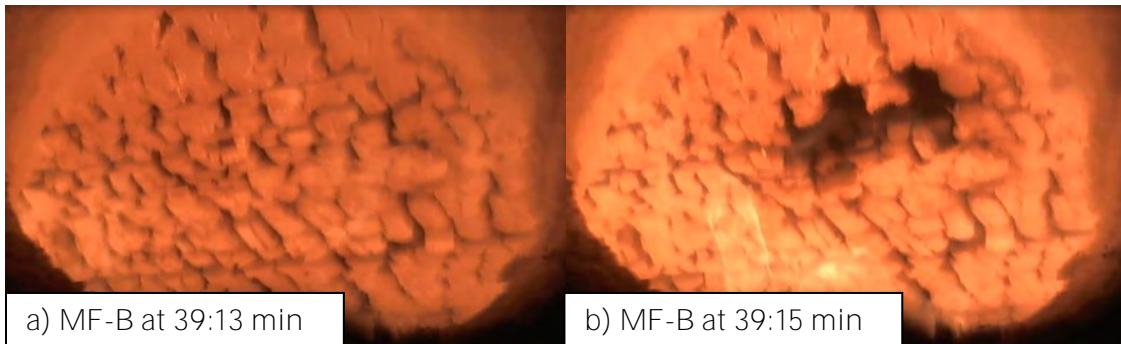


Figure 64: Frames of the video before and after local falling of char during MF-B.

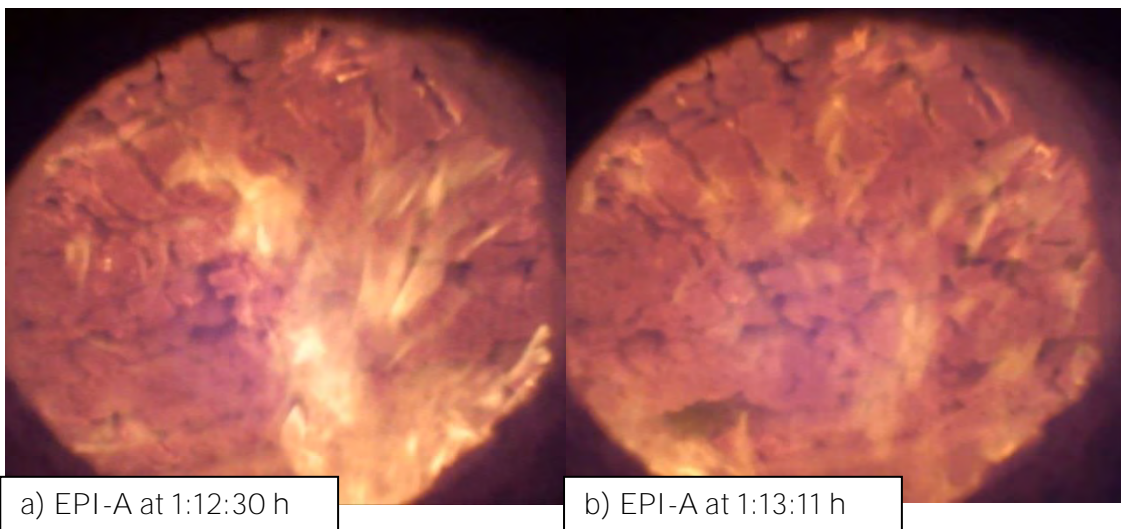


Figure 65: Frames of the video before and after local falling of char during EPI-A.

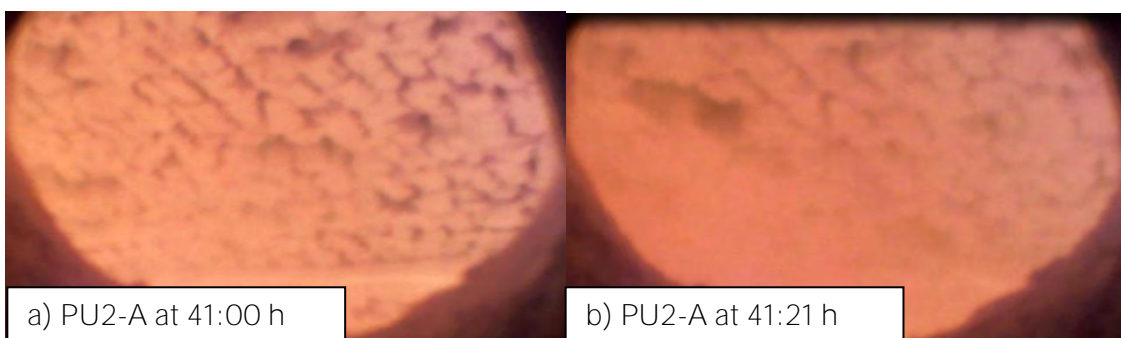


Figure 66: Frames of the video before and after local falling of char during PU2-A.

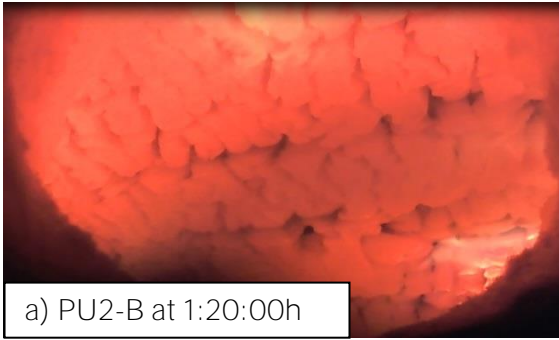


Figure 67: Frame of the video after 80 minutes without falling char PU2-B.

Appendix II

Additional data of the furnace tests.

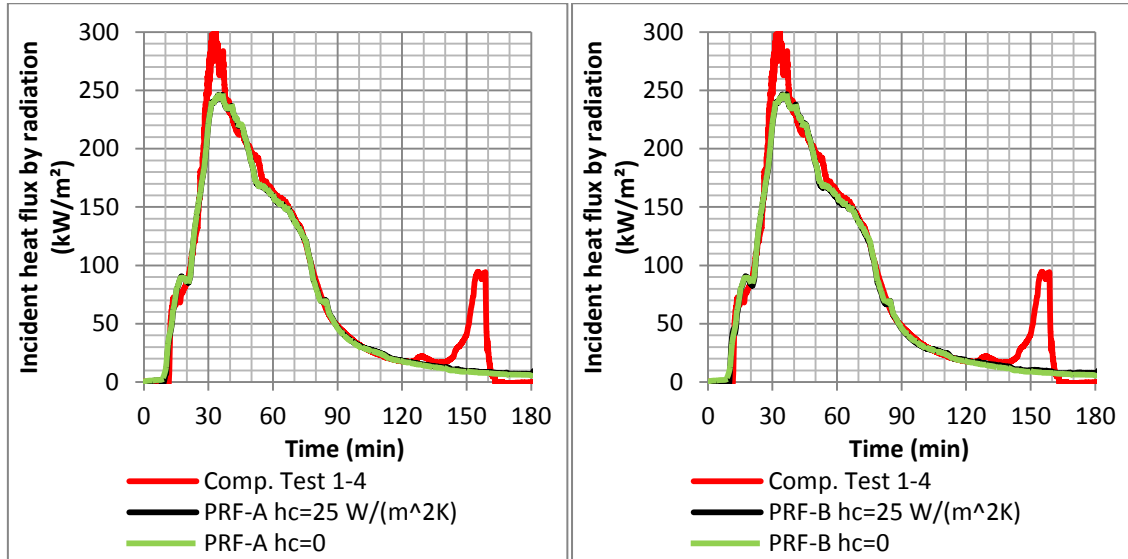


Figure 68: Incident heat flux by radiation of PRF-A (left) and PRF-B (right)

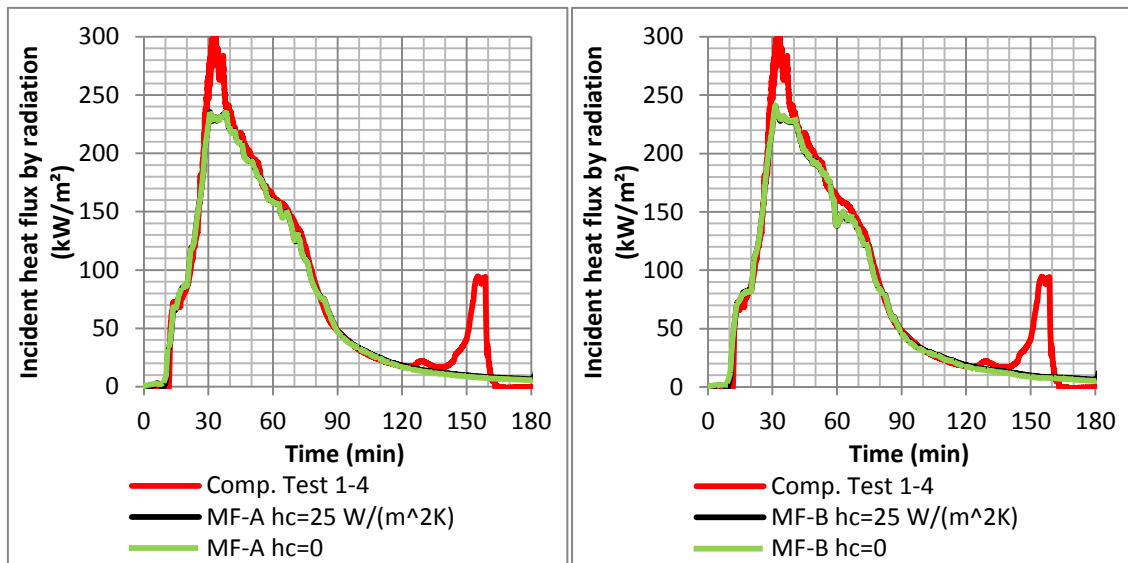


Figure 69: Incident heat flux by radiation of MF-A (left) and MF-B (right)

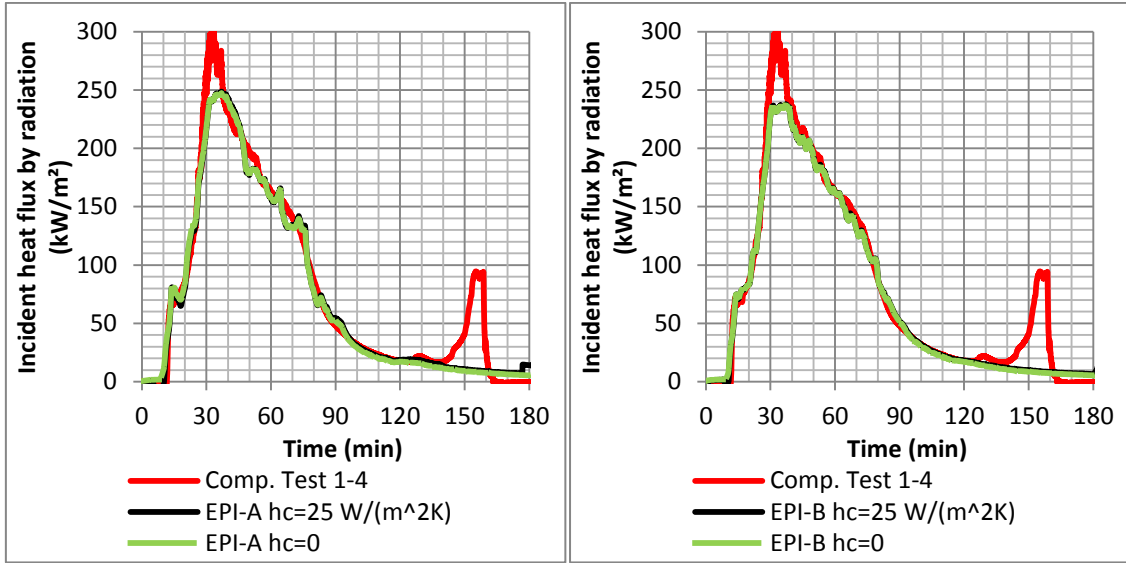


Figure 70: Incident heat flux by radiation of EPI-A (left) and EPI-B (right)

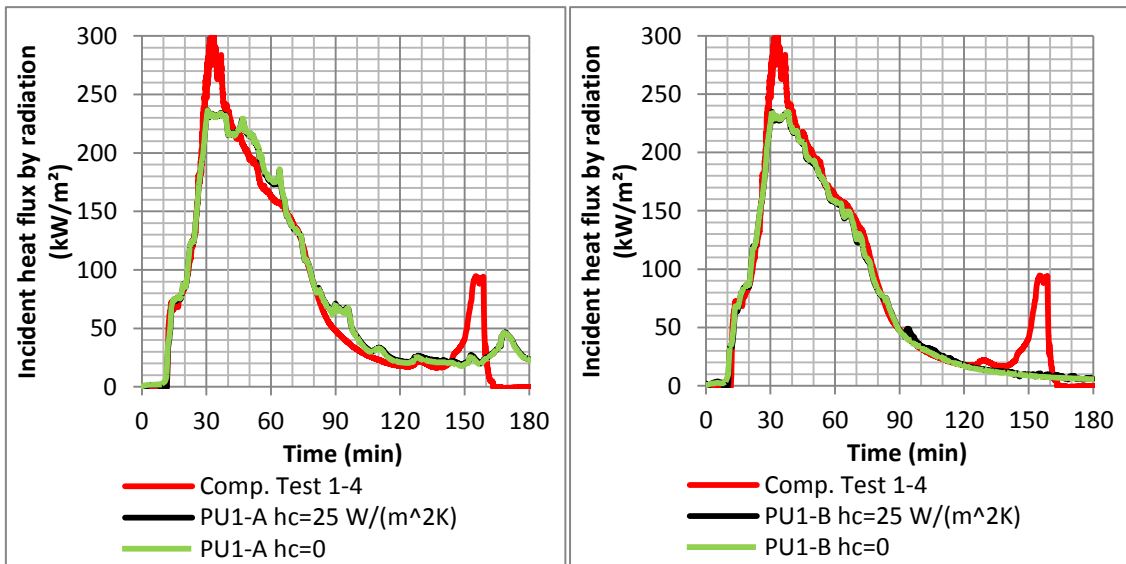


Figure 71: Incident heat flux by radiation of PU1-A (left) and PU1-B (right)

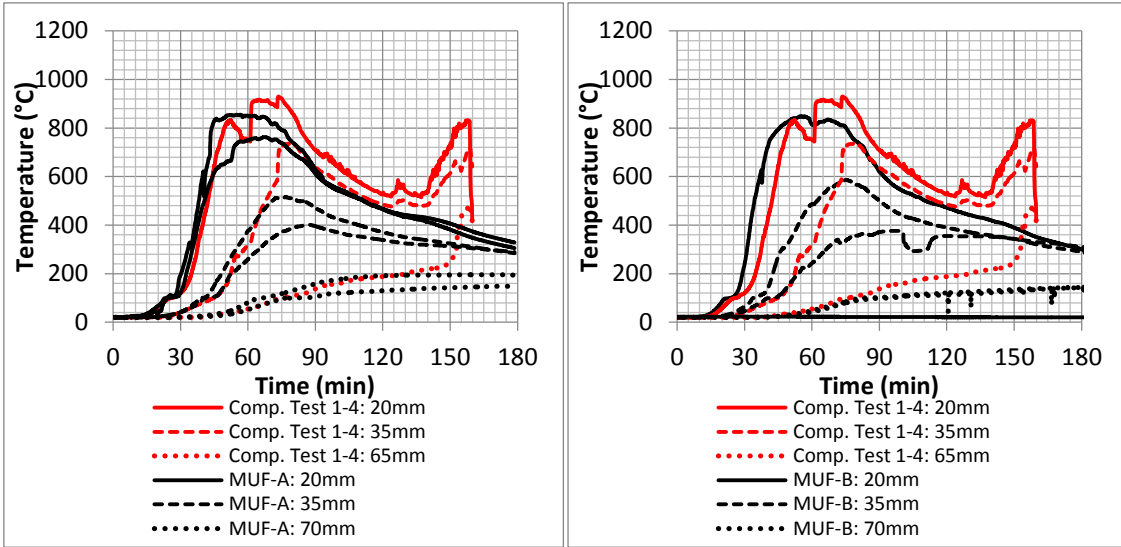


Figure 72: Material temperature comparison with Comp. Test 1-4. MF-A (left) and MF-B (right)

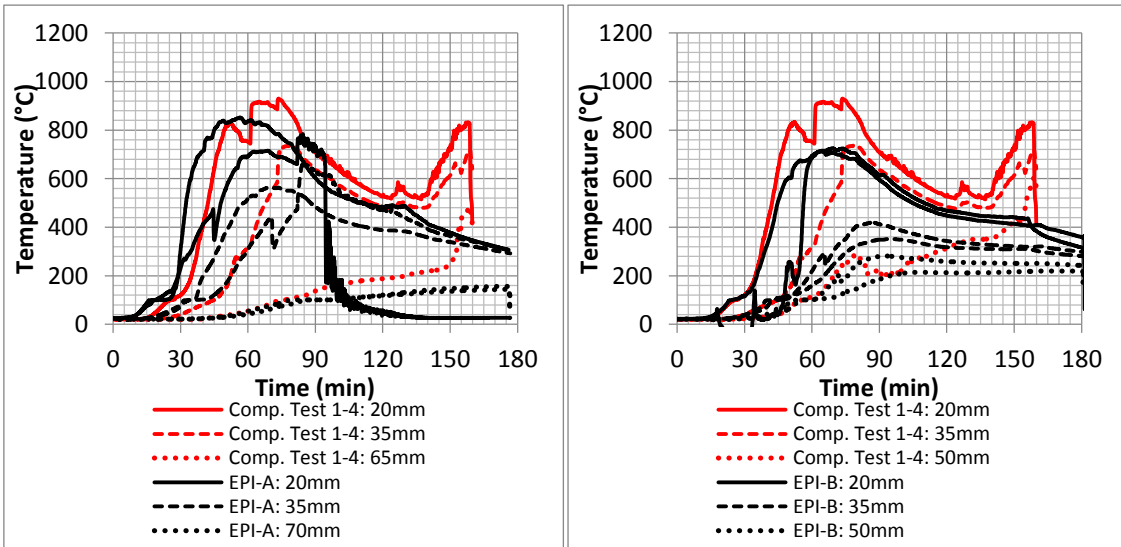


Figure 73: Material temperature comparison with Comp. Test 1-4. EPI-A (left) and EPI-B (right)

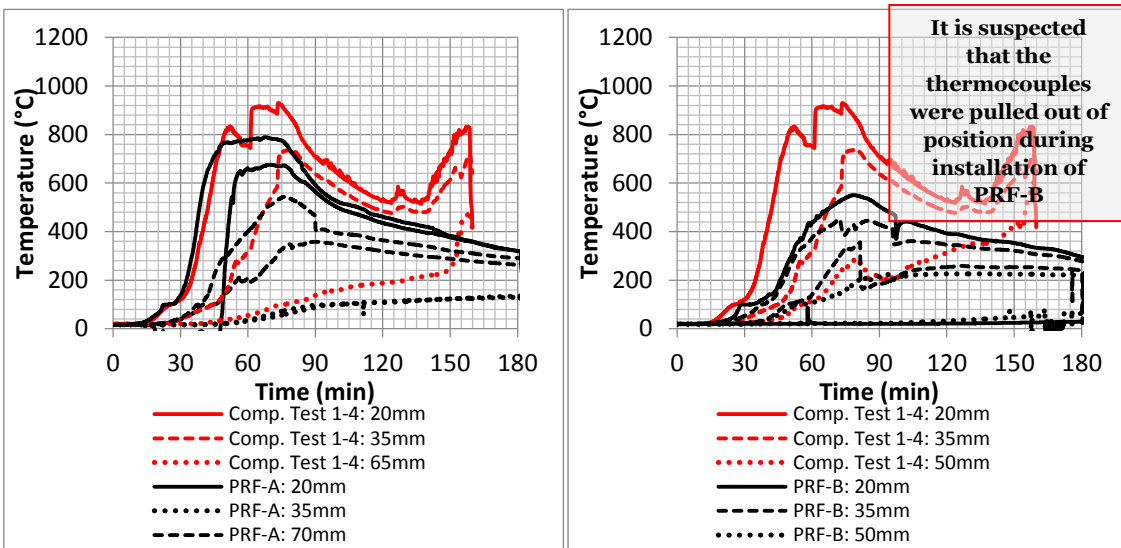


Figure 74: Material temperature comparison with Comp. Test 1-4. PRF-A (left) and PRF-B (right)

Appendix III

Additional pictures of the PS 1 flame tests.



Figure 75: Douglas-Fir veneers for PS 1 testing

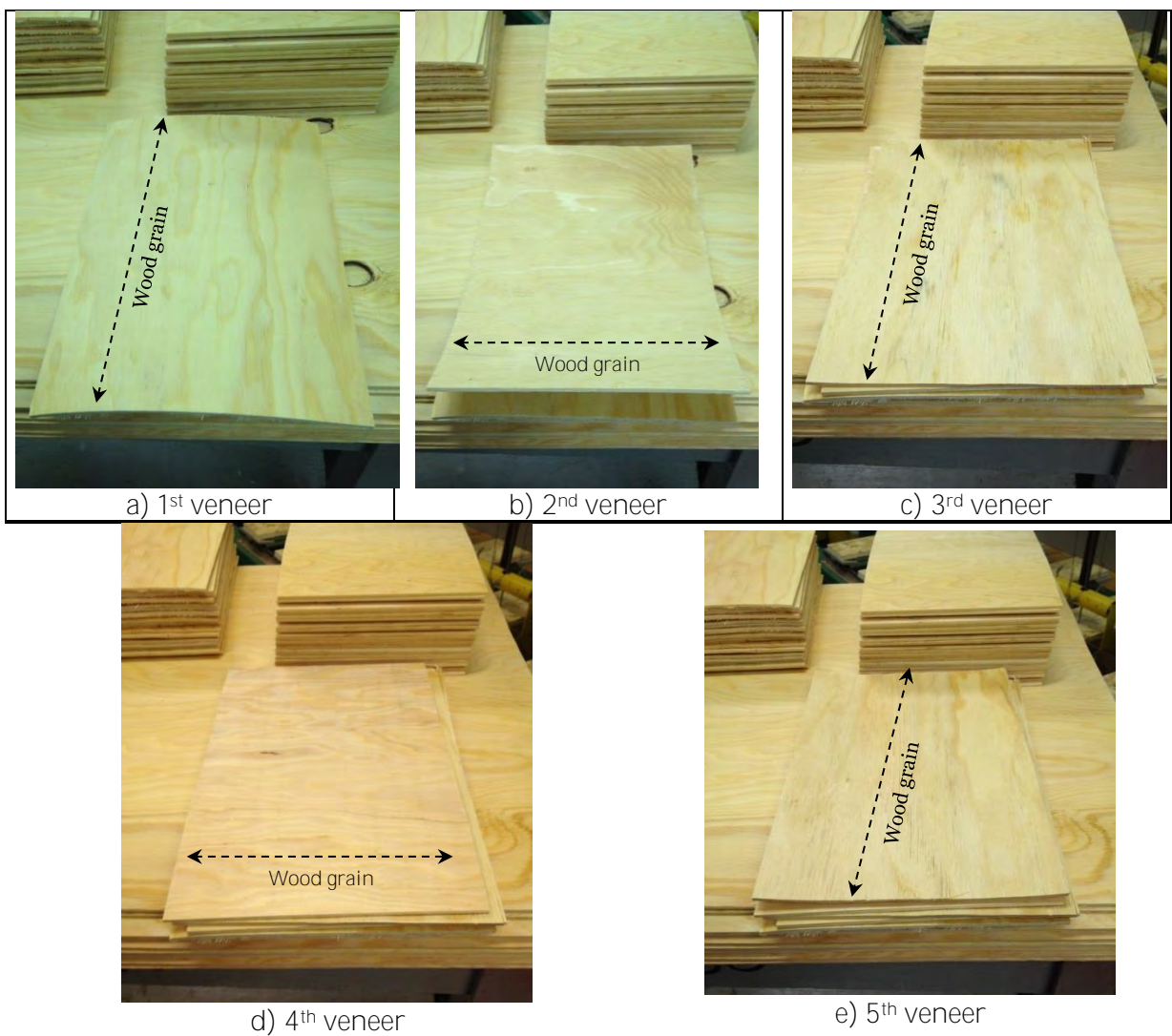


Figure 76: Douglas-Fir veneers used for plywood specimens

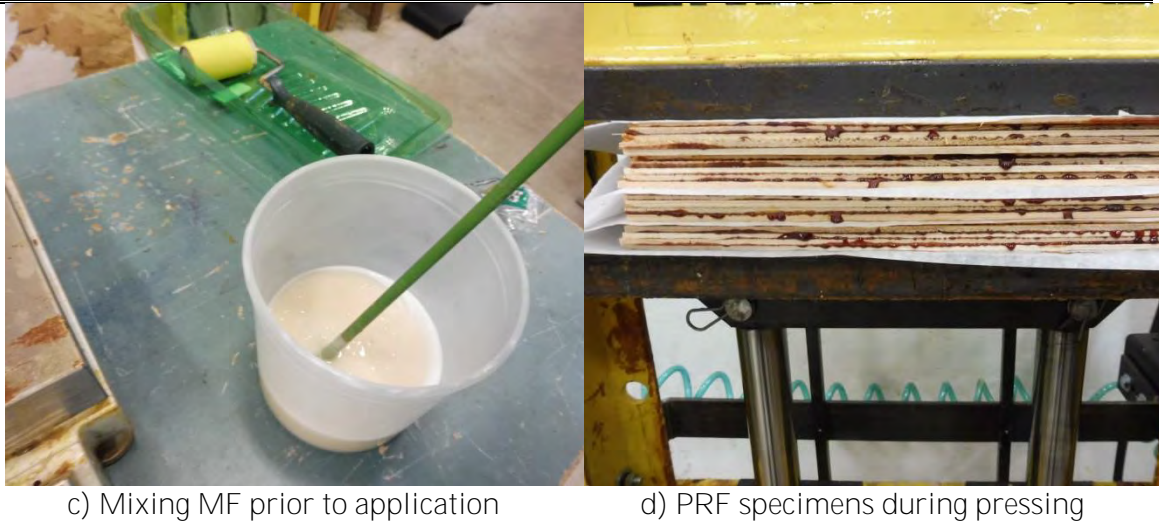
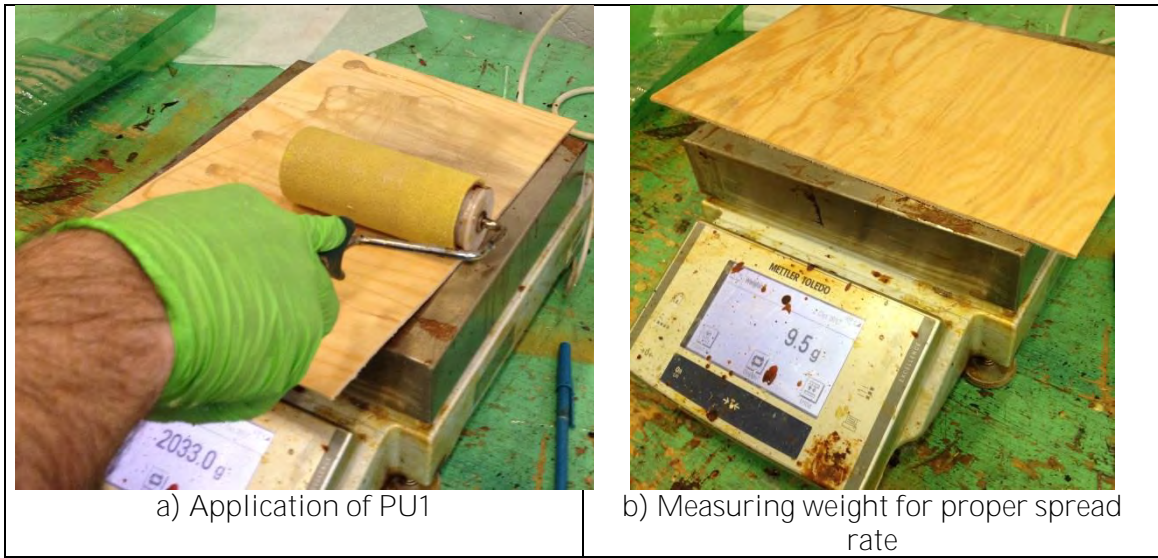


Figure 77: Gluing process of plywood billets

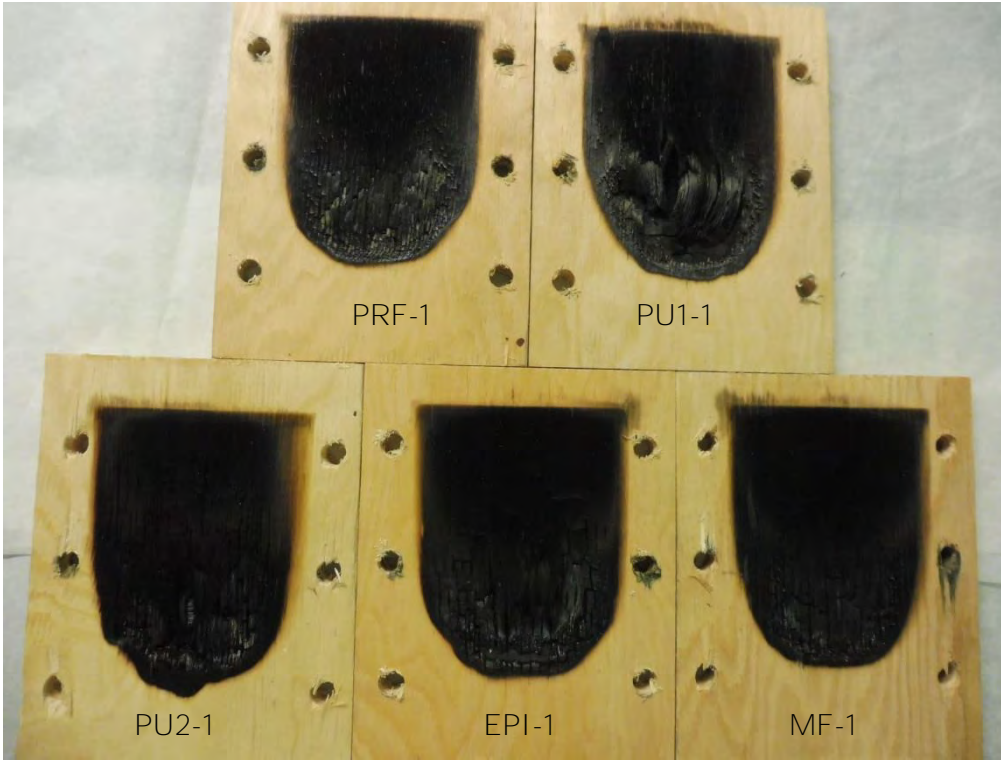


Figure 78: Specimens after PS 1 flame testing (all adhesives)

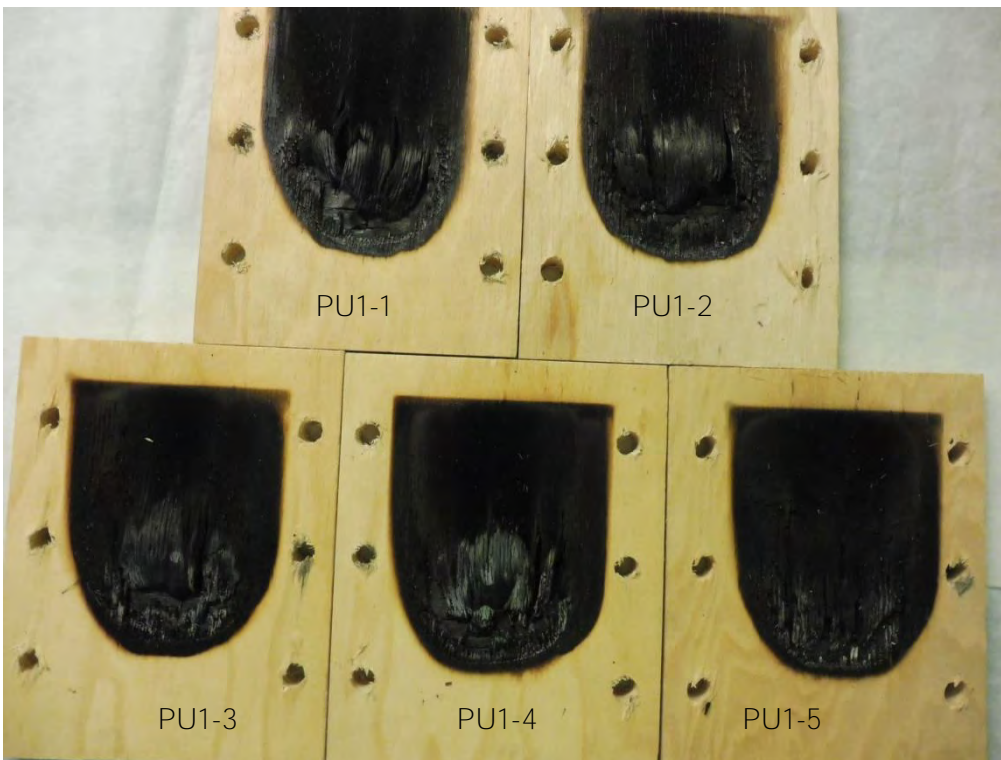


Figure 79: PU1 specimens after PS 1 flame testing

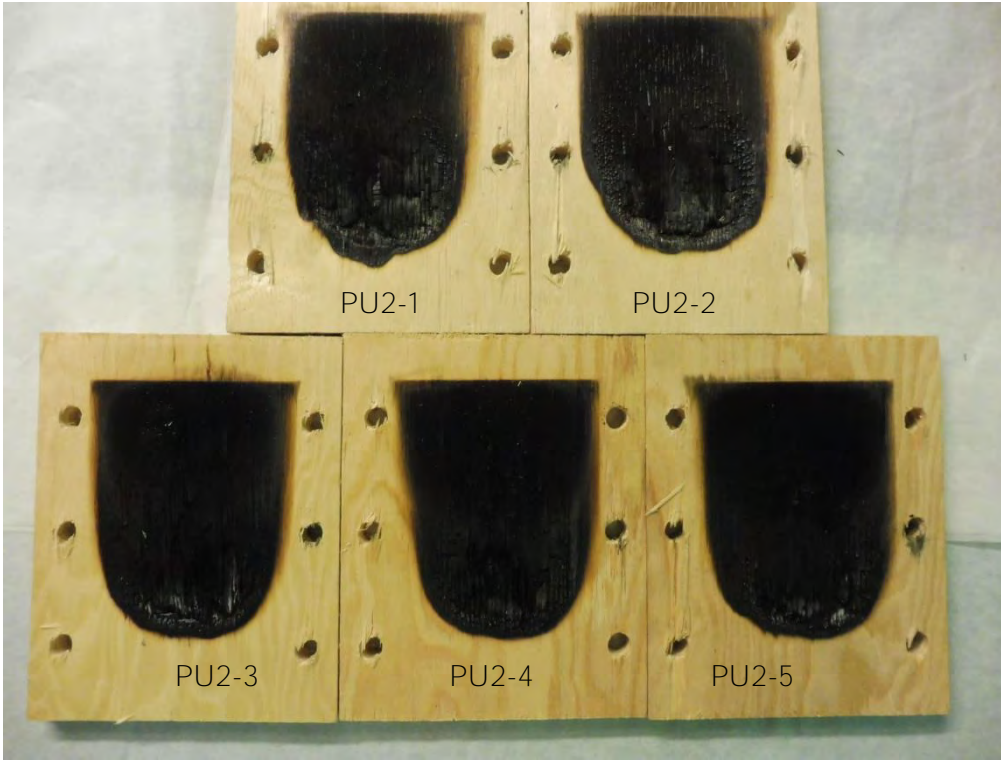


Figure 80: PU2 specimens after PS 1 flame testing

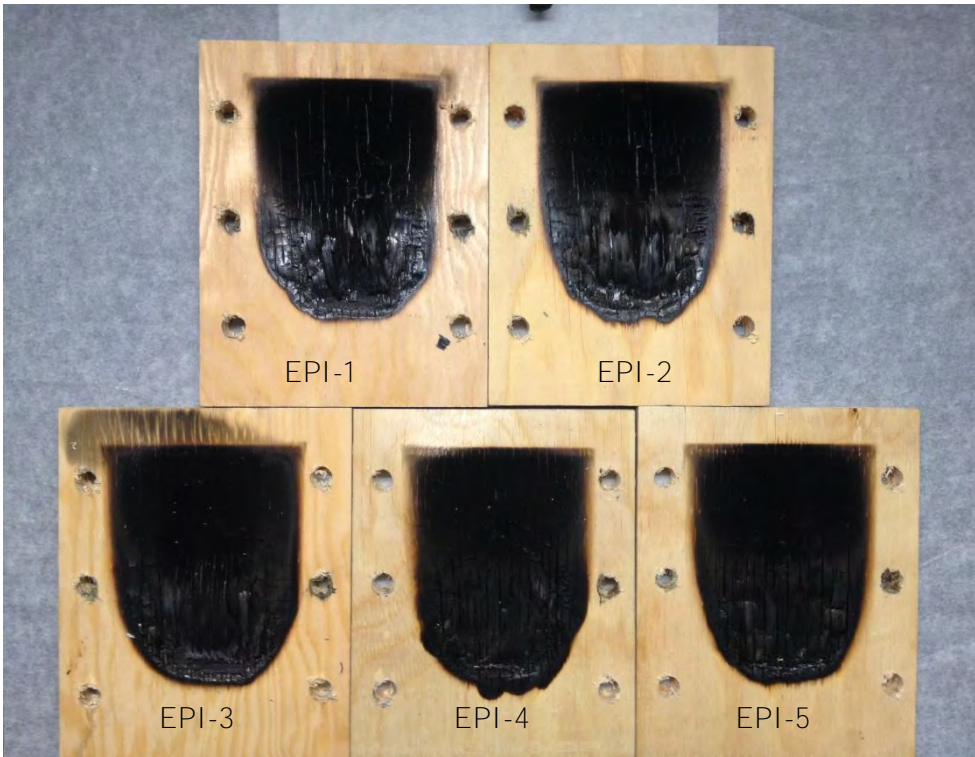


Figure 81: EPI specimens after PS 1 flame testing

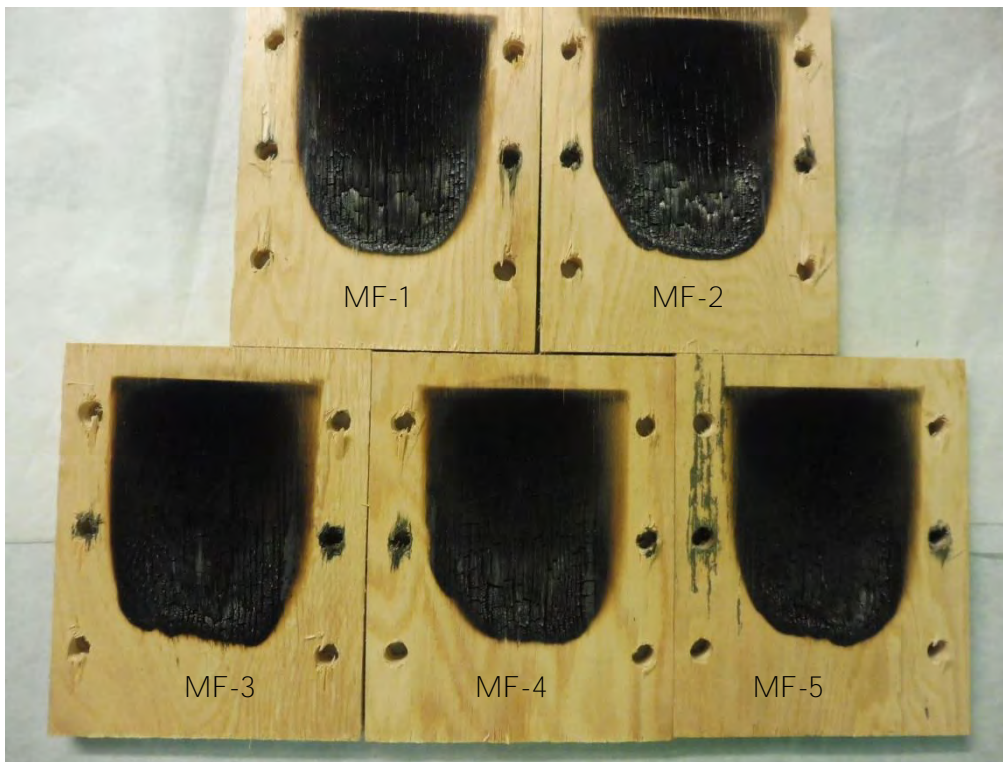


Figure 82: MF specimens after PS 1 flame testing

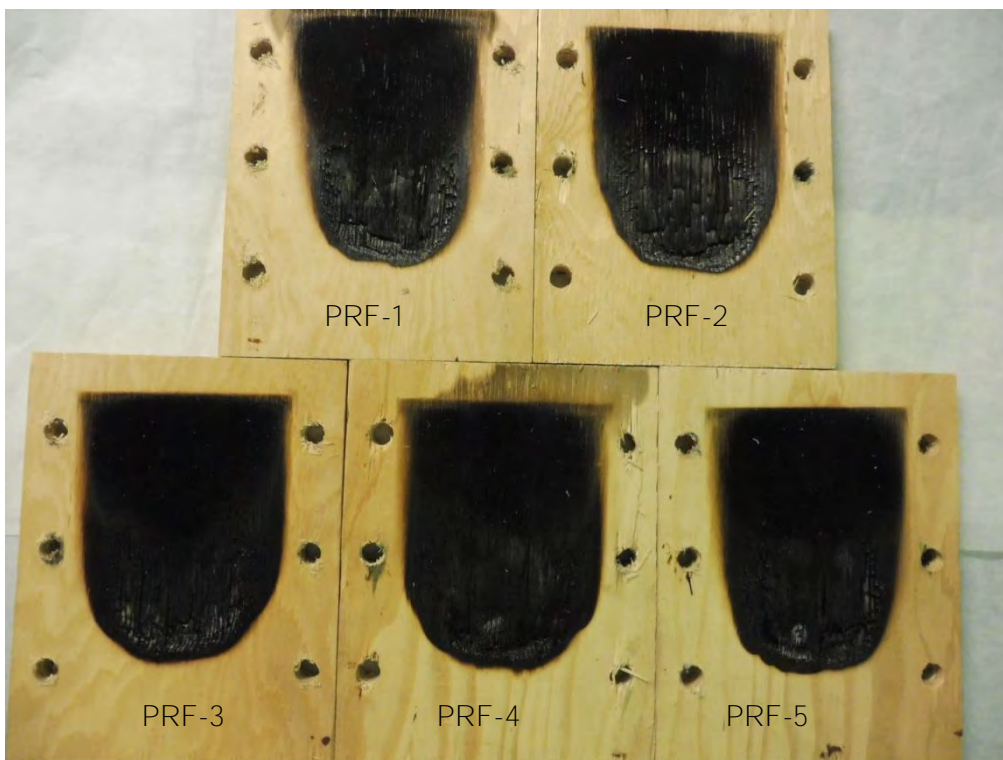


Figure 83: PRF specimens after PS 1 flame testing

Through our international collaboration programmes with academia, industry, and the public sector, we ensure the competitiveness of the Swedish business community on an international level and contribute to a sustainable society. Our 2,200 employees support and promote all manner of innovative processes, and our roughly 100 testbeds and demonstration facilities are instrumental in developing the future-proofing of products, technologies, and services. RISE Research Institutes of Sweden is fully owned by the Swedish state.



RISE Research Institutes of Sweden AB Box 5608, SE-114 86 STOCKHOLM, Sweden Telephone: +46 10 516 50 00 E-mail: info@ri.se , Internet: www.ri.se	Fire Research
--	---------------

